Chapter 2
Nonaqueous Electrolytes with Advances in Solvents

Makoto Ue, Yukio Sasaki, Yasutaka Tanaka, and Masayuki Morita

Abstract Most of the liquid electrolytes used in commercial lithium-ion (Li-ion) cells are nonaqueous solutions, in which roughly 1 mol dm^{-3} of lithium hexafluorophosphate ($LiPF_6$) salt is dissolved in a mixture of carbonate solvents selected from cyclic carbonates—ethylene carbonate and propylene carbonate—and linear carbonates—dimethyl carbonate, ethyl methyl carbonate, and diethyl carbonate. In Sect. 2.1, the physicochemical properties of these carbonate solvents are listed and the phase diagrams and electrolytic conductivity data of mixed carbonate solvent systems are given. However, recent market demands for Li-ion cells with higher energy, higher power, and higher safety requires new solvents to improve the performance of cells in electrolytes based on carbonate solvents only. New heteroatom-containing organic solvents including fluorine, boron, phosphorous, and sulfur, which have been applied to lithium cells in recent years, are reviewed from the viewpoints of synthesis, physicochemical properties, and cell performance by four authors.

M. Ue (✉)
Mitsubishi Chemical Corporation, 1000 Kamoshida, Aoba, Yokohama, Kanagawa 227-8502, Japan

National Institute for Materials Science, Namiki, Tsukuba, Ibaraki 305-0044, Japan
e-mail: macue01@gmail.com

Y. Sasaki
Tokyo Polytechnic University, 1583 Iiyama, Atsugi, Kanagawa 243-0297, Japan
e-mail: sasaki2045@gmail.com

Y. Tanaka
Graduate School of Science and Technology, Shizuoka University, Hamamatsu 432-8561, Japan
e-mail: tcytana@ipc.shizuoka.ac.jp

M. Morita
Graduate School of Science and Engineering, Yamaguchi University, 2-16-1, Tokiwadai, Ube 755-8611, Japan
e-mail: morita@yamaguchi-u.ac.jp

T.R. Jow et al. (eds.), *Electrolytes for Lithium and Lithium-Ion Batteries*, Modern Aspects of Electrochemistry 58, DOI 10.1007/978-1-4939-0302-3_2,
© Springer Science+Business Media New York 2014

Section 2.2 mainly reviews the papers on novel fluorinated organic solvents, which include fluorinated lactones, fluorinated linear carboxylates, fluorinated cyclic carbonates, fluorinated linear carbonates, fluorinated monoethers, fluorinated diethers, and others. The physicochemical properties of typical fluorinated compounds are summarized in comparison with nonfluorinated counterparts.

Section 2.3 summarizes the recent promising progress of electrolyte solvents that contain boron atoms, particularly borate esters and cyclic borate esters. The authors also introduce some boron compounds acting as additives and supporting salts in electrolytes.

Section 2.4 reviews organophosphorous compounds as nonflammable or flame-retardant electrolytes for lithium-ion batteries. These include organic phosphates, phosphites, phosphonates, or phosphazenes, and a phosphonamidate as co-solvents or additives. The author introduces polymeric gel electrolytes containing these flame-retardant components.

Section 2.5 reviews papers on lithium and lithium-ion cells using sulfur-containing organic solvents, including sulfide, sulfoxide, sulfone, sulfite, sulfonate, and sulfate. Particularly, the performance of sulfones such as ethyl methyl sulfone and sulfolane as electrolyte solvents for high-voltage cells is introduced.

2.1 General Remarks

Most lithium cells available in the market utilize nonaqueous electrolyte solutions, where lithium salts are dissolved in organic solvents. The gelled electrolytes used in lithium-ion polymer batteries are also regarded as an organic electrolyte immobilized with a high molecular weight polymer.

There are numerous organic solvents and lithium salts; however, a very limited number of materials fulfill the following physicochemical requirements for practical use.

1. High electrolytic conductivity
2. High chemical and electrochemical stability
3. Wide operational temperature range
4. High safety

The selection of the electrolyte materials is also dependent on the kind of negative and positive electrodes.

Most liquid electrolytes used in commercial lithium-ion cells are nonaqueous solutions, in which roughly 1 mol dm^{-3} of lithium hexafluorophosphate ($LiPF_6$) salt is dissolved in a mixture of carbonate solvents selected from cyclic carbonates, e.g., ethylene carbonate (EC) and propylene carbonate (PC), and linear carbonates, e.g., dimethyl carbonate (DMC), ethyl methyl carbonate (EMC), and diethyl carbonate (DEC), as listed in Table 2.1 [1].

Regarding the practical carbonate solvents, the phase diagrams of mixed-carbonate solvent systems were investigated by Ding [2]. Since these data are very important, a brief explanation is given here. Figure 2.1 shows phase

Table 2.1 Physical properties of carbonate solvents

Solvent	FW	ε_r	η_0 (mPa s)	d_0 (g cm^{-3})	mp (°C)	bp (°C)	fp (°C)	κ^a (mS cm^{-1})	$E_{red}{}^a$ (V vs. Li/Li$^+$)	$E_{ox}{}^a$ (V vs. Li/Li$^+$)
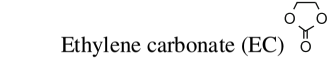 Ethylene carbonate (EC)	88.1	90[b]	1.9[b]	1.32[b]	36	238	143	17	0.0	+6.2
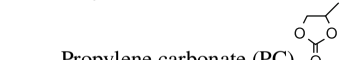 Propylene carbonate (PC)	102.1	65	2.5	1.20	−49	242	138	13	0.0	+6.6
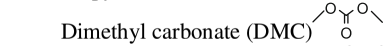 Dimethyl carbonate (DMC)	90.1	3.1	0.59	1.06	5	90	17	2.0[c]	0.0[c]	+6.5[c]
 Ethyl methyl carbonate (EMC)	104.1	3.0	0.65	1.01	−53	108	23	1.1[c]	0.0[c]	+6.7[c]
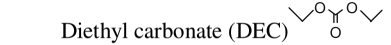 Diethyl carbonate (DEC)	118.1	2.8	0.75	0.97	−74	127	25	0.6[c]	0.0[c]	+6.7[c]

[a]1 mol dm^{-3} Et_4NBF_4 ([c]0.65 mol dm^{-3} Bu_4NBF_4), GC, 5 mV s^{-1}, 1 mA cm^{-2}

25°C ([b]40°C)

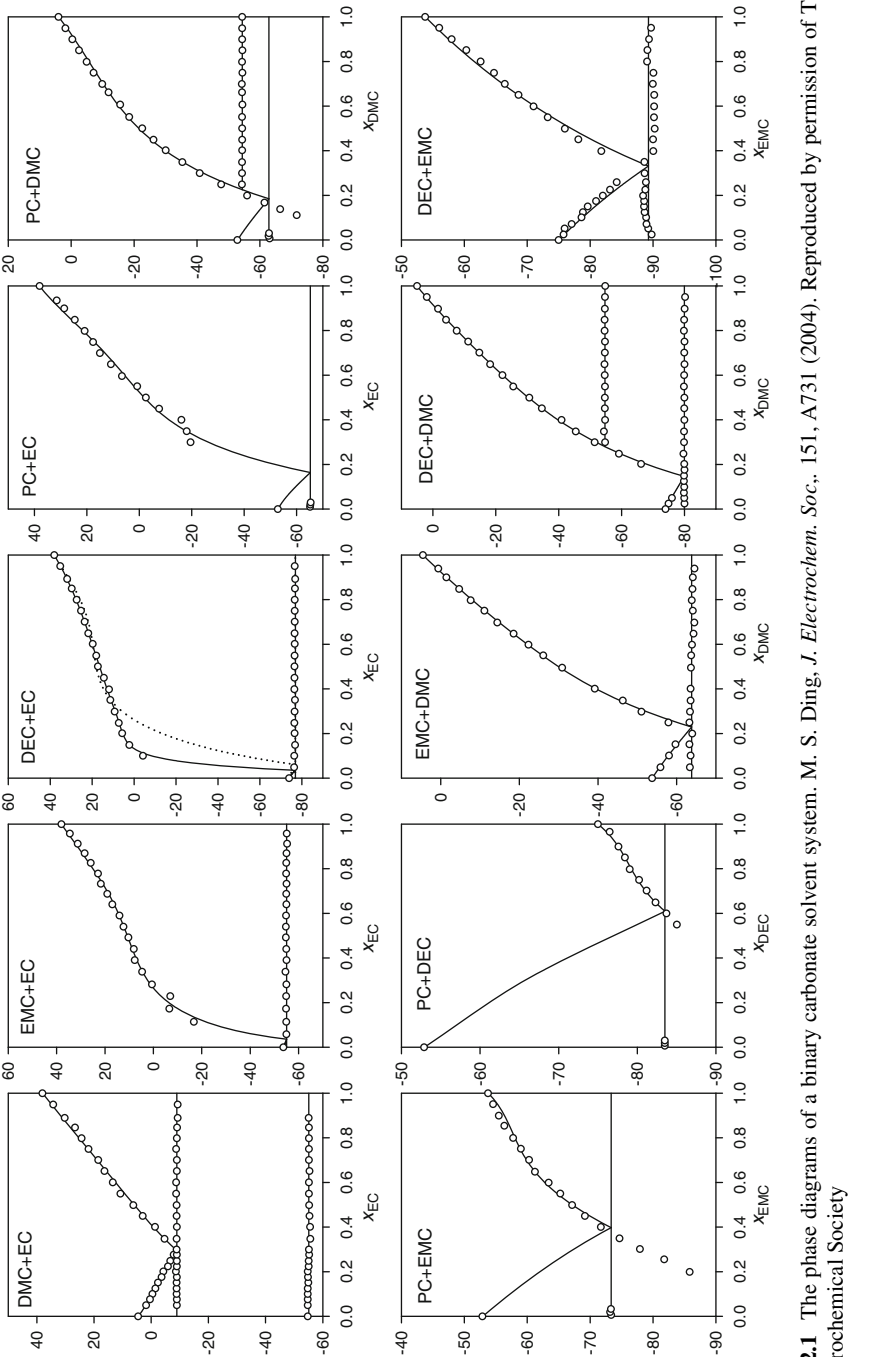

Fig. 2.1 The phase diagrams of a binary carbonate solvent system. M. S. Ding, *J. Electrochem. Soc.*, 151, A731 (2004). Reproduced by permission of The Electrochemical Society

diagrams of binary solvent systems selected from five carbonate solvents, where χ and θ are mole fraction and temperature, respectively. All systems exhibit a eutectic point and a typical phase diagram of binary systems, where both components mutually dissolve in the liquid state and do not dissolve in the solid state. Compositions near the eutectic point are preferred to expand the lower limit of the operation temperature. The eutectic point falls remarkably when both components have similar freezing points and molecular structures (chain or cyclic). Figure 2.2 shows the phase diagram of an EC-DMC-EMC ternary system as (a) a liquidus surface plot and (b) a contour plot of temperature over the composition triangle of the mole fraction. In the surface plot, the binary eutectic temperatures are indicated with the numbers near the respective solidus lines, and the ternary eutectic temperature is also indicated in the figure. In the contour plot, the temperature values of selected contours are indicated by the numbers near them. As shown in the surface plot, the melting point of EC falls progressively with the addition of DMC until it reaches the eutectic point (−8.6 °C) of the EC-DMC binary, thus tracing the solubility curve of EC in DMC on the EC-DMC binary phase diagram as an end-member to the ternary. It does the same with the addition of EMC, forming the solubility curve of EC in EMC with the eutectic point (−55.1 °C) on the EC-EMC binary. With the addition of DMC and EMC together, the melting point of EC expands into a falling solubility surface of EC in DMC-EMC, bounded on the two binary end-members by the solubility curves of EC in DMC and in EMC. It is further bounded within the composition triangle by two more space curves formed when the solubility surface of EC intersects those of DMC and EMC. Further, the three solubility surfaces meet at the eutectic point (−64.7 °C) of the ternary system EC-DMC-EMC, thus forming a complete liquidus surface above which any composition of the ternary is a thermodynamically stable liquid. Below the eutectic temperature of the ternary, which is lower than any of the three binary eutectic temperatures, any composition will be composed of nothing but solid phases. The most striking and important feature in the topography of the liquidus surface of the EC-DMC-EMC ternary is the slow descent of the melting point of EC with the addition of, or the flat solubility surface of EC in, DMC and EMC.

The electrolytic conductivity of $LiPF_6$ in the EC-EMC binary solvent system is given in Table 2.2 over a range of salt concentrations and temperatures [1, 3]. The content of EC is usually less than 50 vol.%, preferably 30 vol.%, because higher EC content causes its precipitation at low temperatures. For high-rate (high-power) applications, further high electrolytic conductivity is required. The addition of DMC is an effective solution to increase the electrolytic conductivity as shown in Fig. 2.3.

In addition to carbonate solvents, much effort has been made to introduce new solvents in order to improve cell performance. In the following section, heteroatom-containing organic solvents applied to lithium cells in recent years are reviewed by each author. The heteroatom includes fluorine, phosphorous, boron, and sulfur.

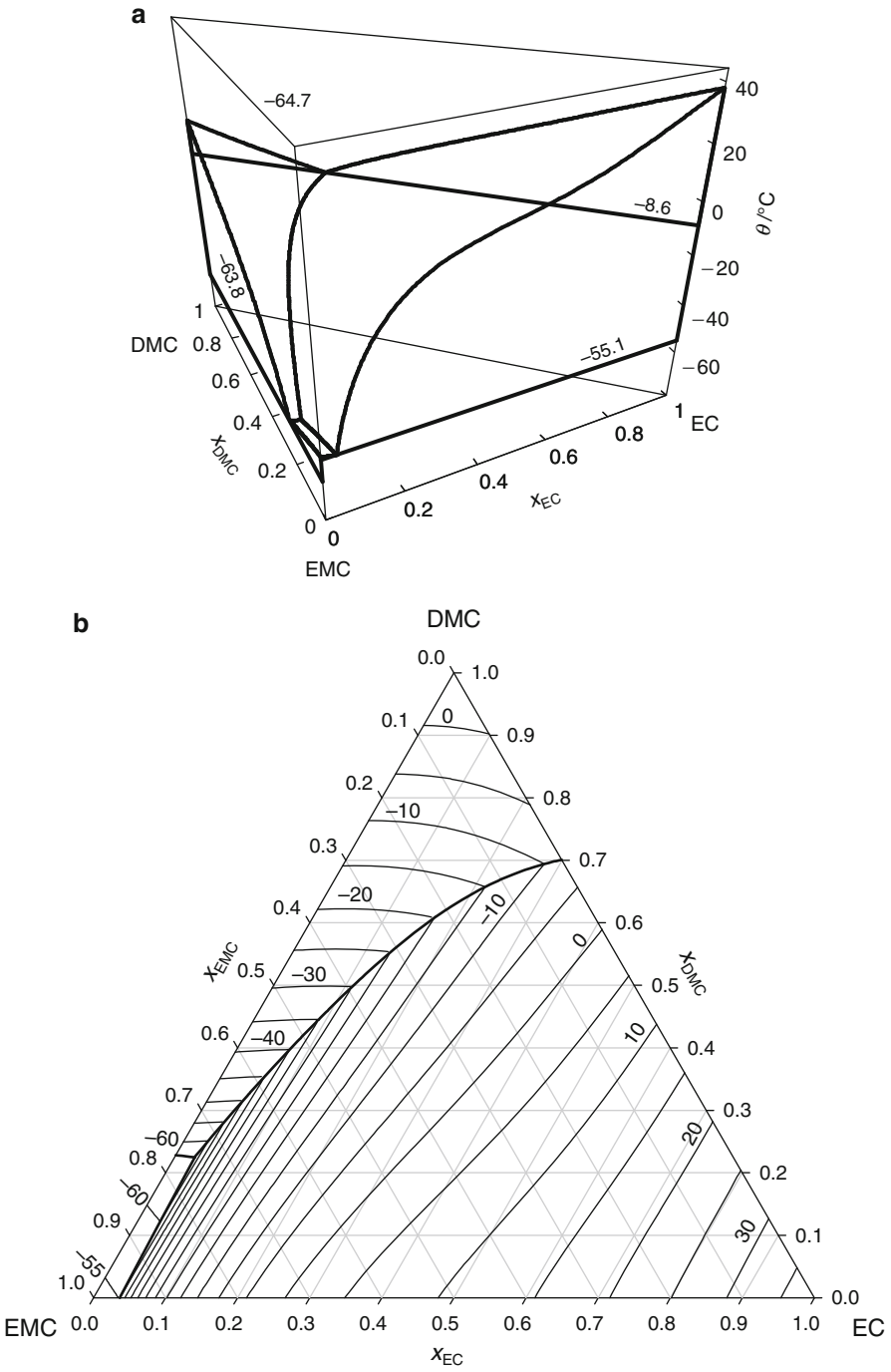

Fig. 2.2 The phase diagram of an EC-DMC-EMC ternary solvent system. M. S. Ding, *J. Electrochem. Soc,*. 151, A731 (2004). Reproduced by permission of The Electrochemical Society

Table 2.2 Electrolytic conductivity of $LiPF_6$ in an EC-EMC binary solvent system

$LiPF_6$, C (M)	EC, χ (vol.%)	EMC, χ (vol.%)	t (°C)											
			−40	−30	−20	−10	0	10	20	25	30	40	50	60
0.50	10	90	0.9	1.4	1.9	2.4	3.0	3.6	4.2	4.4	4.7	5.3	5.8	6.3
0.75	10	90	1.2	1.8	2.6	3.3	4.1	5.0	5.9	6.3	6.7	7.5	8.3	9.1
1.00	10	90	1.0	1.7	2.6	3.5	4.4	5.4	6.5	6.9	7.4	8.4	9.4	10.4
1.25	10	90	1.0	1.7	2.6	3.7	4.8	5.9	7.2	7.6	8.3	9.5	10.7	11.8
1.50	10	90	0.7	1.3	2.1	3.1	4.1	5.4	6.7	7.3	8.0	9.3	10.7	12.0
0.50	30	70		*p*	3.0	4.0	5.1	6.3	7.5	8.0	8.6	9.8	11.1	12.3
0.75	30	70	*p*	2.1	3.1	4.3	5.6	7.0	8.6	9.3	10.0	11.5	13.1	14.6
1.00	30	70	1.1	1.8	2.9	4.1	5.6	7.2	8.8	9.6	10.5	12.2	14.0	15.8
1.25	30	70	0.7	1.3	2.3	3.4	4.8	6.5	8.2	9.0	9.9	11.8	13.7	15.6
1.50	30	70	0.4	1.0	1.8	3.0	4.4	6.0	7.7	8.5	9.4	11.3	13.3	15.5
0.50	50	50			*p*	3.8	4.9	6.3	7.6	8.3	9.0	10.4	11.9	13.4
0.75	50	50		*p*	2.9	4.2	5.6	7.2	8.9	9.8	10.7	12.5	14.5	16.4
1.00	50	50		*p*	2.7	4.0	5.4	7.0	8.8	9.7	10.6	12.6	14.8	16.9
1.25	50	50		*p*	1.9	3.1	4.7	6.4	8.4	9.3	10.4	12.6	14.9	17.3
1.50	50	50							Insoluble					
0.50	60	40						*p*	7.4	8.1	8.8	10.3	11.8	13.3
0.75	60	40				*p*	5.4	7.0	8.8	9.7	10.6	12.5	14.5	16.5
1.00	60	40			*p*	3.5	5.1	6.8	8.6	9.5	10.5	12.6	14.8	17.0
1.25	60	40			*p*	2.9	4.3	6.2	8.2	9.2	10.2	12.5	15.0	17.5
1.50	60	40							Insoluble					

in mS cm^{-1}, *p*: EC precipitation

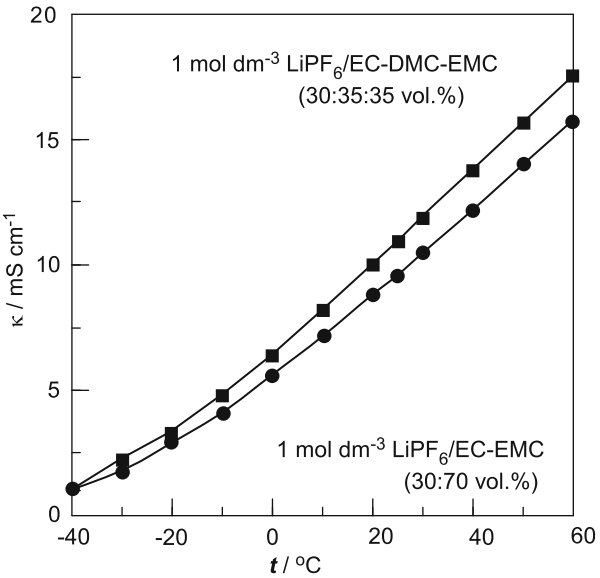

Fig. 2.3 Conductivity increases by the addition of DMC

2.2 Fluorine-Containing Organic Solvents

2.2.1 Introduction

One of the recent methodologies for finding a new appropriate solvent for advanced lithium batteries is the introduction of fluorine atoms into the solvent molecules, because it will improve the various electrochemical properties such as solvent polarity, oxidation durability, liquidus temperature range, and nonflammability, which would result in better cell performances [4, 5]. In general, fluorinated organic solvents show very different physical properties compared to the common organic solvents because of very high electronegativity and low polarizability of the fluorine atom. In addition, partially fluorinated organic solvents show fairly high polarity in comparison with that of fully fluorinated (perfluoro-) organic solvents.

There are three methods for the introduction of fluorine atoms into the solvent molecules, which are common organic chemical synthesis, electrolytic fluorination, and direct fluorination using elemental fluorine (F_2 gas), respectively. The direct fluorination is the simplest method to prepare partially fluorinated organic solvents. It makes possible to obtain many interesting fluorinated organic solvents. Among the important solvents for practical lithium batteries, the direct fluorination has already been applied to propylene carbonate (PC) [6] and 1,2-dimethoxyethane (DME) [7] in the late 1960s.

This section mainly reviews the papers on the novel fluorinated organic solvents, which were investigated for lithium batteries in the past decade. Although their chemical structures were drawn in Schemes, it was difficult to include all detailed data on physical and electrochemical properties of fluorinated solvents. The physical properties of typical fluorinated compounds and non-fluorinated counterparts were summarized in Tables 2.3 and 2.4, respectively [4, 5], where FW, d, ε_r, η, E_{homo}, and E_{lumo} are formula weight, density, relative permittivity, viscosity, and frontier orbital energies, respectively. The frontier orbital energies were recalculated by RHF/6-311+G(2d,p) with structure optimization.

2.2.2 Fluorinated Lactones

γ-Butyrolactone (γ-BL) is one of the good solvents for lithium batteries because of its well-balanced relative permittivity and viscosity, and wide liquidus temperature range. Therefore, it is interesting to modify γ-BL by fluorination. Three kinds of mono-fluorinated γ-butyrolactones, α-fluoro-γ-BL (α-F-γ-BL), β-fluoro-γ-BL (β-F-γ-BL), and γ-fluoro-γ-BL (γ-F-γ-BL) were prepared by direct fluorination as shown in Scheme 2.1 [8]. A mixture of α-F-γ-BL and β-F-γ-BL was obtained by fractional distillation (3:7 in molar ratio, F-γ-BL_{mix}). γ-F-γ-BL was easily decomposed by HF produced during the reaction. It was possible to obtain α-F-γ-BL by direct fluorination using α-acetyl-γ-BL as a starting material [5]. In addition, γ-F-γ-BL was selectively produced by electrolytic fluorination [9].

Table 2.3 Physical properties of fluorinated solvents

Name	FW	d, g cm^{-3}	ε_r	η, mPa s	E_{homo}, eV	E_{lumo}, eV
α-Fluoro-γ-butyrolactone (α-F-γ-BL)	104	1.30	73	3.4	−12.16	1.55
β-Fluoro-γ-butyrolactone (β-F-γ-BL)	104				−12.19	1.52
γ-Fluoro-γ-butyrolactone (γ-F-γ-BL)	104				−12.31	1.61
3:7 mixture of α-and β-Fluoro-γ-butyrolactone (F-γ-BL$_{mix}$)	104	1.30	80	3.9	–	–
Methyl fluoroacetate (MFA)	92	1.17	18	1.2	−12.58	1.71
Methyl difluoroacetate (MDFA)	110	1.26			−12.90	1.67
Ethyl fluoroacetate (EFA)	106	1.09	15	0.89	−12.47	1.75
Ethyl difluoroacetate (EDFA)	124	1.24			−12.78	1.73
2-Fluoroethyl acetate (2FEA)	106	1.09	7.8	0.97	−12.46	1.75
2,2-Difluoroethyl acetate (DFEA)	124	1.20	9.4	1.0	−12.64	1.74
2,2,2-Trifluoroethyl acetate (TFEA)	142	1.24	6.7	0.70	−12.80	1.76
4-Fluoro-1,3-dioxolan-2-one (FEC)	106	1.50	107	4.1	−13.30	1.45
cis-4,5-Difluoro-1,3-dioxolan-2-one (*cis*-DFEC)[a]	124	1.59		2.3 (60 °C)	−13.91	1.34
trans-4,5-Difluoro-1,3-dioxolan-2-one (*trans*-DFEC)[a]	124	1.51	37	2.5	−13.91	1.63
4,4-Difluoro-1,3-dioxolan-2-one (*gem*-DFEC)[a]	124	1.57	34	2.1	−13.70	1.56
4-Fluoromethyl-1,3-dioxolan-2-one (FPC)	120	1.41	190	7.6	−13.00	1.39
4-Trifluoromethyl-1,3-dioxolan-2-one (TFPC)	156	1.58	67	5.0	−13.39	1.31
trans-4-Fluoromethyl-5-methyl-1,3-dioxolan-2-one (F-*t*-BC)	134	1.33	150	13	−12.86	1.44
Fluoromethyl methyl carbonate (FDMC)	108	1.24	9.0	0.92	−13.25	1.79
Bis(fluoromethyl) carboante (DFDMC)	126	1.40	14	1.4	−13.68	1.80
Difluoromethyl fluoromethyl carboante (TFDMC)	144	1.47	11	0.99	−13.75	1.76
2-Fluoroethyl methyl carbonate (FEMC)	122	1.19	7.3	1.4	−12.98	1.84
2,2-Difluoroethyl methyl carbonate (DFEMC)	140	1.29	9.3	2.7	−13.21	1.78
Methyl 2,2,2-trifluoroethyl carbonate (TFEMC)	158	1.33	7.1	0.82	−13.33	1.75
Ethyl 2-fluoroethyl carbonate (FDEC)	136	1.12	6.5	1.3	−12.80	1.86
2,2-Difluoroethyl ethyl carbonate (DFDEC)	154	1.29	6.6	1.3	−13.01	1.82
Ethyl 2,2,2-trifluoroethyl carbonate (TFDEC)	172	1.33	7.1	0.93	−13.11	1.80
3-Fluoropropyl methyl carbonate (FPMC)	136	1.14	7.1	1.7	−12.98	1.83
Methyl 3,3,3-trifluoropropyl carbonate (TrFPMC)	172	1.30	7.5	1.7	−13.13	1.77
Methyl 2,2,3,3-tetrafluoropropyl carbonate (TeFPMC)	190	1.40	8.8	2.6	−13.28	1.73
Methyl 2,2,3,3,3-pentafluoropropyl carbonate (PeFPMC)	208	1.41	6.2	1.3	−13.06	1.75
Methyl nanofluorobutyl ether (MFE)	250	1.52		0.38	−14.03	1.70
Ethyl nanofluorobutyl ether (EFE)	264	1.43		0.38	−13.26	1.77
2-Trifluoromethyl-3-methoxyperfluoropentane (TMMP)[b]	350	1.66	6.1	1.2	−13.08	1.68
2-(Trifluoro-2-fluoro-3-difluoropropxy)-3-difluoro-4-fluoro-5-trifluoropentane (TPTP)[b]	346	1.54	6.3	1.7	−13.81	1.47
2-Fluoroethoxymethoxyethane (FEME)	122	1.01	17	1.0	−11.68	1.95
2,2-Difluoroethoxymethoxyethane (DFEME)	140	1.10	17	1.1	−11.88	1.87
Methoxy-2,2,2-trifluoroethoxyethane (TFEME)	158	1.15	17	0.79	−11.98	1.84
Ethoxy-2-fluoroethoxyethane (EFEE)	136	0.97	14	1.1	−11.58	1.97
2,2-Difluoroethoxyethoxyethane (EDFEE)	154	1.05	14	1.1	−11.77	1.91
Ethoxy-2,2,2-trifluoroethoxyethane (ETFEE)	172	1.10	14	0.85	−11.87	1.89

[a]Reference [20]
[b]Reference [50]

Table 2.4 Physical properties of typical organic solvents

Name	FW	d, g cm^{-3}	ε_r	η, mPa s	E_{homo}, eV	E_{lumo}, eV
γ-Butyrolactone (γ-BL)	86	1.13	39	1.7	−11.86	1.67
Methyl acetate (MA)	74	0.93	6.7	0.36	−12.21	1.85
Ethyl acetate (EA)	88	0.89	6.0	0.43	−12.09	1.87
Ethylene carbonate (EC)	88	1.32 (40 °C)	90 (40 °C)	1.9 (40 °C)	−12.86	1.51
Propylene carbonate (PC)	102	1.20	65	2.5	−12.72	1.52
trans-Butylene carbonate (*t*-BC)	116	1.14	64	3.2	−12.60	1.55
Dimethyl carbonate (DMC)	90	1.06	3.1	0.59	−12.85	1.88
Ethyl methyl carbonate (EMC)	104	1.01	3.0	0.65	−12.71	1.91
Diethyl carbonate (DEC)	118	0.97	2.8	0.75	−12.59	1.93
Propyl methyl carbonate (PMC)	118	0.98	3.0	1.1	−12.67	1.91
Dimethoxyethane (DME)	90	0.86	5.5	0.46	−11.49	2.02
Ethoxymethoxyethane (EME)	104	0.85	5.7	0.52	−11.40	2.03
Diethoxyethane (DEE)	118	0.84	5.0	0.60	−11.36	2.05

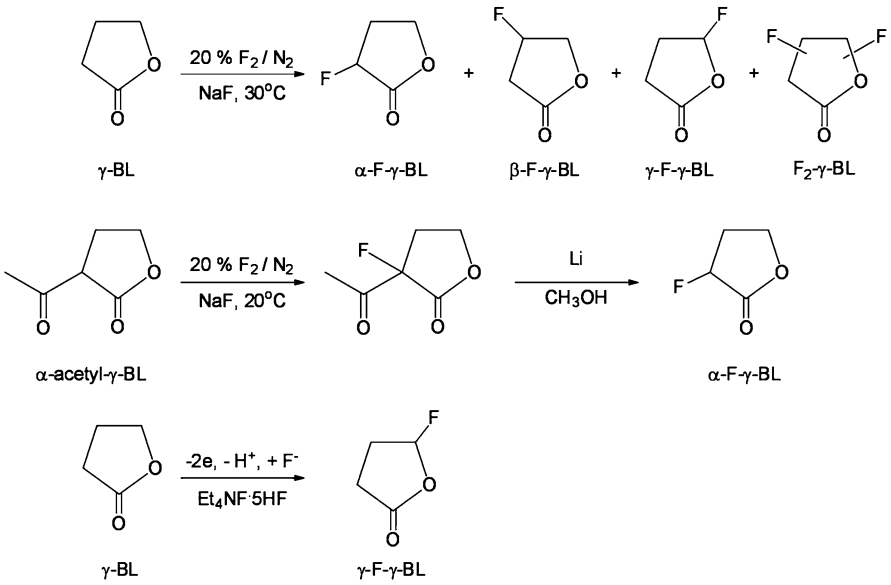

Scheme 2.1 Preparation methods of fluorinated γ-butyrolactones

The melting point of α-F-γ-BL is 26.5 °C, which is very different from that of γ-BL (−43.4 °C) [5]. The relative permittivities of α-F-γ-BL and F-γ-BL$_{mix}$ at 25 °C were 72.6 and 80.3, respectively, and about twice of that of γ-BL in a temperature range from 10 to 80 °C [5, 10]. At the same time, the viscosities of α-F-γ-BL and F-γ-BL$_{mix}$ became much higher than that of γ-BL. The electrolytic conductivities of lithium salts in α-F-γ-BL and F-γ-BL$_{mix}$ in a temperature range from 10 to 80 °C

were in the order; $LiPF_6 > LiClO_4 > LiBF_4$ and F-γ-BL_{mix} > α-F-γ-BL, and always lower than those in γ-BL due to their high viscosities. α-F-γ-BL and F-γ-BL_{mix} showed higher oxidation potentials than γ-BL on Pt electrode. In general, the introduction of fluorine atoms to organic solvents tends to increase their oxidation potentials and decrease their reduction potentials as expected from HOMO and LUMO energies. The lithium cycling efficiency (charge–discharge coulombic efficiency for a lithium electrode) on a Ni electrode was examined as the first step to know the possibility of applying F-γ-BL_{mix} to rechargeable lithium cells. The cycling efficiency is highly dependent on the morphology of the film on the lithium electrode. Among three kinds of solvents tested, F-γ-BL_{mix}, γ-BL, and PC, the lithium cycling efficiency became in the order; F-γ-BL_{mix} > PC > γ-BL and $LiPF_6 > LiBF_4 > LiClO_4$. Furthermore, 1 moldm^{-3} $LiPF_6$/F-γ-BL_{mix}-EC equimolar binary solution showed higher efficiency more than 75 % during 100 cycles, and better than α-F-γ-BL-EC equimolar binary solution. 1 moldm^{-3} $LiPF_6$/F-γ-BL_{mix} electrolyte showed much higher capacity retention in a Li/$LiCoO_2$ cell than γ-BL counterpart, but not as good as PC counterpart [10].

2.2.3 *Fluorinated Linear Carboxylates*

Fluorinated compounds of linear carboxylates were examined for low temperature application. The electrochemical behavior of a graphite electrode at low temperatures was investigated in 1 moldm^{-3} $LiClO_4$/EC-DEC-X (10:10:1 in volume) solution containing a fluorinated carboxylate (X) selected form CHF_2COOCH_3 (methyl difluoroacetate, MDFA), $CF_3CF_2COOCH_2CH_3$, $CF_3CF_2CF_2COOCH_3$, $(CF_3)_2CHCOOCH_3$, $CF_3CF_2CF_2CF_2COOCH_2CH_3$, $CF_3CF_2CF_2CF_2CF_2CF_2COOCH_3$, $CF_3CF_2CF_2CF_2$ $CF_2CF_2CF_2COOCH_2CH_3$ [11], and 1 moldm^{-3} $LiClO_4$/EC-DEC-PC-X (4:4:2:1 in volume) selected from CHF_2COOCH_3, $CF_3CF_2COOCH_2CH_3$, $CF_3CF_2CF_2COOCH_3$, $(CF_3)_2CHCOOCH_3$, $CF_3CF_2CF_2CF_2COOCH_2CH_3$, $CF_3CF_2CF_2CF_2COOCH(CH_3)_2$, $CF_3CF_2CF_2CF_2COOC(CH_3)_3$ [12] in Scheme 2.2.

The electrolytic conductivities of 1 moldm^{-3} $LiClO_4$/EC-DEC-MDFA (10:10:1 in volume) and EC-DEC-PC-MDFA (4:4:2:1 in volume) solutions were a little bit higher than those of EC-DEC and EC-DEC-PC baseline solutions, respectively, and other fluorinated carboxylates gave inferior conductivities in a temperature range from 0 to 50 °C [12]. The reduction potentials of these fluorinated carboxylates (0.87–1.41 vs. Li/Li$^+$) were more positive than that of EC (0.60 V). With decreasing reduction potential of the fluorinated carboxylates, the reversibility of the graphite electrode increased, resulting in higher charge capacity. The lowest reduction potential was observed for a low molecular weight MDFA. 1 moldm^{-3} $LiClO_4$/EC-DEC-MDFA (10:10:1 in volume) solution provided larger charge capacities than EC-DEC baseline solution at 0 and −4 °C. The study was extended to fluorinated graphite electrodes using 1 moldm^{-3} $LiClO_4$/EC-DEC-PC (1:1:1 in volume) solution with 0.15 vol.% MDFA at −10 °C [13].

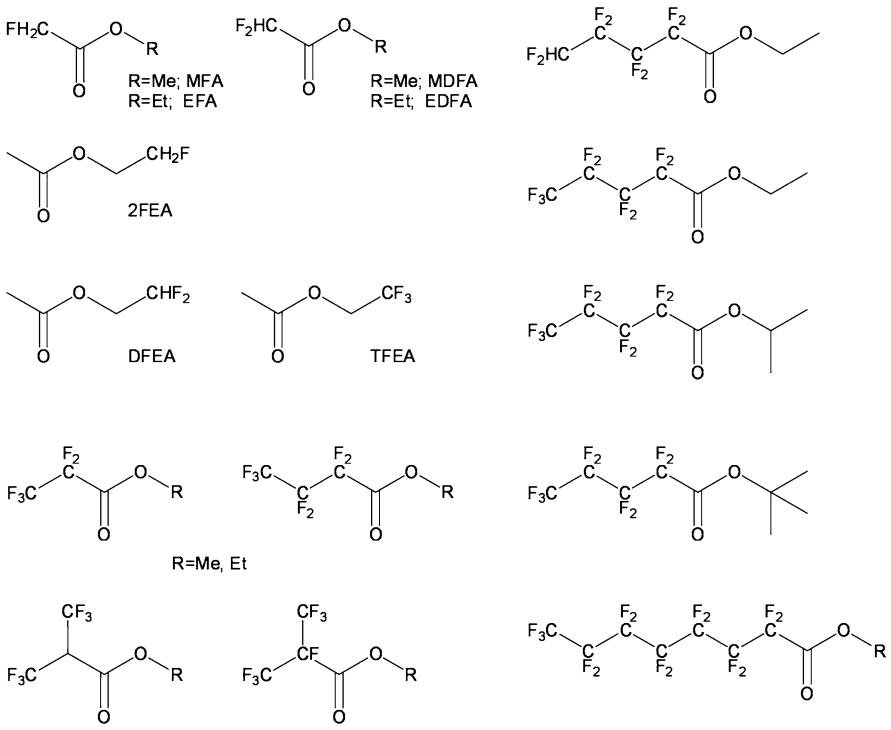

Scheme 2.2 Fluorinated linear carboxylates

Thermal stability and electrochemical properties of fluorinated carboxylates selected from CHF_2COOCH_3 (MDFA), $CHF_2COOCH_2CH_3$ (ethyl difluoroacetate, EDFA), $CF_3CF_2COOCH_3$, $CF_3CF_2COOCH_2CH_3$, $CF_3CF_2CF_2COOCH_3$, $CF_3CF_2CF_2COOCH_2CH_3$, $(CF_3)_2CFCOOCH_3$, $(CF_3)_2CFCOOCH_2CH_3$, $HCF_2CF_2CF_2CF_2COOCH_2CH_3$, and $CF_3CF_2CF_2CF_2CF_2CF_2CF_2COOCH_2CH_3$ in Scheme 2.2 were investigated [14–17]. Most fluorinated carboxylates including 0.2 moldm^{-3} or saturated $LiPF_6$ showed an exothermic reaction peak at higher temperatures in differential scanning calorimetry (DSC) than the corresponding non-fluorinated solvent counterparts even at the coexistence of Li or $Li_{0.5}CoO_2$ [14]. Among these fluorinated carboxylates, 1 moldm^{-3} $LiPF_6$/EC-DMC-MDFA (1:1:2 in volume) solution showed the highest onset temperature and smallest amount of exothermic heat at the coexistence of lithium [15]. However, the volume ratio of MDFA in 1 moldm^{-3} $LiPF_6$/EC-DMC-MDFA, PC-MDFA solutions should be more than 50 % to show the remarkable improvement of the thermal stability. This kind of good behavior was observed only in MDFA and not in EDFA, because the main component of SEI in the MDFA solution was CHF_2COOLi, which dissolved in EC, PC, DMC, DEC, and EDFA solution [16]. The main exothermic peak of 1 moldm^{-3} $LiPF_6$/MDFA solution at the coexistence of a lithiated graphite is around 400 °C and about 100 °C higher than that of EC-DMC (1:1 in volume) solution [17].

The relative permittivities and viscosities of methyl acetate (MA) and ethyl acetate (EA) increased by the introduction of one or two fluorine atoms, which resulted in the decrease of electrolytic conductivity of 1 moldm^{-3} $LiPF_6$ solutions as usual [16, 18]. The oxidation potentials on Pt were also increased by the introduction of fluorine atoms. Depending on the position of fluorine atom, the properties of 2-fluoroethyl acetate (2FEA) and ethyl fluoroacetate (EFA) varied. The electrolytic conductivities of 1 moldm^{-3} $LiPF_6$ solutions at 25 °C were in the order; MA > EA > MDFA > EFA > EC-DMC (1:1 in volume) >2FEA > EDFA >> EMC. However, the electrolytic conductivities of 1 moldm^{-3} $LiPF_6$/EFA and 2FEA solutions became higher than that of EA counterpart at high temperatures [18]. The lithium cycling efficiency of 1 moldm^{-3} $LiPF_6$/MDFA solution was more than 80 % and higher than those of EDFA, MA, or EA solutions [14]. The lithium cycling efficiency of 1 moldm^{-3} $LiPF_6$/EC-2FEA equimolar binary solution was higher than those of EC-EFA, EC-EA, or EC-EMC solutions [18]. The discharge capacity of carbons was smaller in 1 moldm^{-3} $LiPF_6$/MDFA solution than EC-DMC (1:1 in volume) counterpart due to the large resistance of SEI, while the cycling performance was similar to EC-DMC counterpart. A graphite/$LiCoO_2$ cells containing 1 moldm^{-3} $LiPF_6$/MDFA electrolyte exhibited a good cycling performance without any oxidation of the electrolyte on the $LiCoO_2$ cathode [17]. Furthermore, by adding 3 vol.% of vinylene carbonate (VC) in 1 moldm^{-3} $LiPF_6$/MDFA electrolyte resulted in satisfactory reversible capacity and cycling performance in a graphite/$LiCoO_2$ cell [19].

2.2.4 Fluorinated Cyclic Carbonates

Ethylene carbonate (EC) and propylene carbonate (PC) have favorable physical and electrochemical properties such as high relative permittivity, high donicity, and relatively wide potential window. The direct fluorination of EC was successfully carried out to provide 4-fluoro-1,3-dioxolan-2-one (fluoroethylene carbonate, FEC) as shown in Scheme 2.3 [20]. The fluorination of EC was strongly dependent on a choice of a reaction medium and no solvent was preferred from the viewpoint of conversion. FEC was further fluorinated to give three di-fluorinated derivatives. On the other hand, FEC was also prepared from 4-chloroethylene carbonate by exchange with KF [21]. FEC was tested as an electrolyte additive for rechargeable lithium cells [21, 22] and is now practically used [23, 24].

The melting point of FEC was 17 °C and lower than that of EC (37 °C). The relative permittivity and viscosity of FEC were higher than those of EC (Fig. 2.4a, b) [25]. The electrolytic conductivity of $LiPF_6$ in FEC was always lower than that in EC due to its high viscosities (Fig. 2.4c) [4]. FEC showed a higher oxidation potential on Pt than EC (Fig. 2.4d). The lithium cycling efficiency of 1 moldm^{-3} $LiPF_6$/FEC was as high as 90 % (Fig. 2.4e). The cycling efficiency of a graphite/$LiCoO_2$ cell containing 1 moldm^{-3} $LiPF_6$/FEC-PC-EC (1:3.5:3.5 in volume) electrolyte was higher than 99.5 % and the discharge capacity retention of the cell was 63 % at the 200th cycle [5].

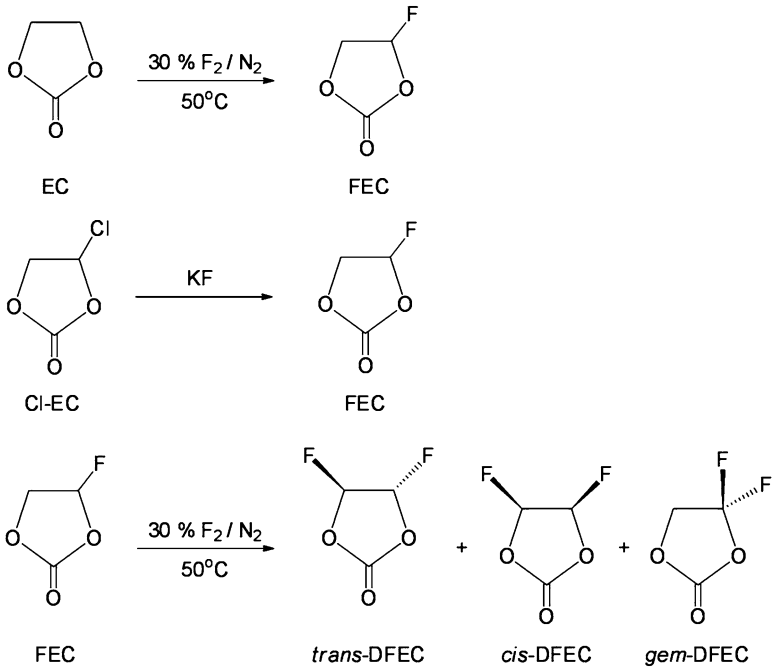

Scheme 2.3 Preparation methods of fluorinated ethylene carbonates

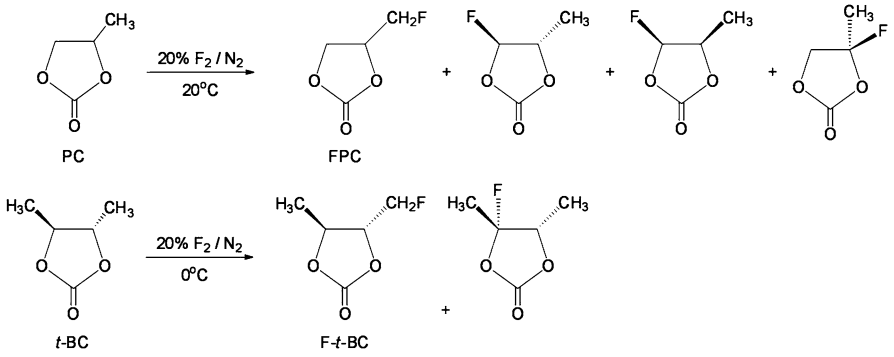

Scheme 2.4 Preparation of fluorinated propylene carbonates and *trans*-butylene carbonates

The direct fluorination of PC and *trans*-butylene carbonate (*t*-BC) gave four and two mono-fluorinated derivatives, respectively as shown in Scheme 2.4 [5, 26]. 4-Fluoromethyl-1,3-dioxolan-2-one (fluoromethylethylene carbonate, FMEC; hereafter renamed as FPC for easy understanding), 4-fluoromethyl-5-methyl-1,3-dioxolan-2-one (fluormethylmethylethylene carbonate, FMMEC; hereafter renamed as F-*t*-BC for easy understanding) were obtained by fractional distillation of the fluorinated samples.

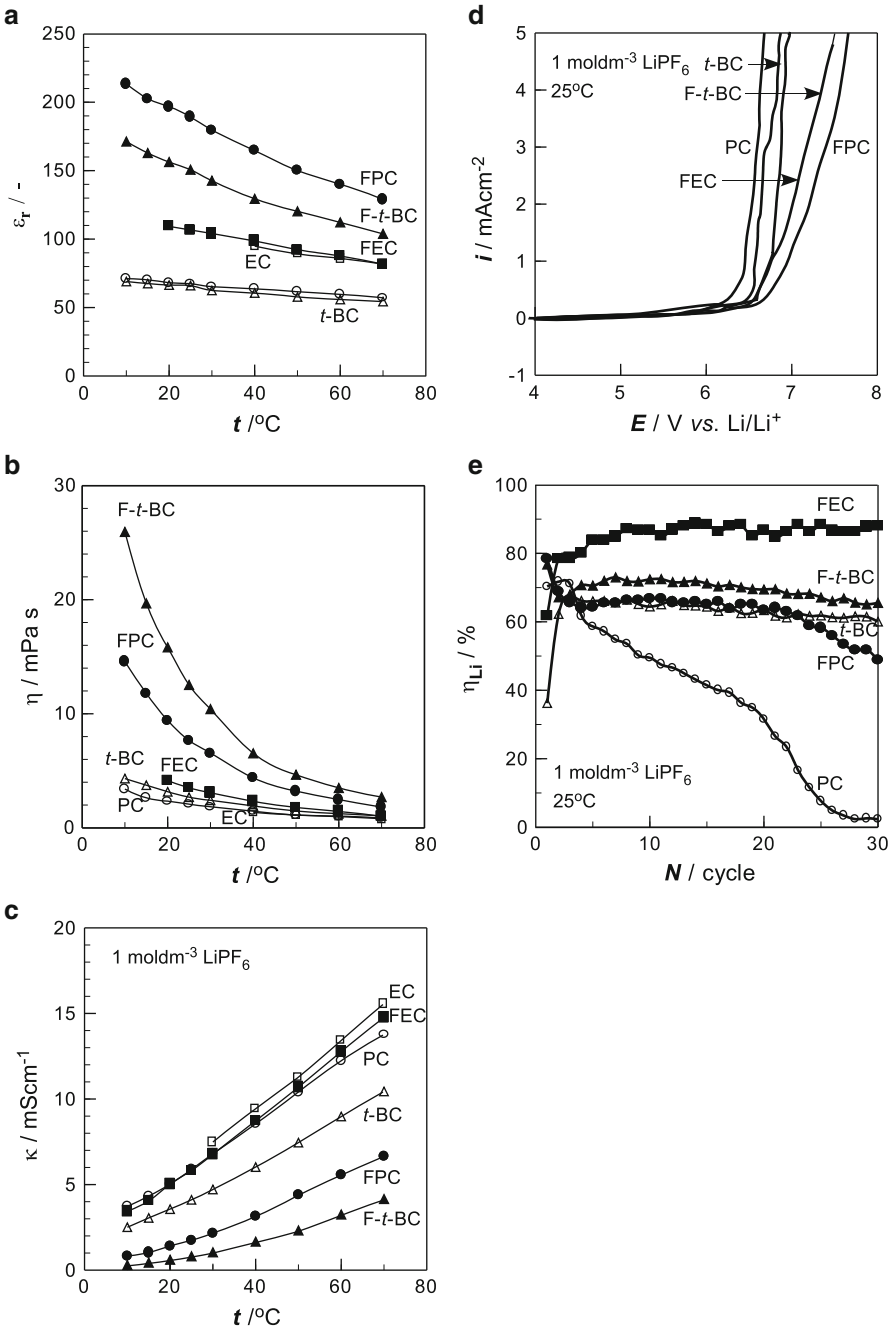

Fig. 2.4 Properties of cyclic carbonates and its mono-fluorinated derivatives. (**a**) relative permittivity (**b**) viscosity (**c**) electrolytic conductivity (**d**) oxidation potential (**e**) lithium cycling efficiency

The relative permittivities and viscosities of FPC and F-*t*-BC were higher than those of PC and *t*-BC, respectively (Fig. 2.4a, b) [27, 28]. The electrolytic conductivities of lithium salts in FPC and F-*t*-BC were always lower than those in PC and *t*-BC, respectively, due to their high viscosities (Fig. 2.4c) [4]. FPC and F-*t*-BC showed higher oxidation potentials on Pt than PC and *t*-BC, respectively (Fig. 2.4d). The lithium cycling efficiency in 1 moldm^{-3} $LiPF_6$/FPC and F-*t*-BC solutions was higher than those in PC and *t*-BC counterparts, respectively, but lower than FEC counterpart (Fig. 2.4e). The cycling efficiencies of Li/$LiCoO_2$ and graphite/$LiCoO_2$ cells containing 1 moldm^{-3} $LiPF_6$/FPC electrolyte were more than 95 % at a large cycle number. The cycling efficiency and discharge capacity of a graphite/$LiCoO_2$ cell containing 1 moldm^{-3} $LiPF_6$/FPC-EMC (1:3 in molar ratio) electrolyte was lower than those of EC-EMC counterpart at 25 °C; however, they were reversed at 60 °C [28].

As the novel fluorinated cyclic carbonates, the Li^+ intercalation of a graphite and SEI formation in 4-trifluoromethyl-1,3-dioxolan-2-one (trifluoromethylpropylene carbonate, TFPC) in Scheme 2.5 was investigated [29] and its 1 moldm^{-3} $LiPF_6$ binary mixed electrolytes with EC, PC, and ClEC were examined in graphite/Li and $LiMn_2O_4$/Li half cells [30]. The electrochemical behavior of 4-(2,2,3,3-tetrafluoropropoxymethyl)-1,3-dioxolan-2-one, 4-(2,3,3,3-tetrafluoro-2-trifluoromethylpropyl)-1,3-dioxolan-2-one, and 4,5-difluoro-4,5-dimethyl-1,3-dioxolan-2-one in Scheme 2.5 has been studied in EC-DEC and EC-DEC-PC mixtures [31, 32]. Electrochemical oxidation using a Pt microelectrode was largely suppressed by mixing these fluorinated derivatives with 0.67 moldm^{-3} $LiClO_4$/EC-DEC (1:1 in volume) or EC-DEC-PC (1:1:1 in volume). The oxidation current on a natural graphite was much smaller in 0.67 moldm^{-3} $LiClO_4$/EC-DEC-X (1:1:1 in volume) than in EC-DEC (1:1 in volume) or EC-DEC-PC (1:1:1 in volume) baseline solutions, and the reduction potentials of these fluorinated derivatives on the natural graphite were about 2 V vs. Li/Li^+, which were higher than those of EC, DEC, and PC. These fluorinated carbonates increased the first coulombic efficiencies on natural graphites due to the quick SEI formation in PC-containing solutions. Thermal stability was also increased by the use of these fluorinated derivatives. In addition, these fluorinated derivatives gave antioxidation ability to electrolyte solutions.

2.2.5 Fluorinated Linear Carbonates

Among the carbonate solvents used in practical lithium batteries, linear carbonates such as dimethyl carbonate (DMC), ethyl methyl carbonate (EMC), and diethyl carbonate (DEC) are well-known good co-solvents (thinner) for EC and PC. The direct fluorination of DMC gave fluorinated derivatives such as mono-fluorinated one, fluoromethyl methyl carbonate (FDMC), two di-fluorinated ones (bis(fluoromethyl) carbonate, DFDMC, and difluormethyl methyl carbonate, *gem*-DFDMC), and trifluorinated ones (difluoromethyl fluoromethyl carbonate, TFDMC) as shown in Scheme 2.6 [33]. Three kinds of partially fluorinated DMCs except *gem*-DFDMC were obtained by fractional distillation of the fluorinated sample.

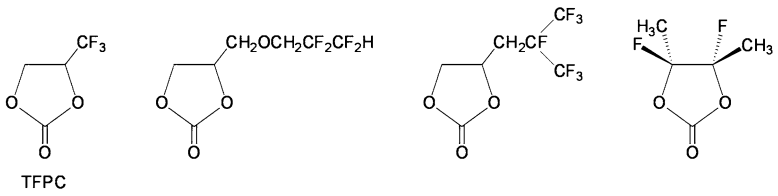

Scheme 2.5 Other fluorinated cyclic carbonates

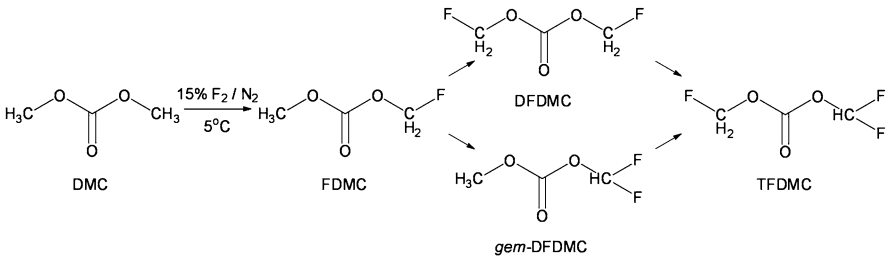

Scheme 2.6 Preparation of fluorinated dimethyl carbonates

The relative permittivity and viscosity of FDMC were higher than those of DMC (Fig. 2.5a, b) [34–36]. The electrolytic conductivities of 1 moldm^{-3} lithium salts ($LiClO_4$, $LiBF_4$, $LiPF_6$) in FDMC or EC-FDMC at 25 °C were always lower than those in DMC or EC-DMC counterparts due to their high viscosities (Fig. 2.5c). FDMC showed a higher oxidation potential on Pt than DMC (Fig. 2.5d). The lithium cycling efficiency in 1 moldm^{-3} $LiPF_6$/FDMC and EC-FDMC equimolar solution was higher than that in EC-DMC counterpart (Fig. 2.5e). The cycling efficiency of a Li/$LiCoO_2$ cell containing 1 moldm^{-3} $LiPF_6$/EC-FDMC equimolar electrolyte was higher than 95 % and the discharge capacity retentions of the cells were also higher than those of EC-DMC counterpart [36].

The relative permittivity and viscosity increased in the order; DMC < FDMC < TFDMC < DFDMC (Fig. 2.5a, b) [37, 38]. The electrolytic conductivities of 1 moldm^{-3} $LiPF_6$ solutions were in the order; DFDMC < FDMC < DMC over the concentration range from 0.5 to 2.0 moldm^{-3} (Fig. 2.5c). The electrolytic conductivities of 1 moldm^{-3} $LiPF_6$ in EC equimolar solutions were in the order; DFDMC < FDMC < DMC influenced by their viscosities. The oxidation potentials of these fluorinated DMC on Pt was in the order; DMC < FDMC < DFDMC as expected from HOMO energies (Fig. 2.5d). In general, the oxidation potential of the fluorinated organic solvents tends to increase with the increase in the number of fluorine atoms introduced to the solvent molecule; however, TFDMC with very poor solubility of $LiPF_6$ was excluded from the experiments. DFDMC and EC-DFDMC equimolar binary solutions containing 1 moldm^{-3} $LiPF_6$ showed higher lithium cycling efficiencies; especially, EC-DFDMC solution exhibited more than 80 % at the 100th cycle (Fig. 2.5e).

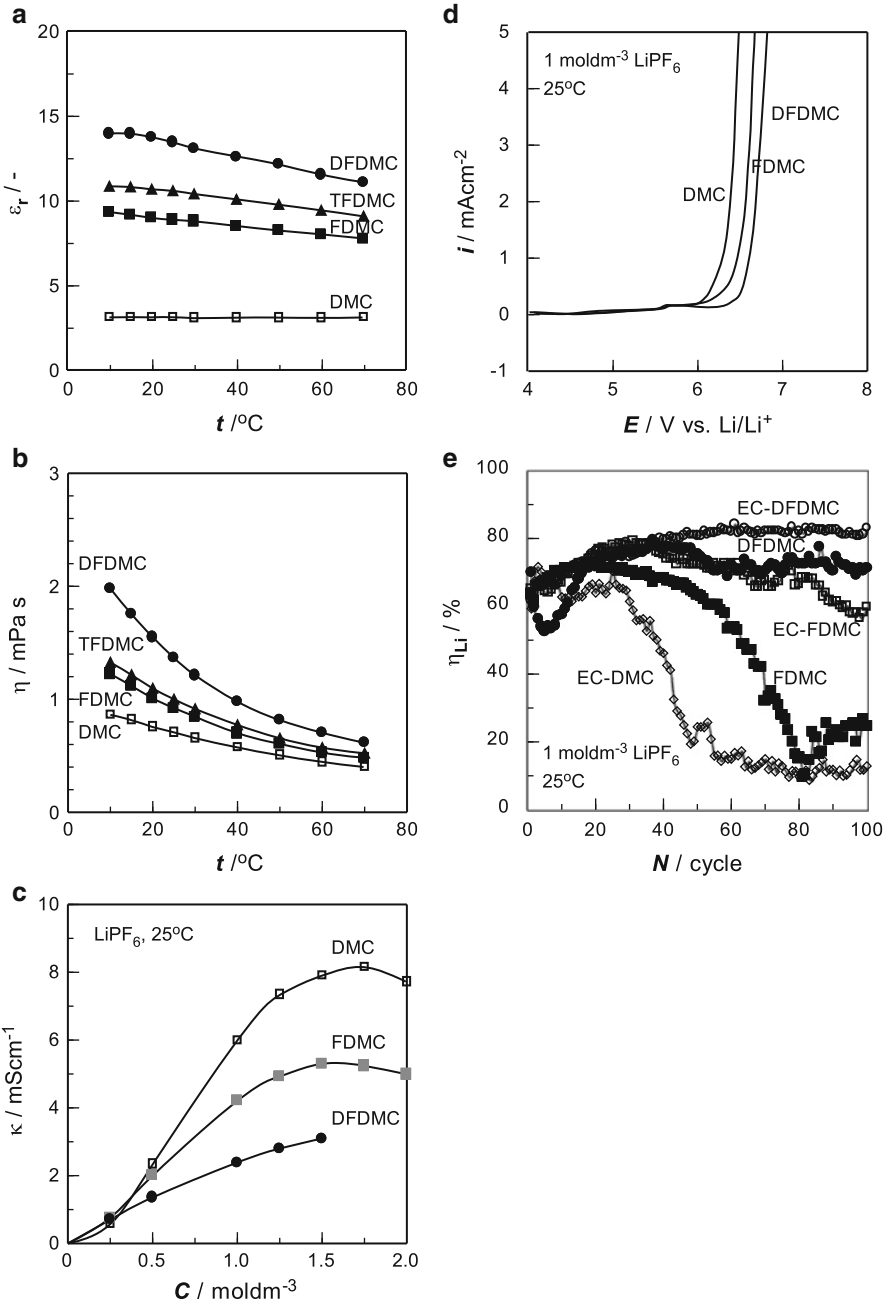

Fig 2.5 Properties of dimethyl carbonates and its fluorinated derivatives. (**a**) relative permittivity (**b**) viscosity (**c**) electrolytic conductivity (**d**) oxidation potential (**e**) lithium cycling efficiency

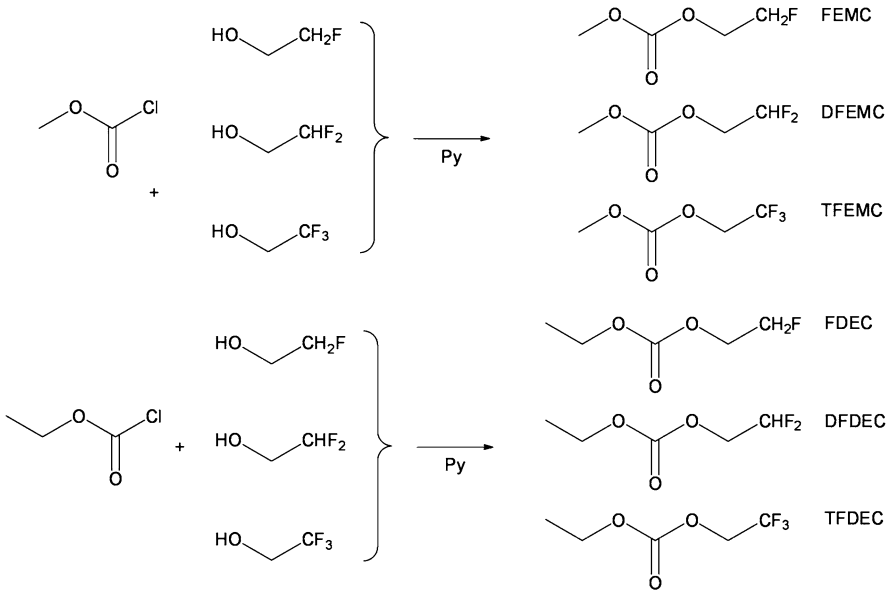

Scheme 2.7 Preparation of fluorinated ethyl methyl carbonates and diethyl carbonates

As partially fluorinated EMC and DEC derivatives, 2-fluoroethyl methyl carbonate (FEMC), 2,2-difluoroethyl methyl carbonate (DFEMC), methyl 2,2,2-trifluoroethyl carbonate (TFEMC), ethyl 2-fluoroethyl carbonate (FDEC), ethyl 2,2-difluoroethyl carbonate (DFDEC), and ethyl 2,2,2-trifluoroethyl carbonate (TFDEC) in Scheme 2.7 were examined [4, 5, 39, 40]. These fluorinated EMC and DEC derivatives were synthesized by use of the corresponding three kinds of fluoroethanols and methyl chlorocarbonate or ethyl chlorocarbonate in the presence of pyridine.

The relative permittivities and viscosities of these fluorinated linear carbonates were higher than those of EMC and DEC, respectively. The relative permittivity and viscosity were in the order; DEC < EMC << FDEC, DFDEC < TFEMC, TFDEC, FEMC << DFEMC and EMC < DEC < TFEMC < TFDEC << FEMC, FDEC, DFDEC << DFEMC, respectively, over the temperature range from 10 to 70 °C (Figs. 2.6a, b and 2.7a, b) [4]. The electrolytic conductivities of 1 moldm^{-3} $LiPF_6$ solutions at 25 °C were in the order; TFDEC < TFEMC, DFDEC < FDEC, DFEMC, DEC < FEMC < EMC (Figs. 2.6c and 2.7c) [4]. The electrolytic conductivities of lithium salts ($LiClO_4$, $LiBF_4$, $LiPF_6$) in FEMC or FDEC were not always lower than those of EMC or DEC counterparts, respectively, depending on the kind of lithium salts, its concentration, and temperature. For example, $LiPF_6$/FEMC or FDEC solutions showed higher conductivities than EMC or DEC counterparts at 25 °C and 0.5 moldm^{-3}, and 1 moldm^{-3} $LiPF_6$/FDEC showed higher conductivity than DEC counterpart above 40 °C [40, 41], which indicates the high degree of dissociation of $LiPF_6$ due to the increase of relative permittivity in spite of the increase of viscosity.

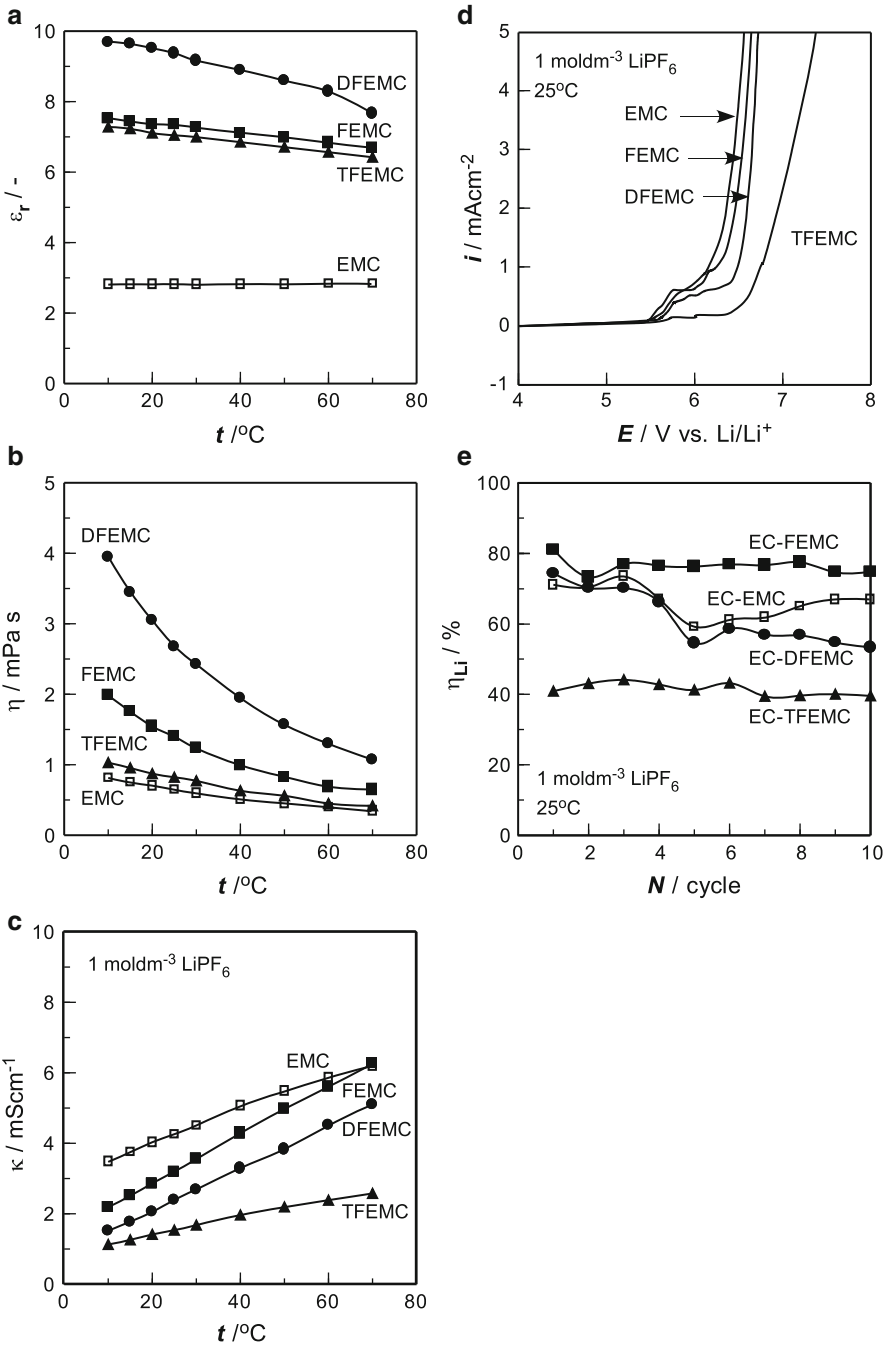

Fig. 2.6 Properties of ethyl methyl carbonates and its fluorinated derivatives. (**a**) relative permittivity (**b**) viscosity (**c**) electrolytic conductivity (**d**) oxidation potential (**e**) lithium cycling efficiency

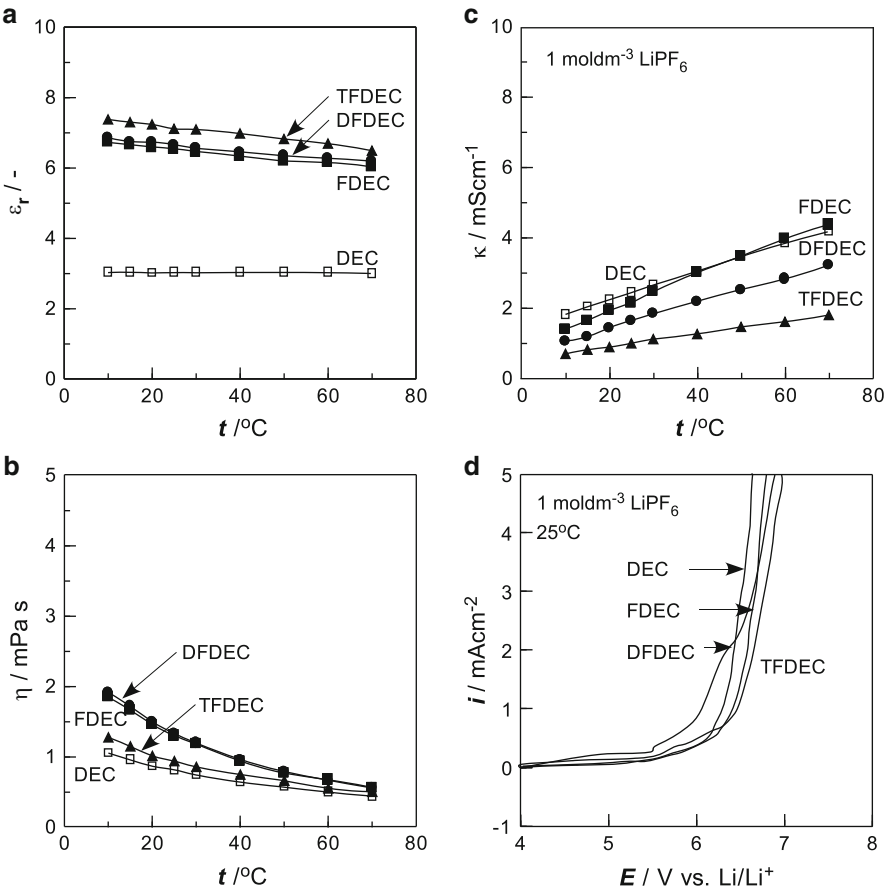

Fig. 2.7 Properties of diethyl carbonates and its fluorinated derivatives. (**a**) relative permittivity (**b**) viscosity (**c**) electrolytic conductivity (**d**) oxidation potential

The electrolytic conductivities of 1 moldm^{-3} $LiPF_6$/EC-FEMC or EC-FDEC equimolar solutions at 25 °C were always lower than those in EC-EMC or EC-DEC counterparts due to their high viscosities. The oxidation potentials on Pt were in the order; EMC, DEC < FEMC, FDEC < DFEMC, DFDEC < TFEMC, TFDEC with increasing the number of fluorine atom (Figs. 2.6d and 2.7d) [4, 5]. The lithium cycling efficiencies in 1 moldm^{-3} $LiPF_6$/EC-FEMC and EC-FDEC equimolar solutions were higher than those in EC-EMC and EC-DEC counterparts, whereas those in EC-DFEMC and EC-TFEMC equimolar electrolytes were lower (Fig. 2.6e). The cycling efficiencies and discharge capacity retentions of a Li/$LiCoO_2$ cell containing 1 moldm^{-3} $LiPF_6$/EC-FEMC and EC-FDEC equimolar electrolytes were higher than those of EC-EMC and EC-DEC counterparts. On the other hand, the cycling

efficiency and discharge capacity retention of a graphite/$LiCoO_2$ cell containing 1 moldm^{-3} $LiPF_6$/EC-FEMC equimolar electrolyte was lower than those of EC-EMC counterpart [4].

Methyl propyl carbonate (MPC) is a structural isomer of DEC. Physical and electrochemical properties of four kinds of partially fluorinated MPC derivatives, 3-fluoropropyl methyl carbonate (FPMC), methyl 3,3,3-trifluoropropyl carbonate (TrFPMC), methyl 2,2,3,3-tetrafluoropropyl carbonate (TeFPMC), and methyl 2,2,3,3,3-pentafluoropropyl carbonate (PeFPMC) in Scheme 2.8 were examined [42].

The relative permittivities and viscosities of these fluorinated MPC derivatives except PeFPMC with five fluorine atoms increased with increasing the number of fluorine atom. The relative permittivity and viscosity of FPMC were higher than those of MPC and lower than those of other fluorinated MPC derivatives. Donor numbers (DN) of these fluorinated solvents, which were estimated by ^{29}Si NMR chemical shifts of triphenylsilanol [42], decreased with increasing the number of fluorine atom except PeFPMC. The electrolytic conductivities of 1 moldm^{-3} $LiPF_6$ in the fluorinated MPC derivatives at 25 °C were in the order; MPC = FPMC > TrPMC > TePMC = MPC. However, the electrolytic conductivity of 1 moldm^{-3} $LiPF_6$/FPMC became higher than that of MPC counterpart above 25 °C. The oxidation potentials of the fluorinated MPC derivatives on Pt increased with increasing the number of fluorine atom. The lithium cycling efficiency in 1 moldm^{-3} $LiPF_6$/PC-FPMC equimolar solution was higher than those in PC and PC-MPC counterparts. In addition, the discharge capacity retention of a Li/$LiCoO_2$ cell containing 1 moldm^{-3} $LiPF_6$/PC-FPMC equimolar electrolyte was higher than those of PC and PC-MPC counterparts.

Electrochemical properties of many ternary and quaternary electrolyte formulations based upon a partially fluorinated carbonate solvent selected from methyl 2,2,2-trifluoroethyl carbonate (TFEMC), ethyl 2,2,2-trifluoroethyl carbonate (TFDEC), propyl 2,2,2-trifluoroethyl carbonate (TFEPC), 2,2,2,2′,2′,2′-hexafluoro-i-propyl methyl carbonate, ethyl 2,2,2,2′,2′,2′-hexafluoro-*i*-propyl carbonate, and bis(2,2,2-trifluoroethyl) carbonate in Scheme 2.9 were examined in detail [43]. A number of electrolyte formulations containing a partially fluorinated aliphatic carbonate showed excellent reversibility, with most of the formulations resulting in higher reversible capacity after the formation cycles compared to the baseline electrolyte formulations in experimental Li/MCMB carbon half cells. Good low temperature performance was observed in many cases, with TFDEC- and TFEPC-containing cells performing the best. The electrodes in contact with the novel electrolytes generally displayed low film resistance and low charge transfer resistance, especially at low temperature. In addition, when Tafel polarization measurements were performed, the novel electrolytes resulted in the least amount of electrode polarization and the highest limiting current densities implying facile lithium intercalation/de-intercalation kinetics. Similar results were reported on bis(2,2,3,3-tetrafluoropropyl) carbonate and bis(2,2,3,3,3-pentafluoropropyl) carbonate in Scheme 2.9 [31].

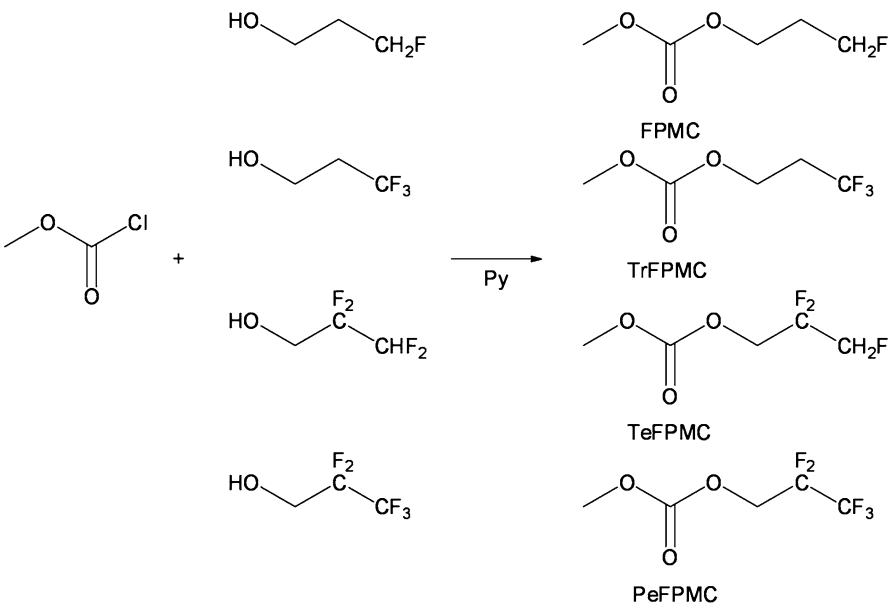

Scheme 2.8 Preparation of fluorinated methyl propyl carbonates

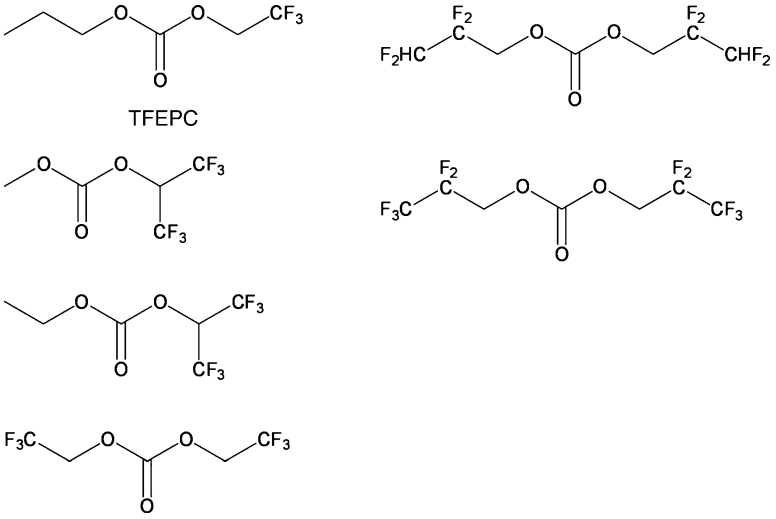

Scheme 2.9 Other fluorinated linear carbonates

2.2.6 *Fluorinated Monoethers*

The addition effect of the hydrofluoroethers such as $CF_3CF_2CH_2OCH_3$, $(CF_3)_2CHCF_2OCH_3$, $HCF_2CF_2CH_2OCHF_2$, $CF_3CHFCF_2OCH_2CH_3$, and $CHClFCF_2OCH_2CF_3$ in Scheme 2.10 to EC-DEC or EC-DEC-PC was investigated using graphite electrodes [12, 32]. The charge capacities higher than in EC/DEC were observed in these electrolytes when the reduction potentials of the fluoroethers are slightly higher than that of EC. The reduction potentials and irreversible capacities decreased with increasing LUMO energies of the fluoroethers. 1,1,2,2-Tetrafluoro-3-(1,1,2,2-tetrafluoroethoxy)-propane (TFTFEP) mixed with FEC was used for high voltage application. A Li/$LiCoO_2$ cell containing 1 moldm^{-3} $LiPF_6$/FEC-TFTFEP (1:1 in volume) exhibited high and stable discharge capacity in 30 cycles even with a high upper cutoff voltage of 4.5 V when compared with a cell containing 1 moldm^{-3} $LiPF_6$/EC-DMC (1:1 in volume). This electrolyte provided lower resistant SEI at the cathode before and after cycles [44].

Use of nonflammable hydrofluoroethers such as methyl nanofluorobutyl ether (MFE) and ethyl nanofluorobutyl ether (EFE) in Scheme 2.10 was studied in terms of the flammability, electrolytic conductivity, and charge–discharge cell performances of a graphite/$LiCoO_2$ and an amorphous carbon/$LiMn_2O_4$ cylindrical cells [45–47]. These fluorinated ethers have no flash point and are nonviscous; however, their low polarity and permittivity make difficult to dissolve lithium salts. By mixing appropriate amounts of MFE with linear carbonate co-solvents, the mixed solution showed no flash point. MFE-EMC (8:2 in volume) solution containing 0.94 moldm^{-3} $LiN(SO_2CF_3)_2$ (LiTFSA) showed a maximum conductivity of 0.97 mScm^{-1}. However, less than 0.2 moldm^{-3} $LiBF_4$ and $LiPF_6$ were dissolved in this mixed solvent. A graphite/$LiCoO_2$ cylindrical cell assembled with 1 moldm^{-3} $LiN(SO_2C_2F_5)_2$ (LiBETI)/MFE-EMC (8:2 in volume) discharged the designed capacity (1400 mAh) at a 0.1 C rate and sustained 80 % of their initial capacity up to 50 cycles. No thermal runaway was detected and cell surface temperature increased very slowly in the nailing test.

EFE was also tested as a co-solvent of nonflammable electrolyte for lithium ion batteries [48]. A typical composition satisfying both nonflammability and the rechargeability of a graphite electrode was 1 moldm^{-3} $LiPF_6$/EFE-DEC-EC (50:48:2 in volume), whose electrolytic conductivity is 1.7 mScm^{-1} at 25 °C. High reversible capacity was obtained for the graphite negative electrode but less rechargeability of the metal oxide positive electrode ($LiCr_{0.1}Mn_{1.9}O_4$) was observed in this EFE-based electrolyte, which was improved by the SEI modification by the addition of a small amount of biphenyl.

Another nonflammable hydrofluoroethers such as 2-trifluoromethyl-3-methoxyperfluoropentane (TMMP) and 2-(trifluoro-2-fluoro-3-difluoropropxy)-3-difluoro-4-fluoro-5-trifluoropentane (TPTP) in Scheme 2.10 were studied in terms of the flammability, electrolytic conductivity, and charge–discharge cell performances of a MCMB/$LiCoO_2$ cells [49, 50]. Effective nonflammability was achieved with adding 50 vol.% of TMMP or TPTP for the co-solvent of EC-DEC.

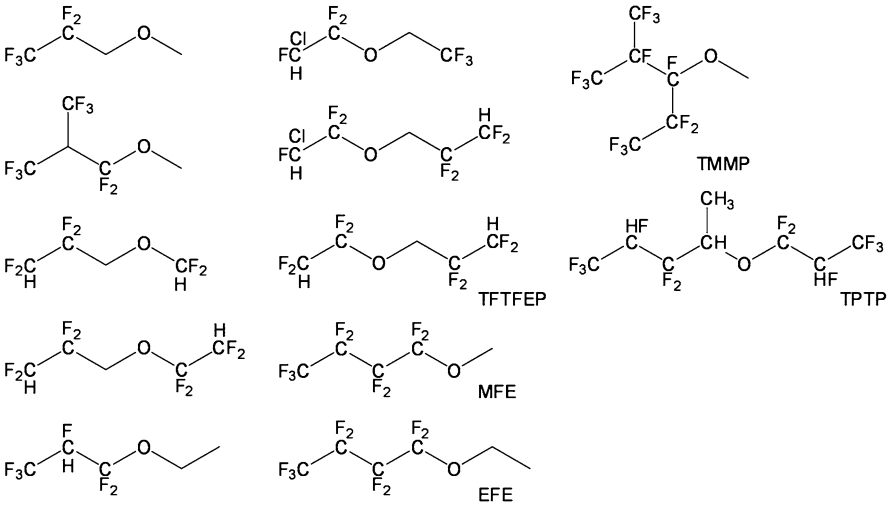

Scheme 2.10 Fluorinated monoethers

The cell containing 1 moldm^{-3} LiBETI/TMMP-EC-DEC (50:5:45 in volume) showed better discharge capacities than EC-DEC counterparts (5:95 and 50:50 in volume) as the discharge rate was increased from 0.2 to 12 C and the operation temperature was decreased from 25 to −20 °C, even though the electrolytic conductivity of 1 moldm^{-3} LiBETI/TMMP-EC-DEC is much lower than those of EC-DEC counterparts. TPTP showed better miscibility with 1 moldm^{-3} $LiPF_6$ in EC-DEC than that of TMMP, because TPTP was expected to show a higher intermolecular force due to lower F/H ratio (EFE = 1.8, TPTP = 2.0, MFE = 3.0, TMMP = 4.3). Similarly, 1 moldm^{-3} $LiPF_6$/TPTP-EC-DEC (50:5:45 in volume) showed better discharge capacities than EC-DEC counterparts (5:95 and 50:50 in volume) as the discharge rate was increased from 0.2 to 12 C and the operation temperature was decreased from 25 to −20 °C. This behavior was attributed to the decrement in the activation energy for the Li^+ desolvation process due to the decrease of solvation number of Li^+ by the addition of the hydrofluoroethers. Thus, the rate capability improvements by adding TMMP or TPTP are exerted by both enhancements of the intercalation kinetics and Li^+ diffusion at the $LiCoO_2$ interface, where the hydrofluoroethers preferentially exist by their affinity with the hydrophilic $LiCoO_2$ surface [50, 51].

2.2.7 Fluorinated Diethers

In addition to fluorinated linear diethers of 1,2-dimethoxyethane (DME) [6], fluorinated cyclic diethers such as 2,2-bis(trifluoromethyl)-1,3-dioxolane, 2,2-dimethyl-4,5-difluoro-1,3-dioxolane, and 2,2-dimethyl-4,4,5,5-tetrafluoro-1,3-dioxolane having low melting points were disclosed in a patent [52].

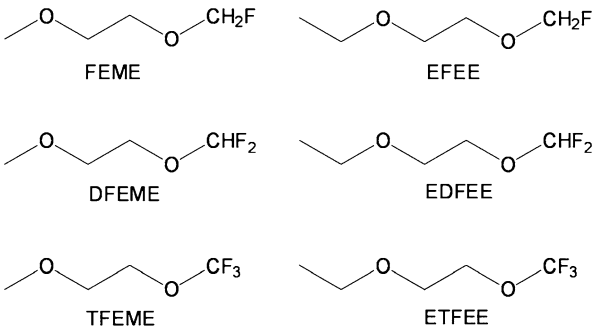

Scheme 2.11 Fluorinated dialkoxyethanes

Physical and electrochemical properties of partially fluorinated 1-ethoxy-2-methoxyethane (EME) and 1,2-diethoxyethane (DEE) derivatives such as 2-fluoroethoxymethoxyethane (FEME), 2,2-difluoroethoxymethoxyethane (DFEME), methoxy-2,2,2-trifluoroethoxyethane (TFEME), ethoxy-2-fluoroethoxyethane (EFEE), 2,2-difluoroethoxyethoxyethane (EDFEE), and ethoxy-2,2,2-trifluoroethoxyethane (ETFEE) in Scheme 2.11 were examined [53]. EME and DEE have higher relative permittivities and lower viscosities compared with those of EMC and DEC with similar molecular weights and boiling points. These fluorinated EME and DEE derivatives were obtained by reacting methoxyethanol or ethoxyethanol and each fluorinated ethyl p-toluenesulfonate synthesized with p-toluenesulfonyl chloride and each fluoroethanol. The relative permittivities and viscosities of these fluorinated EME and DEE derivatives were higher than those of EME and DEE (Figs. 2.8a, b and 2.9a, b). In addition, the relative permittivities of these fluorinated derivatives are almost independent on the number of fluorine atoms. The viscosities of TFEME and ETFEE with three fluorine atoms become smaller than those of mono- and di-fluorinated EME and DEE derivatives. The donar numbers (DNs) of the fluorinated EME and DEE derivatives decreased with increasing the number of fluorine atoms. The electrolytic conductivities of 1 moldm^{-3} $LiPF_6$ solutions decreased with increasing the number of fluorine atoms (Figs. 2.8c and 2.9c). The electrolytic conductivities of 1 moldm^{-3} $LiPF_6$/EC-equimolar binary solutions are always lower than those of EME and DEE counterparts (Figs. 2.8d and 2.9d). The oxidation potentials of the fluorinated derivatives on Pt increased with increasing the number of fluorine atoms (Figs. 2.8e and 2.9e). However, variation of the oxidative potentials among the fluorinated DEE derivatives is very small. The lithium cycling efficiencies in 1 moldm^{-3} $LiPF_6$/EC-TFEME and ETFEE solutions were higher than those in EC-EMC and EC-DEC counterparts, respectively (Figs. 2.8f and 2.9f). In general, the cycling efficiencies and discharge capacity retentions of a Li/$LiCoO_2$ cell containing 1 moldm^{-3} $LiPF_6$/EC-fluorinated EME and DEE derivative equimolar electrolytes were equivalent to those of EC-EME and EC-DEE counterparts.

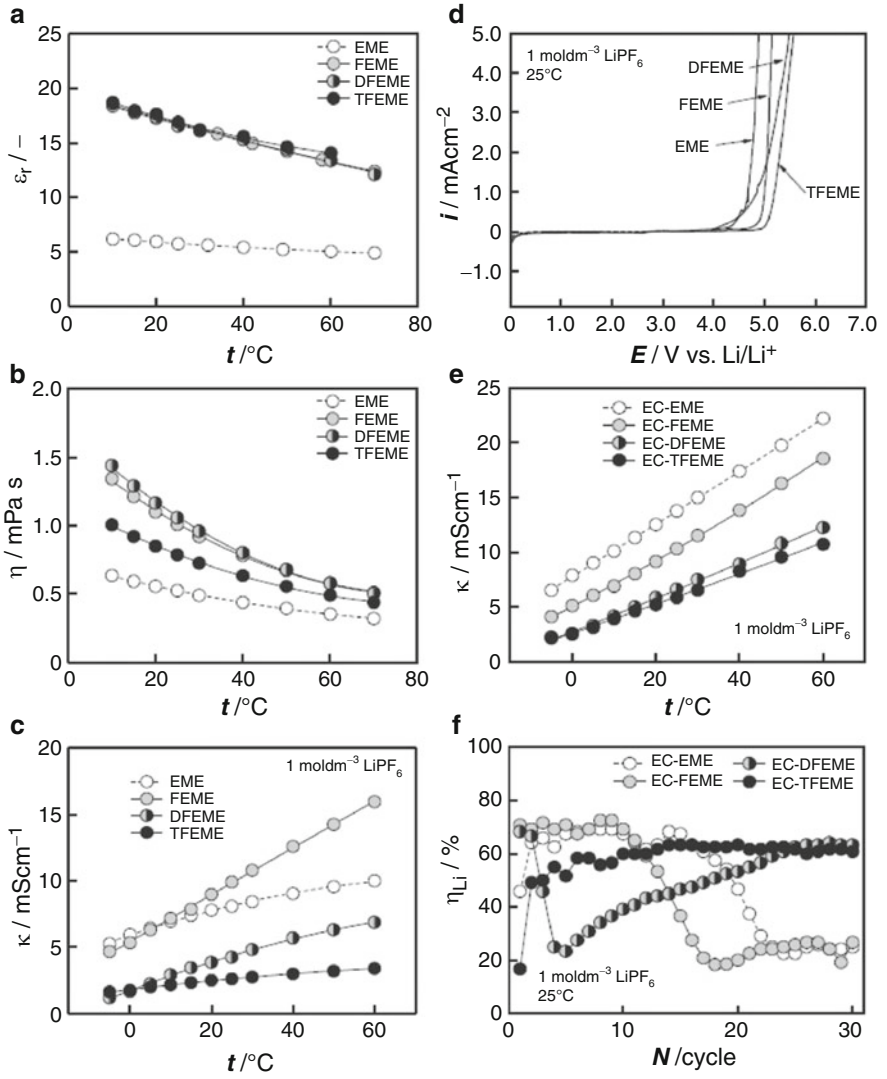

Fig. 2.8 Properties of ethoxymethoxyethane and its fluorinated derivatives. (**a**) relative permittivity (**b**) viscosity (**c**) electrolytic conductivity (**d**) oxidation potential (**e**) electrolytic conductivity (EC equimolar solution) (**f**) lithium cycling efficiency

2.2.8 Other Fluorinated Solvents

3-Methyl-2-oxazolidinone (NMO) is isostructural with EC with an N-CH_3 group substituted for one of the EC ring oxygen atoms. It is a highly polar solvent ($\varepsilon_r = 78$ at 25 °C) and was once used in primary lithium cells [54]. However, its oxidation potential on a glassy carbon is much lower than that of PC [55]. To increase its

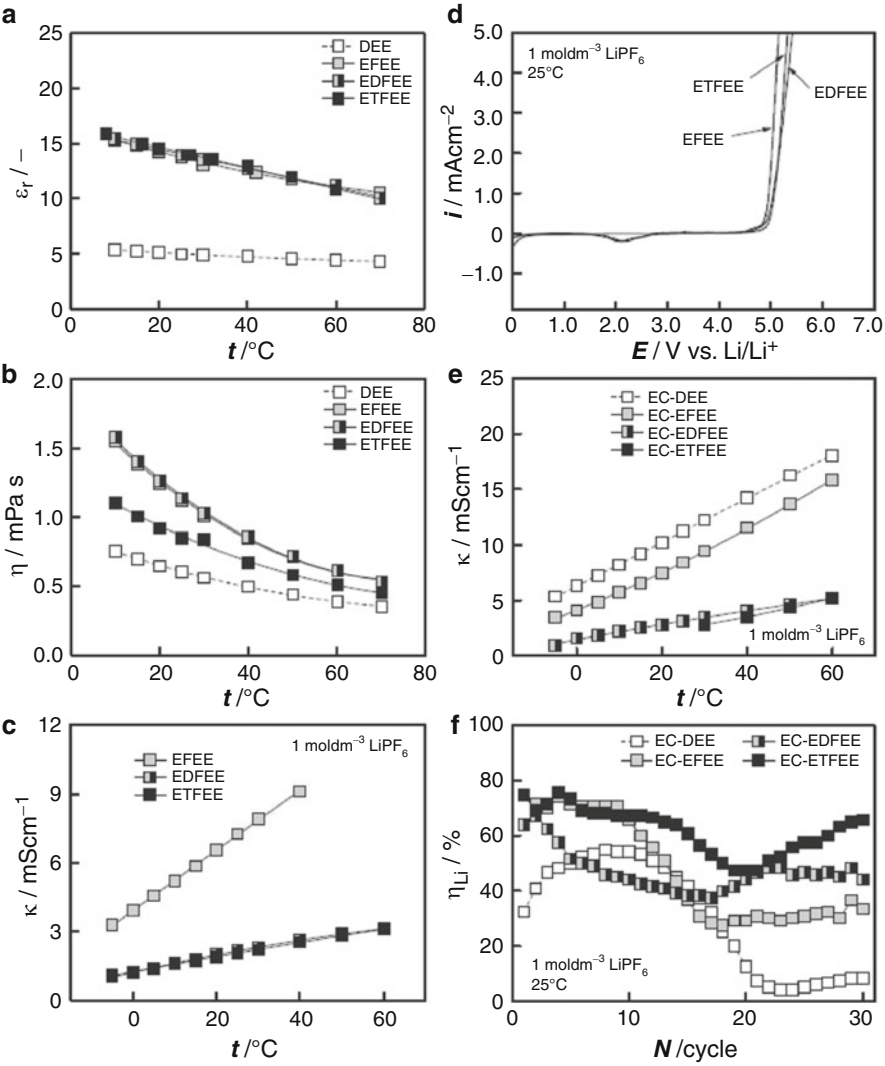

Fig. 2.9 Properties of diethoxyethane and its fluorinated derivatives. (**a**) relative permittivity (**b**) viscosity (**c**) electrolytic conductivity (**d**) oxidation potential (**e**) electrolytic conductivity (EC equimolar solution) (**f**) lithium cycling efficiency

oxidation potential, the direct fluorination of NMO was carried out, and an 3:7 isomeric mixture ($DFNMO_{mix}$) of 4,4-difluoro-3-methyl-2-oxazolidinone (4,4-DFNMO) and 4,5-difluoro-3-methyl-2-oxazolidinone (4,5-DFNMO) in Scheme 2.12 was obtained [56]. The relative permittivity of $DFNMO_{mix}$ was lower than that of NMO, although the viscosity of $DFNMO_{mix}$ was higher than that of NMO. This kind of opposite behavior was observed for fluoroacetonitrile [57].

Scheme 2.12 Fluorinated carbamates

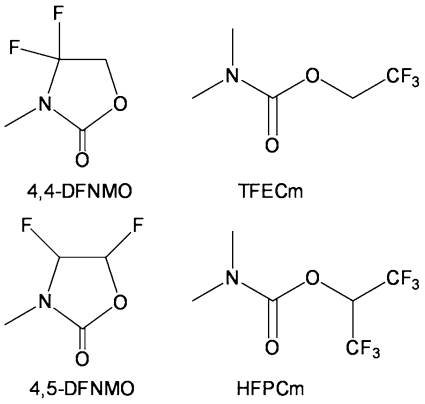

The electrolytic conductivity of 1 moldm^{-3} $LiPF_6$/$DFNMO_{mix}$ was much lower than that of NMO due to the high viscosity and low permittivity. The oxidation potential of $DFNMO_{mix}$ on Pt was increased but still lower than that of PC. The addition of $DFNMO_{mix}$ to 1 moldm^{-3} $LiPF_6$/EC-DEC equimolar binary solution suppressed discharge capacity fading in a Li/$LiCoO_2$ cell.

Partially fluorinated carbamates such as 2,2,2-trifluoroethyl *N*,*N*-dimethyl carbamate (TFECm) and hexafluoro-i-propyl *N*,*N*-dimethyl carbamate (HFPCm) in Scheme 2.12 were also applied to lithium cells, but no marked results were obtained [43].

The direct fluorination of *N*-methylpyrrolidinone (NMP) was also carried out to afford α-fluoro-*N*-methylpyrrolidinone (α-F-NMP). Its relative permittivity (70) and viscosity (3.6) were almost doubled those of NMP (32, 1.7), respectively. The electrolytic conductivity of 1 moldm^{-3} $LiPF_6$/α-F-NMP solution at 25 °C was 2.5 mScm^{-1}, less than half of that of NMP (6.1) [58].

2.2.9 Summary

Fluorinated organic solvents show very different physical and electrochemical properties. In particular, mono- or di-fluorinated organic solvents show very fairly high polarity, which generally results in the increases of relative permittivity, viscosity, and oxidation potential. Although the electrolytic conductivity of lithium salts decreases due to the increase of viscosity, the lithium cycling efficiency is always enhanced by the good SEI formation, and usually results in low capacity fading in a Li/$LiCoO_2$ cell. In addition, the nonflammability of solvents increases with increasing of the number of fluorine atoms; however, the solubility of lithium salts decreases.

The enhancement of both energy density and cell safety of rechargeable lithium(−ion) batteries is important for electric vehicle and power grid applications. Therefore, partially fluorinated organic compounds are expected as a good solvent

for rechargeable lithium(−ion) batteries. It is still necessary to study harder finding the novel fluorinated solvents giving not only high electrolytic conductivity, high oxidation potential, and nonflammability, but also good cell performances.

2.3 Boron-Containing Organic Solvents

2.3.1 Introduction

The urgent requirement for secondary batteries such as lithium-ion batteries for vehicle installation is that they be small and light. The indexes of the smallness and lightness are energy densities of per-unit volume (=V A h/dm^3) and mass (=V A h/kg). Thus, these numbers are expressed as a product of the capacity of electrodes and the operating voltage of the cell. Recently, cathodes possessing high capacity as well as high redox-potential have been developed to increase these numbers [59]. In contrast, the development of liquid electrolytes with a high oxidation potential falls far behind since organic compounds consisting of liquid electrolytes such as carbonate esters are generally being oxidized with facility (~4.3 V (Li/Li$^+$), Fig. 2.10a). Attention has thus been paid to seek or design an organic compound with a high oxidation potential as the electrolyte solvent. The organic compounds also come equipped with the following physical and electrochemical properties: high dielectric constant to dissociate the supporting electrolyte salt; high fluidity to acquire the enough ionic conductivity; low flammability to be absolutely secure; and low toxicity. During the last decade, some novel organic compounds have been proposed.

Organic sulfones exhibited high oxidation potential but low fluidity, eventually decreasing ionic conductivity (Fig. 2.10b) [60]. The sulfones also caused the abruption of carbon anodes. Nitriles such as adiponitrile also showed a high oxidation potential because the nitrile substituents in the strong electron withdrawing group resulted in high oxidation resistance (Fig. 2.10c) [61]. However the nitriles also lack enough fluidity. Fluorinated carbonate esters in which some hydrogen atoms in carbonate esters were substituted with fluorine atoms indicated a high oxidation potential due to the fluorine nature of electron withdrawing (Fig. 2.10d) [62]. The fluorine atoms substituted also created low flammability for the carbonate ester. Moreover, they maintained their intrinsic high fluidity, but were not a good solvent for supporting electrolyte salts. Synthetic complexity also remained.

When designing the electrolyte solvent and salt compounds one can consult the molecular orbital methods with some programs such as the Gaussian [63]. The molecular orbital method calculates the most stable conformation as well as the highest occupied molecular orbital (HOMO) and the lowest unoccupied molecular orbital (LUMO) levels of the compound concerned. Figure 2.11 indicates the relationship between molecular orbitals and their energy levels in a molecule. When the oxidation takes place an electron is removed from the HOMO. When the reduction occurs an electron is inserted into the LUMO. Therefore, the lower HOMO level

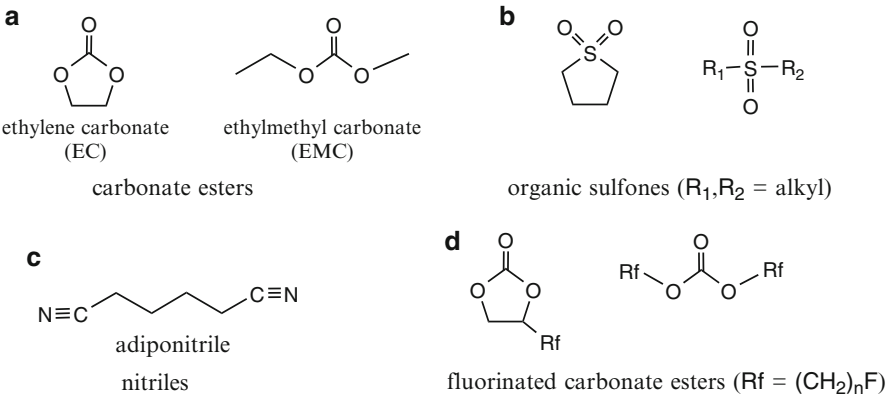

Fig. 2.10 Chemical structures of (**a**) carbonate esters, (**b**) organic sulfones, (**c**) nitriles, and (**d**) fluorinated carbonate esters

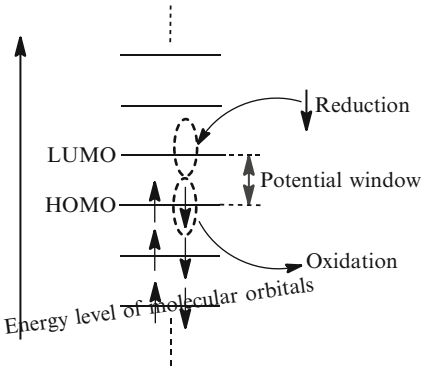

Fig. 2.11 The relationship between molecular orbitals and their energy levels. The *arrow* refers to an electron and its direction does the direction of electron spin

indicates the higher oxidation potential and the higher LUMO level does the lower reduction potential. Therefore the wider differential of HOMO-LUMO levels, i.e., the wider potential window, is preferable to the electrolyte. One can seek a compound with the molecular orbital methods in such a way before synthesizing. However, an organic compound generally has a quite narrow potential window.

2.3.2 Nature of Boron Compounds

According to some statistics, boron is an element with an abundance in the earth's crust of about 10–1,000 ppm and is thus a reasonably rich resource [64]. The output of boron compounds such as borax ($Na_2B_4O_5(OH)_4 \cdot 8H_2O$) is about one million tons a year. Therefore, it is easily supplied. Boric acid ($B(OH)_3$, Fig. 2.12, **1**) is prepared

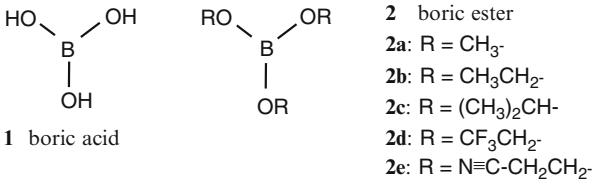

Fig. 2.12 Chemical structures of boric acid (**1**), methylborate (**2a**), ethylborate (**2b**), *iso*-propylborate (**2c**), trifluoroethylborate (**2d**), and 2-cyanoethylborate (**2e**)

from a reaction of $Na_2B_4O_7 \cdot 10H_2O$ with H_2SO_4. One use of boric acid is as an absorbent of neutrons at a nuclear power plant. Natural boron consists of 19.9 % ^{10}B and 80.1 % ^{11}B, where only ^{10}B absorbs neutrons. Boric acid is also used in mouse poison pellets and as an eyedrop ingredient. This means that boric acid has toxicity. However, the LD_{50} for mammals of boric acid is 5.14 g/kg while that of NaCl is 3.75 g/kg [65]. Thus, the toxicity is quite moderate. A further advantage of boron-containing compounds is their ability to reduce weight because the atomic weight of boron is only 10.8.

Both ^{10}B and ^{11}B nuclei are NMR (nuclear magnetic resonance) active. Because of the high content, high resonant frequency, and lower nuclear quadrupole moment, the NMR spectroscopy of the ^{11}B nucleus is generally observed [66]. Trivalent or quadrivalent boron can be comfortably differentiated by means of a chemical shift of ^{11}B: trivalent > 0 ppm > quadrivalent (*d* value). Thus, the electron density on the boron atom can also estimated with the chemical shift. In this way, ^{11}B NMR spectroscopy is a potent tool for structural analyses of boron-containing materials.

2.3.3 Boric Esters

Boric esters ($B(OR)_3$, Fig. 2.12, **2**) are esters prepared from a condensation of boric acid (**1**) and corresponding alcohols as in the case of carbonate esters that form carbonic acid (H_2CO_3) and alcohols (Fig. 2.13a, b). Physical and electrochemical properties of boric esters are tunable due to substituents R in **2**. Methyl, ethyl, *iso*-propyl, and trifluoroethylborates (**2a**, **2b**, **2c**, and **2d**) are transparent liquids, whereas a boric ester possessing nitrile substituent (R = $-CH_2CH_2CN$, **2e**) is solid at room temperature. Thus, **2a**, **2b**, **2c**, and **2d** are highly fluid; **2d** has nonflammability as well. Any lithium salts poorly dissolve in these boric esters. In contrast, **2e** is a good solvent of lithium salts. Once the salt dissolves, the solution in **2e** becomes a liquid. The electrolytes of lithium salts in **2e** exhibit the oxidation potential of over 6.0 V [Pt/(Li/Li^+)] [67]. When a boric ester was blended with the other boric ester, the substituent exchange reaction (ester exchange reaction) spontaneously took place to give mixed boric esters (Fig. 2.14). The reaction was in an equilibrium that largely shifted to right. The mixed boric esters obtained acquired all the preferable

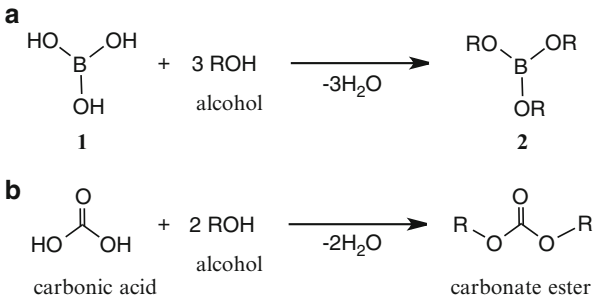

Fig. 2.13 Preparation of (**a**) boric ester (**2**) from boric acid (**1**) and alcohol and (**b**) carbonate ester from carbonic acid and alcohol

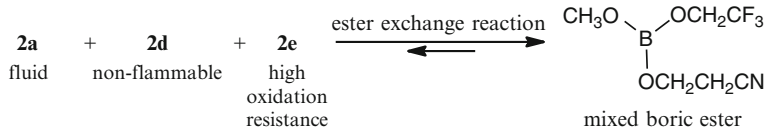

Fig. 2.14 Substituent exchange reaction (ester exchange reaction) among **2a**, **2d**, and **2e** giving the mixed boric ester

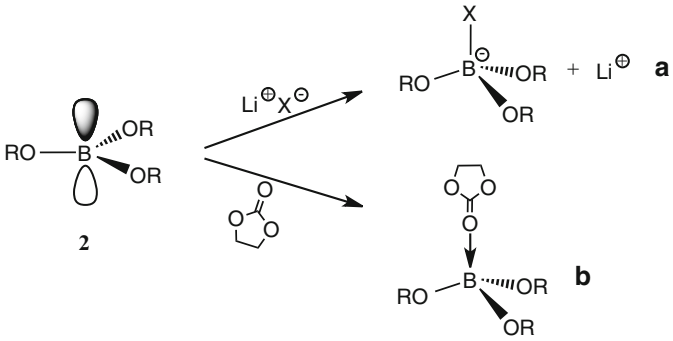

Fig. 2.15 Intermolecular interaction of boric ester (**a**) with lithium salt and (**b**) with carbonyl compound based on Lewis acid-base neutralization

properties that parent boric esters intrinsically bear. In particular, the mixed boric esters showed ionic conductivity of over 10^{-3} S cm^{-1} at room temperature and an oxidation potential of 5.5 V [Pt/(Li/Li^+)] [67]. A coin cell consisting of the $LiNi_{0.5}Mn_{1.5}O_4$ cathode, Li metal anode, and electrolyte of 0.7 mol/kg $LiBF_4$ in **2c** and **2e** (1/2 mol) exhibited stable charge–discharge cycles.

The trivalent boron compounds, including boric esters, are Lewis acids because of the vacant *p*-orbital on the boron atom capable of accepting an electron pair (Fig. 2.15). When the substituents bear electron-withdrawing groups such as nitrile,

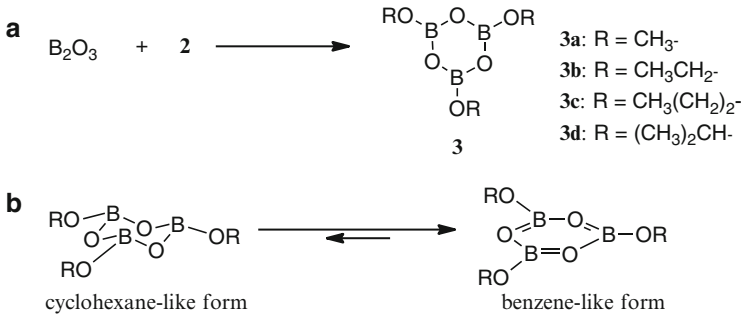

Fig. 2.16 (**a**) Preparation of trialkokyboroxine (**3**) from boric anhydride and boric ester (**2**) and (**b**) the most stable structure of trialkoxyboroxine

the acidity of the Lewis acid increases and then accelerates the dissociation of salts (Fig. 2.15a). In particular, lithium salts are soluble in **2e** but not in **2a**–**2d**. The interaction of boric ester with an anion also causes the lithium transference number to rise (t^{Li+} = Li^+ conductivity/ionic conductivity). In fact, the t^{Li+} is about 0.6 for the boric ester electrolyte, while that for the carbonate ester is about 0.3 [67]. This indicates that the boric esters are acting as an anion receptor. Moreover, a boric ester can bind another Lewis base such as carbonyl compound to decrease the electron density in the carbonyl compound to give it a high oxidation potential (Fig. 2.15b). For example, a blended electrolyte of 1.0 mol/kg $LiBF_4$ in **2e** and carbonate esters (1/1 mol) exhibited the oxidation potential of over 5.2 V [Pt/(Li/Li^+)] while the decomposition of absolute carbonate ester electrolyte commenced at 4.3 V.

2.3.4 Cyclic Boric Esters

Boric anhydride (boric oxide, B_2O_3) reacts with boric ester to give a cyclic boric ester of trialkoxyboroxine (**3**, Fig. 2.16a). The six-membered ring of the trialkoxyboroxine takes a planar benzenelike structure rather than the cyclohexanelike form where π-electrons of oxygen atoms are delocalized on the six-membered ring including vacant *p*-orbitals of three boron atoms to give a planar structure (Fig. 2.16b). When a small amount of **3** (0.2 wt%) is added to the carbonate ester electrolyte, the anodic reaction is stabilized [68]. The electric current at 5.0 V (vs. Li/Li^+) derived from decomposition of the carbonate ester largely decreased in the presence of **3d** when $LiMn_2O_4$, as a high-potential cathode, was utilized. A unique substituent effect was also observed: the trialkoxyboroxine (**3d**) possessing *isopropyl* moieties was most effective among the trialkokyboroxines (**3a**–**3d**). Presumably only **3d** has the preferable oxidation potential and thus is decomposed at around 4.0 V, resulting in formation of a solid electrolyte interface (SEI) containing boron atoms at the surface of the cathode to prevent further decomposition of the electrolyte.

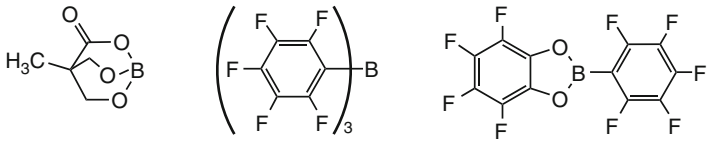

4
triol borate

5
TPFPB

6
PFPBDB

Fig. 2.17 Anion receptor molecules

Another cyclic boric ester of triol borate (**4**, Fig. 2.17) has a highly strained structure owing to the tricyclic skeleton which causes a strong Lewis acid nature [69]. **4** binds counter anions of LiF, Li_2O, and Li_2O_2 to dissociate them and to dissolve them into organic solvents. In addition to **3** and **4,** anion receptor molecules in battery electrolytes have recently received attention. As described above the required functions for an anion receptor are (a) to dissociate an insoluble salt into the cation and anion, (b) to dissolve the salt into a solvent, (c) to increase the lithium transference number (t^{Li+}) as the result of immobilizing anions, and (d) to interact with the solvent molecule to withdraw the electrons on the molecule to prevent the facile oxidation of it. Tris-(pentafluorophenyl)borane (TPFPB, **5**, Fig. 2.17) also functions as an anion receptor and combines the required functions above [70]. **5** also stabilizes the charge–discharge behavior when the electrolyte containing **5** constitutes a battery. 2-(2,3,4,5,6-pentafluorophenyl)-4,5,6,7-tetrafluoro-1,3,2-benzodioxaborole (PFPBDB, **6**, Fig. 2.17) also acts as an anion receptor [71]. **6** exhibits the reversible redox-potential at 4.43 V and is expected to behave as a redox shuttle molecule in the electrolyte. The redox shuttle molecule protects the electrodes from their overcharge with own redox-reaction.

2.3.5 Other Boron Compounds

Lithium tetrafluoroborate ($LiBF_4$) is thermally stable and is not extremely moisture sensitive when compared with lithium hexafluorophosphate ($LiPF_6$). $LiPF_6$ easily reacts with H_2O to exhaust HF and decomposes at 80 °C. However, the ionic conductivity of the $LiPF_6$ electrolyte is superior to that of the $LiBF_4$ electrolyte due to the difference in the degree of dissociation. Novel supporting salt molecules therefore are designed to be thermally stable, moisture insensitive, and have a high dissociation. Orthoborates in which the central boron atom has four B–O bonds are thermostable compounds and thus are suitable for anions of lithium salts. Although lithium bis(oxalate)borate (LiBOB, **7**, Fig. 2.18) initially commanded attention as a lithium salt and was well described in the literature [72], recently it has been viewed less as a support salt and more as an additive because of its low solubility in organic solvents, low fluidity in solution, and difficulty in purifying [73]. **7** stabilizes the cathodic reaction at the surface of the carbon anodes.

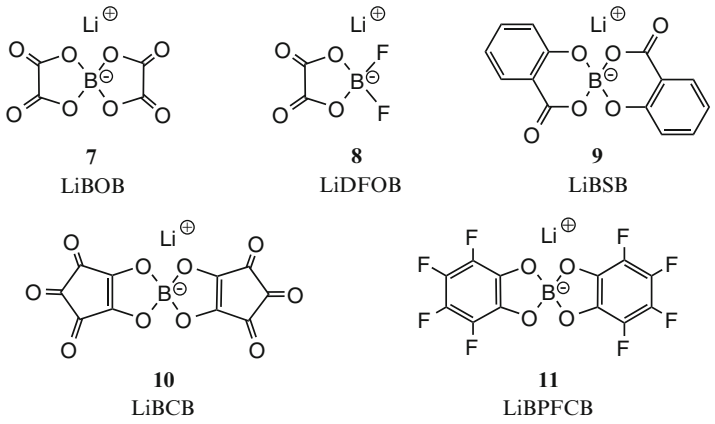

Fig. 2.18 Orthoborate lithium salt molecules

Lithium difluoro(oxalato)borate (LiDFOB, **8**, Fig. 2.18) also shows the same effect as the additive for an electrolyte [74]. Lithium bis[salicylato(2-)]-borate (LiBSB, **9**) [75], lithium bis[croconate]-borate (LiBCB, **10**) [76], and lithium bis[1,2-tetrafluorobenzenediolato(2-)-O,O′] borate (LiBPFCB, **11**) [77] have also been proposed as novel orthoborate lithium salts (Fig. 2.18).

2.3.6 Summary

Boron is a fascinating atom when designing the novel functional solvent, additive, or supporting salt molecules because of its intrinsic electronic structure, giving rise to unique physical and electrochemical properties for boron-containing molecules. The properties differ quite a lot from those of molecules involving carbon, nitrogen, and oxygen atoms even if B, C, N, and O share similar atomic weights. Therefore, the boron-containing molecules may give an initial clue to novel functions for battery materials.

2.4 Phosphorous-Containing Organic Solvents

2.4.1 Introduction

Lithium-ion batteries (LIBs) have been developed as advanced electric power sources for wide variety of portable electronics such as cellular phones, laptop comports, and camcorders. Larger-size LIBs are now considered fit to power systems such as electric vehicles (EV) and energy storage systems (ESS) due to their merits

Table 2.5 Classification of nonflammable electrolytes for lithium-ion batteries

Category	Composition	Example	Characteristics
Organic electrolyte solutions (with nonflammable components)	Nonflammable components as co-solvents or additives	Fluorinated esters Organic phosphorous compounds	High ionic conductivity; trade-off between nonflammability and electrode performances
Polymeric solid electrolytes	Polymer complexes with lithium salts (LiX)	LiX/Poly(ethylene oxide) (PEO) LiX/PEO-grafted polymer	Low ionic conductivity at lower temperature; low Li^+ transport number
Polymeric gel electrolytes	Polymer complexes swollen with organic solutions	LiX/alkylcarbonate/PEO with nonflammable component	High ionic conductivity; trade-off between nonflammability and electrode performances
Ionic liquids	Ionic liquids (IL) dissolving lithium salt (LiX)	LiX/IL, IL: 1-ethyl-3methylimidazolium fluorosulfonylamide (EMIFSA)	High ionic conductivity; low rate capability of electrode performances
Inorganic solid electrolytes	Li^+-containing oxides, sulfides, glass, ceramics	Li_2S-P_2S_5 glass, $Li_{10}GeP_2S_{12}$ crystal	High ionic conductivity; high Li^+ transport number; low interfacial properties

of high-energy density, high power, and long cycle life. Much attention has been focused on the safety issue of LIBs as battery sizes have increased and they have been more widely used [78]. The organic solvent-based electrolytes presently used in LIBs are highly flammable and can cause safety problems. Different approaches have so far been adopted to establish a safer electrolyte [79]. Some of these are: a polymeric solid electrolyte generally composed of lithium salt with a polyether-based polymer [80–82], room-temperature ionic liquids (RTIL) as nonflammable solvents [83–86], flame-retardant co-solvents or additives including phosphorous-containing organic esters or fluorinated esters/ethers [87–91]. Use of inorganic solid electrolytes that conduct lithium-ion (Li^+) at an ambient temperature is another option to construct nonflammable LIBs [92, 93]. Table 2.5 shows the classification and fundamental properties of nonflammable electrolyte systems so far proposed to build safer LIBs. Unfortunately, these approaches generally meet difficulties in compatibility when assessing the basic battery performance, and reliabilty of the system. That is, the use of a safer electrolyte system tends to decrease the charge–discharge performance including the rate capability of the cell and/or the reliability of the system. Thus, composite electrolyte systems consisting of several components have so far been proposed as the practical electrolytes of LIBs: e.g.,, polymeric gels composed of nonflammable organic solvents [94], inorganic glass--ceramic electrolytes dispersed in polymeric matrices [95], ionic liquids mixed with nonflammable, and low-viscosity organic solvents [96–99].

In the present chapter, the use of a phosphorous-containing organic compound, typically alkylphosphates and related compounds, has been reviewed as a

nonflammable component in LIB electrolytes. Generally, phosphorous-containing organic compounds are well known and practically used as fire-retardant materials that suppress the flammability of organic polymers [100, 101]. In the following sections, research papers on organic electrolyte solutions containing alkylphosphates and related compounds for LIBs are reviewed first, and then successful results on the development of polymeric gel electrolytes containing alkyl phosphates are described next.

2.4.2 Alkylphosphates and Related Compounds as Flame-Retardant Additives/Co-solvents

2.4.2.1 Alkylphosphates

The use of alkylphosphates as a nonflammable component in LIB electrolytes was first proposed by Wang and colleagues [87]. They reported that trimethylphosphate (TMP) works as a flame-retardant additive or co-solvent in a mixed alkylcarbonate-based electrolyte solution. The most alkylcarbonate solvents used in conventional LIB shows good compatibility with TMP. That is, the solubility of TMP is generally high in alkylcarbonates. Figure 2.19 shows the results of qualitative evaluation for nonflammability and a self-extinguishing property of TMP-containing mixed alkyl carbonate, ethylene carbonate (EC) and diethyl carbonate (DEC) [94]. In a binary system of EC+TMP, the amount of 20 vol.% of TMP is enough to suppress the flammability. However, more than 50 vol.% of TMP is needed to keep nonflammability in the DEC+TMP binary system. These results are consistent with those reported by other research groups [87, 102–104]. As clearly shown in Fig. 2.19, the flame-retardant ability of TMP depends on the composition of the base solution. In EC+DEC (2:1 by vol), addition of TMP with 20 vol.% or higher suppresses the flammability of the electrolyte solution. In a mixed system of EC with ethyl methyl carbonate in 1:1 mass (weight) ratio (EC+EMC, 1:1), however, greater amounts of TMP are needed to suppress the flammability of the solution. The nonflammability of the electrolyte solution was more quantitatively evaluated by a self-extinguish time (SET) [103, 105]. According to the SET examination, the minimum amount of TMP suppressing the combustion was 30 % (in mass) in a mixed EC+EMC (1:1 by mass) solvent system [103].

Changes in physicochemical properties of the electrolyte solution when adding TMP have also been reported by Morimoto et al. [106]. Because the viscosity of TMP is lower than ethylene carbonate (EC) but higher than linear alkylcarbonates such as dimethyl carbonate (DMC) and DEC, the viscosity of the solution slightly increases with the addition of TMP. In Fig. 2.20, ionic conductivity of 1.0 mol dm^{-3} (M) $LiPF_6$ and $LiBF_4$ in the mixed alkyl carbonates is shown as a function of the solvent composition [106]. The conductivity of $LiPF_6$ decreases with the TMP content. This is because the viscosity of the solution increases with the TMP content. However, in the $LiBF_4$ solution, the conductivity increases with the TMP blending,

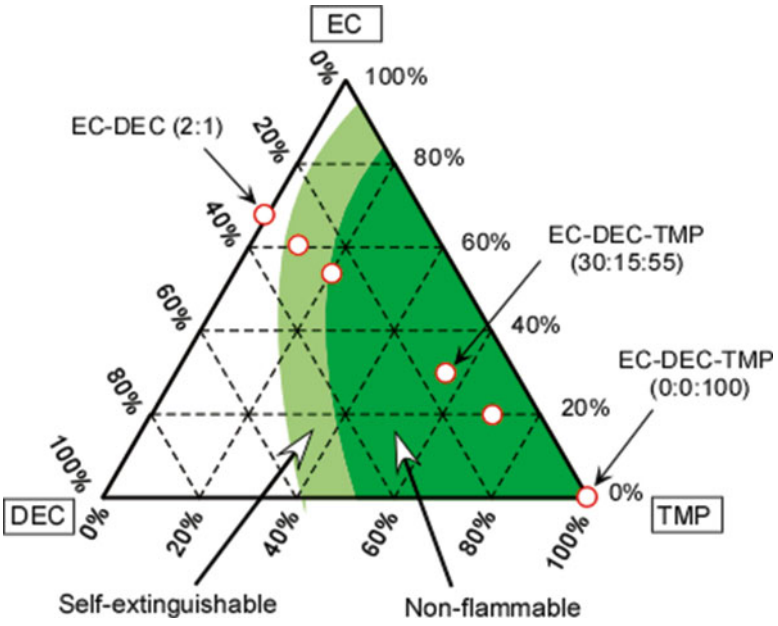

Fig. 2.19 Nonflammable and self-extinguishable compositions in $LiPF_6$/EC + DEC + TMP system

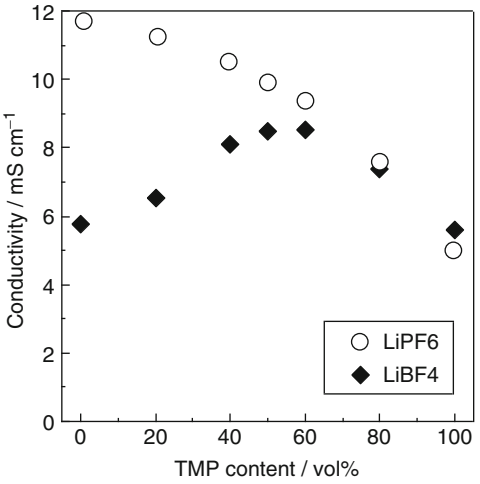

Fig. 2.20 Ionic conductivity of 1 mol dm^{-3} $LiPF_6$ and $LiBF_4$ solutions as a function of TMP content in EC + DMC (1:1 by vol.) at 25 °C

and then decreases in the solution containing higher TMP content than 80 %. Because the $LiBF_4$ salt has rather strong interaction between the cation (Li^+) and anion (BF_4^-), the degree of ionic association is rather high in the system containing a high concentration of $LiBF_4$. Thus, the increase in the conductivity with the addition of TMP up to 50 vol.% is attributable to the decrease in the ionic association caused by the introduction of the higher permittivity component TMP.

Besides nonflammability, the contribution of TMP to the thermal stability of the $LiPF_6$ solution with EC-based mixed solvents is significant [94]. It is well known that $LiPF_6$ is thermally decomposed at around 60 °C or higher. The addition of TMP with 20 vol.% or higher suppresses the decomposition of the PF_6 salt dissolved in the EC-based solvent. Possible reaction schemes have been proposed, in which radical propagation in the oxidation process of alkyl esters will be terminated by TMP [94]. The thermal decomposition of PF_6^- anion evolves an acid HF, which would assist the oxidative decomposition of alkyl esters. The component TMP would act as a scavenger of organic radicals in such oxidation processes. With respect to the fire-retardant ability of TMP, some reaction mechanisms have been proposed. One of the proposed schemes is shown in Fig. 2.21 [87], in which a phosphorous-containing radical, [P]•, evolved by partial decomposition of TMP traps the hydrogen radical, H•, being a main carrier in the oxidative chain reaction (i.e., combustion) of alkyl esters. This radical trapping by the phosphorous-containing radical can be effective for suppressing the thermal decomposition of mixed alkyl ester solutions containing the PF_6^- anion. The effects of TMP addition on the thermal stability of an LIB system are also examined in alkylcarbonate-based electrolytes in contact with fully charged graphite negative and $LiCoO_2$ positive electrodes [107]. The addition of TMP improves the thermal stability of the positive electrode side, while it does not suppress the highly exothermic reaction at the fully charged negative electrode. Thus, only a limited contribution of the flame-retardant component to the thermal stability of the LIB system is generally recognized.

The basic properties of the LIB electrode in the electrolyte solutions containing TMP have also been presented by Wang et al. [87, 103]. For the graphite negative electrode, the addition of considerable amounts of TMP causes the irreversibility of the charge--discharge process. This is because the surface process at the graphite in the electrolyte-containing TMP is different from the EC-based electrolyte [87]. As already discussed, the electrochemical Li-intercalation into graphite structure occurs through a thin layer, the so-called SEI (solid electrolyte interphase) formed at the graphite electrode [108–110]. In the EC-based electrolyte, the decomposition product of the EC component produces good SEI structure, while the electrochemical process in the solution containing TMP does not form compact SEI. The addition of an SEI-forming component, such as vinylene carbonate (VC), improves the rechargeability of the graphite electrode, as shown in Fig. 2.22 [111]. A small amount of the additive is effective in forming a film on the graphite surface. On the other hand, nongraphitizable carbon (hard carbon) shows rather good rechargeability as the negative electrode even in the solution containing TMP, because it does not need the formation of compact SEI that is required for the graphite electrode [103]. Also, common lithiated transition-metal oxides, such as $LiCoO_2$ and $LiMn_2O_4$, work well as positive electrodes in TMP-containing electrolytes [87, 106]. As shown in Fig. 2.23 [87], sufficiently high rechargeable capacity was reported for the $LiCoO_2$ positive electrode in a $LiPF_6$ solution dissolved in EC + DEC + TMP (35:35:30). Almost the same discharge capacity and cycle performance are reported for $LiMn_2O_4$ in $LiBF_4$/EC + DMC + TMP as those in the conventional electrolyte solutions without TMP [106].

1. Thermal decomposition of organic compounds

$RH \rightarrow R\cdot + H\cdot$ (1)

$H\cdot + O_2 \rightarrow HO\cdot + O\cdot$ (2)

$HO\cdot + H_2 \rightarrow H\cdot + H_2O$ (3)

$O\cdot + H_2 \rightarrow HO\cdot + H\cdot$

2. Evolution of P-containing radical from TMP

$TMP_{gas} \rightarrow [\,P\,]\cdot$

3. Trapping $H\cdot$ by radical $[\,P\,]\cdot$, suppressing the reaction of step (2)

$[\,P\,]\cdot + H\cdot \rightarrow [\,P\,]H$

$\rightarrow$Terminating the chain-reaction

Fig. 2.21 A proposed mechanism for suppressing the decomposition reaction by addition of a phosphorous-containing compound

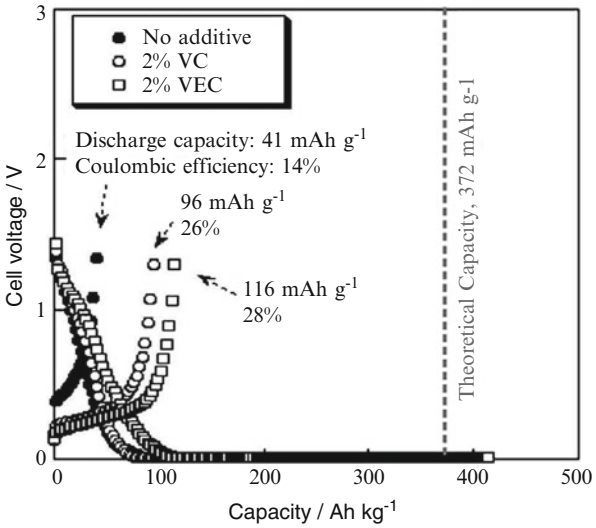

Fig. 2.22 First-cycle charge–discharge curves of Li/graphite (STG) half-cell using 1 mol dm^{-3} LiBETI/TMP electrolyte with and without additives

Other alkylphosphates have also been examined as fire-retardant additives or co-solvents in LIB electrolytes [112]. With respect to fire-retardant ability, the length of the alkyl chain in the phosphates is critical. The SET values of the solutions containing different alkylphosphates tend to be longer as the length of the alkyl chain when the systems contain the same mole fraction for different phosphates. That is, the P/C atomic ratio in the system determines SET. On the other hand, the reduction potential of alkylphosphate, which is strongly related to the SEI formation process at the graphite negative electrode, tends to shift to negative one when increasing the carbon in the alkyl group. Viscosity and dielectric properties are also influenced by the length of the alkyl chain in the phosphates.

Feng et al. [112] reported the use of dimethyl methyl phosphate (DMMP) as a nonflammable solvent. The basic properties of DMMP are between those of TMP

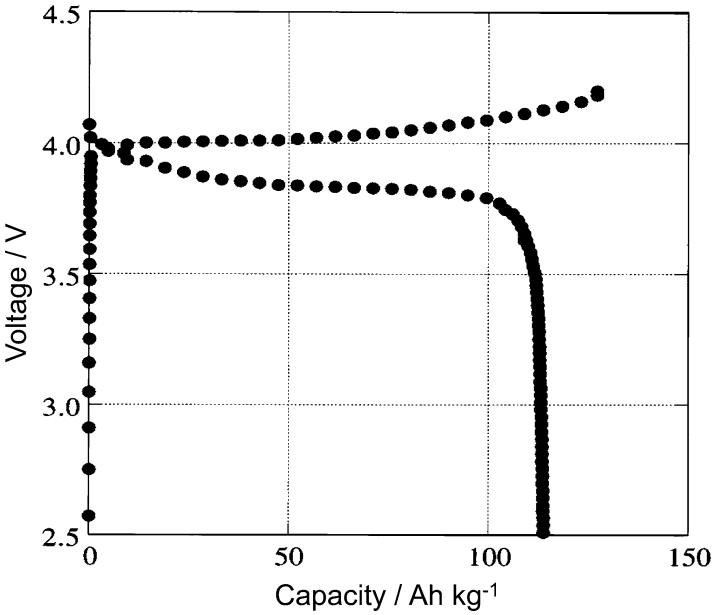

Fig. 2.23 First-cycle charge–discharge curves of Li/$LiCoO_2$ half-cell with1 mol dm^{-3} $LiPF_6$/EC + DEC + TMP (35:35:30)

and triethylphosphate (TEP). With respect to rechargeability of the graphite negative electrode, highly irreversible behavior was observed in the electrolyte ($LiClO_4$) solution using a DMMP solvent. However, reasonable cycling capacity was given by adding 10 vol.% of chloroethylene carbonate (Cl-EC) to the DMMP-based solution. Charge–discharge performances of a graphite/$LiCoO_2$ cell were also reported for the case using $LiClO_4$/DMMP + Cl-EC. Consequently, possible alkylphosphates as the co-solvents giving both sufficient nonflammability and electrochemical performances of the LIB electrolyte would be limited to such lower molecular weight compounds as TMP, TEP, and related compounds.

2.4.2.2 Fluoroalkylphosphates

Organic compounds that contain C–F bonds generally show nonflammability or fire-retardant property. Thus, fluoroalkyl-ethers and -esters have been attempted as nonflammable or flame-retardant solvents for LIB electrolytes [88, 89, 113]. Fluorinated alkylphosphates, or fluoroalkylphosphates, have higher flame-retardant properties than the corresponding alkylphosphates. Jow and co-workers [104, 114–116] reported a series of fluoroalkylphosphate, i.e., tris(2,2,2-trifluoroethyl) phosphate (TFP), bis(2,2,2-trifluoroethyl)-methyl phosphate (BMP) and (2,2,2-trifluoroethyl)-diethyl phosphate (TDP) (Fig. 2.24), as nonflammable additives or co-solvents of

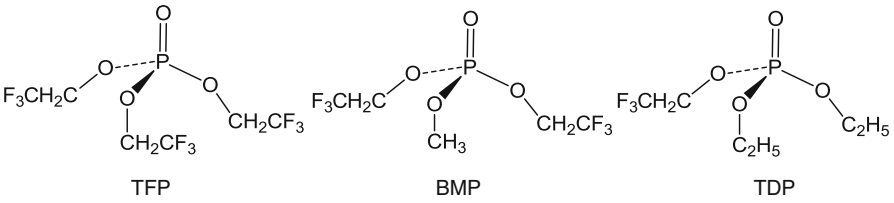

Fig. 2.24 Chemical structures of typical fluorinated alkylphosphates

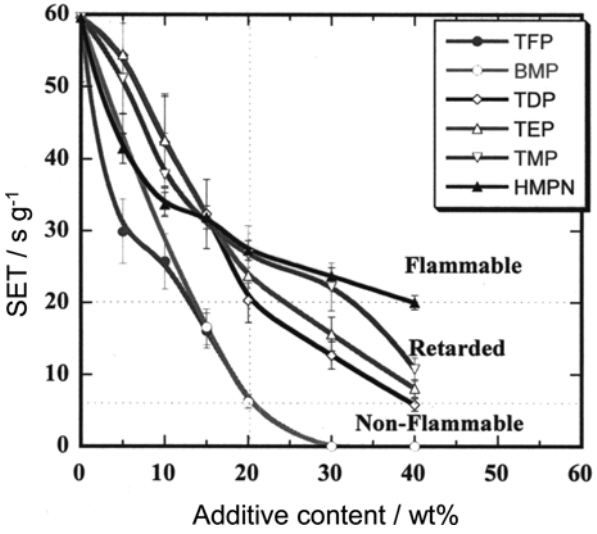

Fig. 2.25 Comparison in flammability of the electrolyte solutions with different fire-retardant additives. The base electrolyte: 1.0 mol dm^{-3} $LiPF_6$/EC + EMC (1:1)

LIBs. Among them, TFP shows high nonflammability of the electrolyte and good compatibility with the graphite-based negative electrode. Introduction of fluorine atoms to ethyl groups of TEP decreases its boiling point (bp) and viscosity. In Fig. 2.25 [115], SET values of the electrolytes containing fluoroalkylphosphates are compared with those of the solutions containing alkylphosphates. The results clearly imply that fluorinated alkylphosphates have higher nonflammability than that of TEP-containing solutions, with respect to the same amount (in mass%) of the flame-retardant components.

Because the dielectric constant (relative permittivity) of TFP is lower than that of EC (ε_r: 11 for TFP, 90 for EC), the ionic conductivity of $LiPF_6$ solution decreases when adding TFP to mixed EC + EMC solvent in the wide temperature range [115]. Also the higher concentration of TFP tends to decrease the rechargeability of the graphite-based negative electrode. Thus, about 40 % of the TFP component in the electrolyte satisfies both the nonflammability and the reversibility of the electrode in the LIB system.

2.4.2.3 Alkyl Phosphonates and Phosphites

The use of alkyl phosphonates as the co-solvent of EC-based electrolytes has been proposed by Xiang and co-workers [91, 117, 118]. Dimethyl methylphosphonate (DMMPp), a typical alkyl phosphonate, has low viscosity (η: 1.75 mPa s) and moderate permittivity (ε_r: 22.3) with a low melting point (−50 °C) and a high boiling point (180 °C). Nonflammability of DMMPp seems to be superior to or comparable with that of a corresponding alkyl phosphate [91]. That is, the addition of 10 mass% DMMPp to $LiPF_6$/EC + DEC showed a self-extinguishing property. However, sufficient nonflammability was observed for the system containing about 50 vol.% of DMMPp [117]. In those systems, a huge irreversible capacity was also observed for graphitic carbon, MCMB (mesocarbon microbead), as the negative electrode. Addition of such SEI-forming reagents as vinyl ethylene carbonate (VEC) improved the reversibility of the MCMB negative electrode (Fig. 2.26). Xiang et al. also reported that the DMMPp-based nonflammable electrolyte works for a cell consisting of $Li_4Ti_5O_{12}$ negative and $LiNi_{0.5}Mn_{1.5}O_4$ positive electrodes, in which about 3 V of the operation voltage is available [118]. The effects of DMMPp addition in the electrolyte consisting of lithium bis(oxalatoborate) (LiBOB) salt have been more recently reported [119]. Better compatibility between nonflammability and the electrode performances was obtained. Further, Wu et al. [120] reported dimethyl(2-methoxyethoxy)methylphosphonate (DMMEMPp) as a new flame-retardant solvent in a Li/$LiFePO_4$ system. They confirmed the nonflammability of the LiTFSA/DMMEMPp electrolyte system (TFSA: trifluoromethylsulfonyl amide) and good cycling performance of the $LiFePO_4$ positive electrode.

Alkylphosphites are another family of phosphorous-containing organic esters, in which the oxidation state of phosphorous is III. Chen et al. [121, 122] first reported the use of trimethylphosphite (TMPi) as a flame-retardant additive in $LiPF_6$/EC + DEC. The effect of TMPi on the nonflammability of the electrolyte is unclear, but some positive effects on the thermal stability of $LiCoO_2$ and $LiNiO_2$ electrodes have been demonstrated. The experimental results on thermal and FT-IR analyses gave a possible mechanism for improving the thermal stability and electrode performance in the electrolyte containing TMPi.

Jow and co-workers have reported fluorinated alkyl phosphites as the additive components in EC-based electrolytes. Among them, tris(2,2,2-trifluoroethyl) phosphite (TTFP) was first reported as a thermal stabilizer for $LiPF_6$-based electrolytes [90, 123].

2.4.2.4 Other Phosphorous-Containing Compounds

Arylphosphates are also possible candidates of flame-retardant additives. Wang et al. [124, 125] reported the effects of 4-isopropyl phenyl diphenyl phosphate (IPPP) addition on the thermal stability of $LiPF_6$/EC + DEC electrolyte. Addition of 5 mass% of IPPP showed positive effects on the decrease in the onset temperature and exothermic behavior of the electrolyte solution [125]. A flame-propagation test was also examined for the electrolyte containing IPPP. Addition of 15 wt% (% in

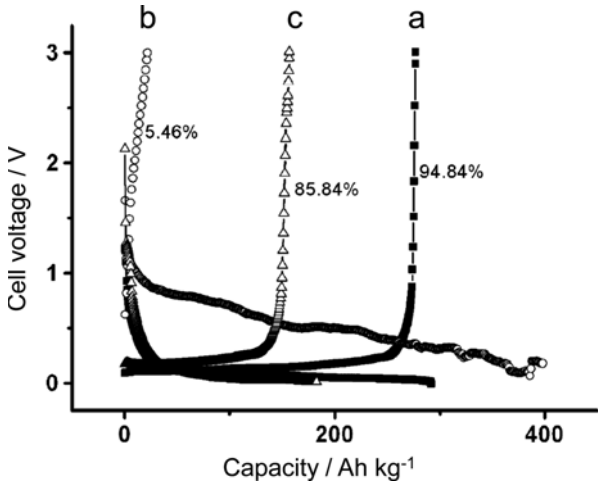

Fig. 2.26 First-cycle charge–discharge curves of Li/graphite (MCMB) half-cells with different electrolytes. (a): 1 M $LiPF_6$/EC + DEC(1:1), (b) 1 M $LiPF_6$/EC + DEC + DMMPp (1:1:2), (c) 1 M $LiPF_6$/EC + DEC + DMMPp (1:1:2) + 5 wt% VEC

mass) or more gave a good result for the nonflammability of the electrolyte, but decreased the discharge capacity and the cycleability of the $LiCoO_2$ positive electrode [124].

As another phosphate-based flame-retardant additive, cresyldiphenyl phosphate (CDP) has been examined in $LiPF_6$/EC + DEC (1:1) [126] and $LiPF_6$/EC + DMC + EMC (1:1:1) [127]. The addition of 5 % (in mass) CDP decreased SET, but its ability for nonflammability was not so high. The effect of CDP on the battery performance of the graphite/$LiCoO_2$ system was small when the addition to the electrolyte solution was limited to a lower level (~5 %). The effect of tris-(4-methoxyphenyl)phosphate (TMMP) on the overcharge protection is also reported in a graphite/$LiFePO_4$ system using [128]. The addition of TMMP in $LiClO_4$/EC + DMC electrolyte shows a decrease in the SET and shifts the oxidation potential of the electrolyte to a less positive one.

Phosphazenes have also been known as effective flame retardants for plastics [129]. Several research groups reported the utility of this family as the flame-retardant component in the LIB electrolytes. Lee et al. [130] examined hexamethoxycyclotriphosphazene $[NP(OCH_3)_2]_3$: HMPN, in $LiPF_6$/EC + DMC (1:1). The addition of HMPN delays the exothermal reaction of lithiated graphite with the electrolyte in a DSC measurement and decreased the self-heating rate in an ARC (accelerating rate calorimater) test [130]. A relatively small amount (1.5 wt%) of HMPN does not show a significant influence on the cycling performance of the $LiNi_{0.8}Co_{0.2}O_2$ positive electrode [130]. Xu et al. [103] reported that, in SET experiments, a considerable amount of HMPN (>40 wt%) is needed to establish sufficient nonflammability for the $LiPF_6$/EC + EMC electrolyte. In

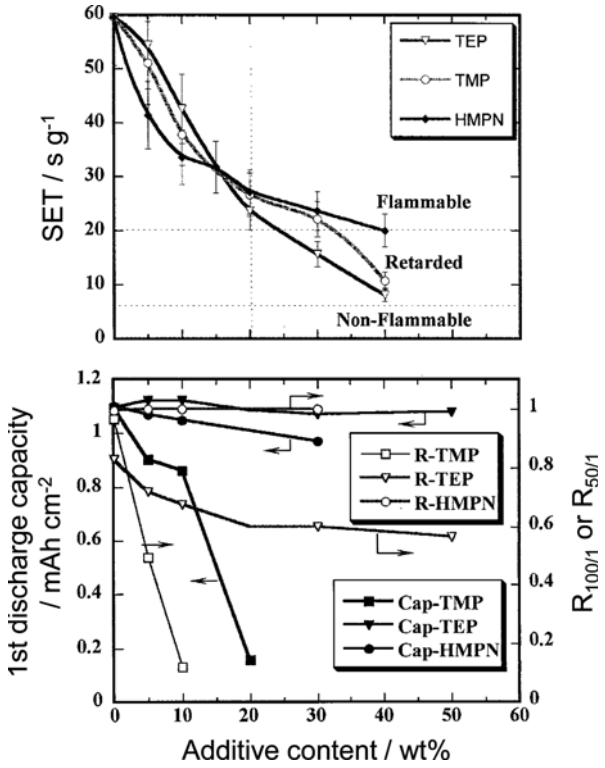

Fig. 2.27 Trade-off between low flammability and electrolyte performance. Capacity utilization of first cycle and retention at hundredth (for TMP, TEP) or fiftieth cycle (HMPN)

Fig. 2.27 [103], the SET value of the electrolyte solution and the discharge capacity of the graphite/$LiNiO_x$ cell using the additive-containing electrolytes are shown as a function of the flame-retardant content. We can see trade-off behavior between low flammability and the electrode performance for the HMPN-added electrolyte, which is commonly observed in the electrolyte systems containing organophosphorous compounds as the flame-retardant components. Sazhin et al. [131] synthesized two kinds of phosphazene compounds and evaluated the nonflammability in EC + EMC-based electrolyte. They observed a significant increase in the flash point of the electrolyte with the content of the additives.

Hu et al. reported a phosphonamidate, bis(*N*,*N*-diethyl) (2-methoxyethoxy) methylphosphonamidate (DEMEMPA), as a new P-N-containing organic flame-retardant additive [132]. Addition of 10 wt% of DEMEMPA to $LiPF_6$/EC + DMC decreases the SET value. The effects of DEMEMPA addition on the cycling performances are rather small for MCMB negative and $LiFePO_4$ positive electrodes.

2.4.3 *Polymeric Gel Electrolytes Containing Alkylphosphates*

Polymeric gel electrolytes that consist of polymer matrices swollen with organic electrolyte solutions are promising quasi-solid electrolytes that contribute to establishing safer and more reliable LIB systems for stationary and vehicle uses [94, 133]. The author's research group has proposed polymeric gel electrolytes containing nonflammable organic components [133, 134]. The key technology of such gel electrolytes is ensuring compatibility of the nonflammability with the cell performance. In this section, basic properties and LIB electrode characteristics of polymeric gel systems containing alkylphosphates are reviewed.

2.4.3.1 Gel Electrolytes Containing Trimethylphosphate

Nonflammable polymeric gel films can be obtained by swelling a polymer matrix with a lithium salt solution containing sufficient amount of nonflammable component. Typically, a polar polymer matrix such as poly(vinylidenefluoride-co-hexafluoropropylene) (PVdF-HFP) is chosen as the host polymer and mixed EC + DMC solution dissolving lithium salt ($LiPF_6$ or $LiBF_4$) is utilized as the liquid component. It is confirmed that nonflammability is established for the gel consisting of 20 vol.% or more of TMP in the liquid phase. Gelation of the flame-retardant EC + DMC + TMP solution decreases the ionic conductivity, but still maintains high values of over 10^{-3} S cm^{-1} at room temperature, as shown in Fig. 2.28 [135]. Similar to the case in liquid electrolyte solutions, addition of VC as an SEI modifier in the liquid phase of the gel is also effective for rechargeability of graphite-based negative electrode in TMP-containing gel electrolyte systems. Figure 2.29 shows the changes in the discharge capacity of the graphite (KS6, TIMICAL) electrode in the gels consisting of $LiPF_6$/EC + DEC + TMP (55:25:20) with and without VC (2 wt%), compared with that observed in conventional liquid electrolyte, $LiPF_6$/EC + DEC (2:1) [134]. For both gel electrolytes, several cycles were initially required to obtain stable capacity. During the initial cycles, the liquid component will be introduced into the pore structure of the electrode to form a good electrode/electrolyte interface. The addition of VC leads to high rechargeability of graphite in the gel containing the nonflammable component TMP.

On the rechargeability of the oxide-based positive electrode, the TMP-containing nonflammable gel electrolyte shows good compatibility with positive electrode materials. With respect to the electrolytic salt, however, $LiBF_4$ is better than $LiPF_6$ for the rechargeability of the $LiMn_2O_4$ positive electrode [135]. In the gel electrolyte dissolving $LiPF_6$, trace amounts of water in the system assist thermal decomposition of PF_6^- anion during the gelation with heat treatment. The resulting gel contains a small amount of HF that promotes the dissolution of Mn species in $LiMn_2O_4$, leading to the degradation of the cycleability of the positive electrode.

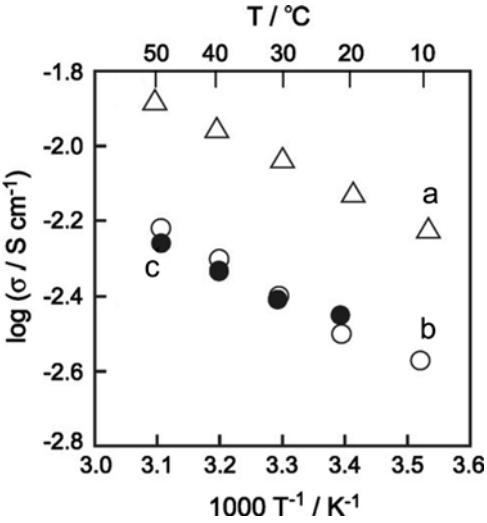

Fig. 2.28 Temperature dependence of ionic conductivity for (a) 0.8 M $LiPF_6$/EC + DEC + TMP (55:25:20) solution, (b) 0.8 M $LiPF_6$/EC + DEC + TMP (55:25:20) gel, and (c) 0.8 M $LiBF_4$/EC + DEC + TMP (55:25:20) gel

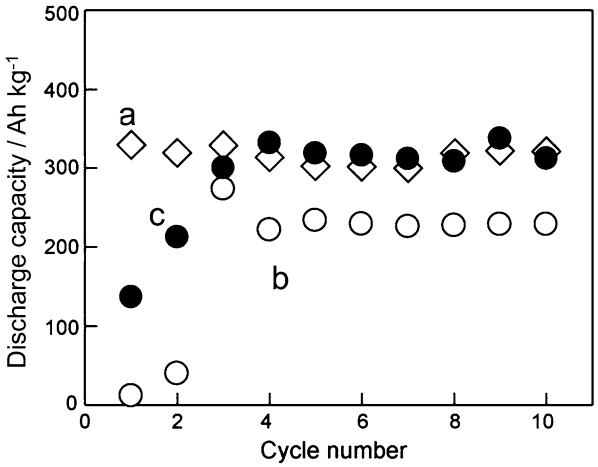

Fig. 2.29 Discharge capacity of a graphite (KS6) electrode in (a) 1 M $LiPF_6$/EC + DEC (2:1) solution, (b) 0.8 M $LiPF_6$/EC + DEC + TMP (55:25:20) gel, and (c) 0.8 M $LiPF_6$/EC + DEC + TMP (55:25:20) + VC (2 wt%) gel

2.4.3.2 Gel Electrolytes Containing Triethylphosphate

The fire-retardant ability of TEP itself is somewhat lower than that of TMP because of the lower P/C ratio in its chemical structure. However, the former would be superior to the latter with respect to compatibility with the graphite-based negative

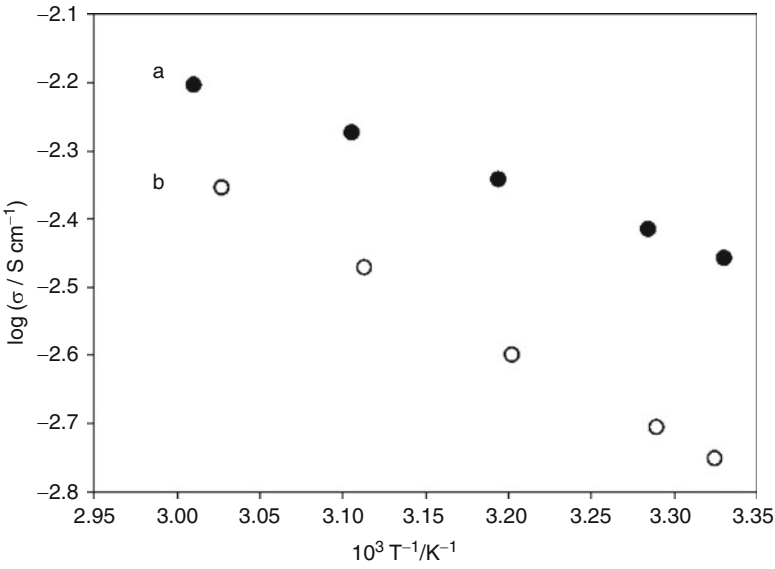

Fig. 2.30 Temperature dependence of ionic conductivity for (a) 1 M $LiBF_4$/EC + DEC + TEP (55:25:20) solution and (b) 1 M $LiBF_4$/EC + DEC + TEP (55:25:20) gel

electrode. Similar to the system containing TMP, an electrolyte solution of 1.0 M $LiBF_4$ in mixed EC + DEC + TEP (55:25:20 in volume) is easily solidified by PVdF-HFP to form transparent self-standing film with sufficient mechanical strength. From the experimental results of thermal analyses, the addition of TEP also shows higher on-set temperature for exothermic decomposition than that of the gel without TEP. Thus, a gel system containing TEP would be promising for practical LIB as nonflammable polymeric gel electrolyte (NPGE). In Fig. 2.30, ionic conductivity of NPGE is compared with that of the base solution electrolyte, $LiBF_4$ (1.0 M)/EC + DEC + TEP [136]. The gel system containing TEP shows a high ionic conductivity of ca. 2 mS cm^{-1} at room temperature, which is a value comparable to that of the gel consisting of TMP [94, 134].

The compatibility of NPGE containing TEP with LIB electrodes is examined for graphite (KS6) negative and $LiMn_2O_4$ positive electrodes by cyclic voltammetry and constant-current charge/discharge cycling. In Fig. 2.31 [136], a typical cyclic voltammetric response of the graphite electrode in the NPGE containing TEP is compared with that in the gel containing TMP. The voltammogram in the gel containing TEP shows reversible current response corresponding to Li-insertion/desertion, which is similar to that in the gel without TEP and completely different from the behavior in the gel containing TMP. This difference in the current responses among the gel composition would be caused by the difference in the interfacial properties between the graphite electrode and the gel electrolyte. That is, the chemistry and electrochemical properties of SEI formed at the graphite surface would depend much on the flame-retardant additives, TEP and TMP, as already discussed

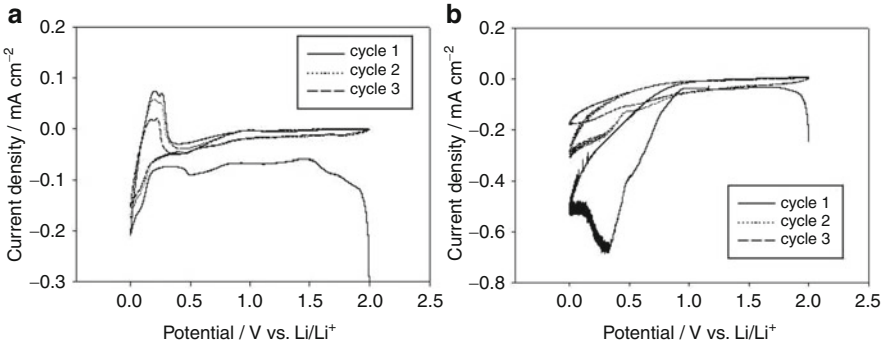

Fig. 2.31 Cyclic voltammograms of graphite (KS6) electrode in (a) 1 M $LiBF_4$/EC + DEC + TEP (55:25:20) gel and (b) 1 M $LiBF_4$/EC + DEC + TMP (55:25:20) gel electrolytes

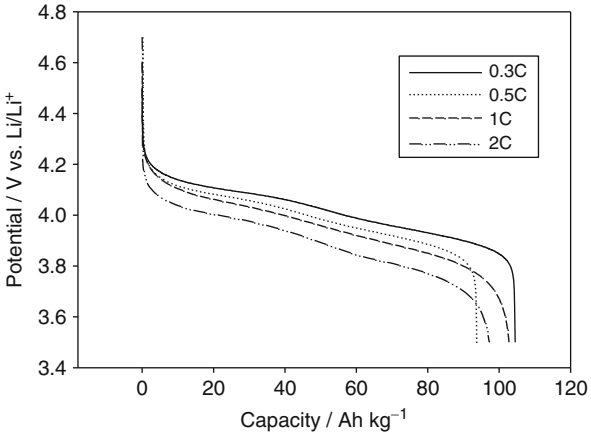

Fig. 2.32 Discharge capacity of a $LiMn_2O_4$ electrode in 1 M $LiBF_4$/EC + DEC + TEP (55:25:20) gel electrolyte (NPGE) at a different discharge rate

above. Figure 2.32 shows an example of the rate-capability of the $LiMn_2O_4$ positive electrode in NPGE containing TEP [136]. More than 90 % of the utility is obtained at a 2C-rate discharge under room temperature conditions.

In order to examine the general features of NPGE, alkylcarbonate-based electrolyte solutions containing different phosphorous-containing additives have been prepared. Free-standing polymeric gel films are easily obtained by a thermal casting method using a PVdF-HFP host polymer. In most cases, the gel films containing a sufficient amount of the fire-retardant additives show excellent nonflammability and ionic conductivity. However, the compatibility of NPGE with the electrode materials is strongly dependent on the sort of the additive component. For example, NPGE containing diphenylphosphite (DPP) as the fire-retardant additive shows excellent nonflammability but poor cycleability of the $LiMn_2O_4$ positive electrode. Anodic

oxidation of DPP inhibits the rechargeability of the positive electrode. If one uses electrode material having a lower redox potential, such as $LiFePO_4$, NPGE containing DPP shows a reversible electrode reaction with high coulombic efficiency [137].

2.4.3.3 Effects of Lewis-Acid Polymer in Gels Containing Triethylphosphate

In order to improve the mass-transport properties, especially at the interface of the solid electrode and the gel electrolyte, different attempts have been reported. The introduction of Lewis-acid polymers (LAPs) into gel electrolyte systems is effective to enhance the Li^+ ion mobility and compatibility of quasi-solid (gel) electrolytes with solid electrode materials [138–140]. With respect to the gel containing the flame-retardant additive, the authors' group reported the utility of LAP in a polymeric gel containing TEP [141]. Typical LAP is synthesized by dehydrated condensation of boron oxide (B_2O_3) with tri(ethylene glycol) monomethylether (TEGMME) and poly(ethylene glycol) (PEG) with a molecular weight of 300. The resulting polymer is blended in a PVdF-HFP-based polymeric gel electrolyte containing TEP (NPGE: PVdF-HFP/$LiBF_4$/EC + DEC + TEP). The effects of the addition of LAP on the ionic conductivity of NPGE are shown in Fig. 2.33 [141]. The addition of a small amount of LAP, with a molar ratio of $[Li^+]/B = 10/1$, improved the ionic conductivity across the whole temperature range examined (−20 to +60 °C). The excess amount of LAP added to NPGE is practically avoided because the higher content of LAP tends to deteriorate the mechanical strength of NPGE.

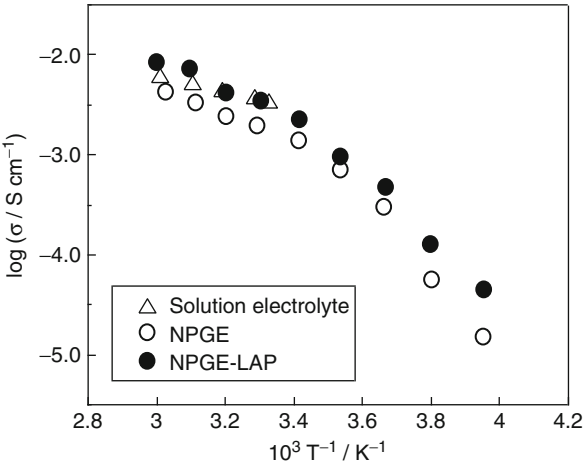

Fig. 2.33 Temperature dependence of ionic conductivity for 1 M $LiBF_4$/EC + DEC + TEP (55:25:20) solution (*open triangle*), 1 M $LiBF_4$/EC + DEC + TEP (55:25:20) gel (NPGE, *open circle*), and 1 M $LiBF_4$/EC + DEC + TEP (55:25:20) + LAP gel (NPGE-LAP, *filled circle*)

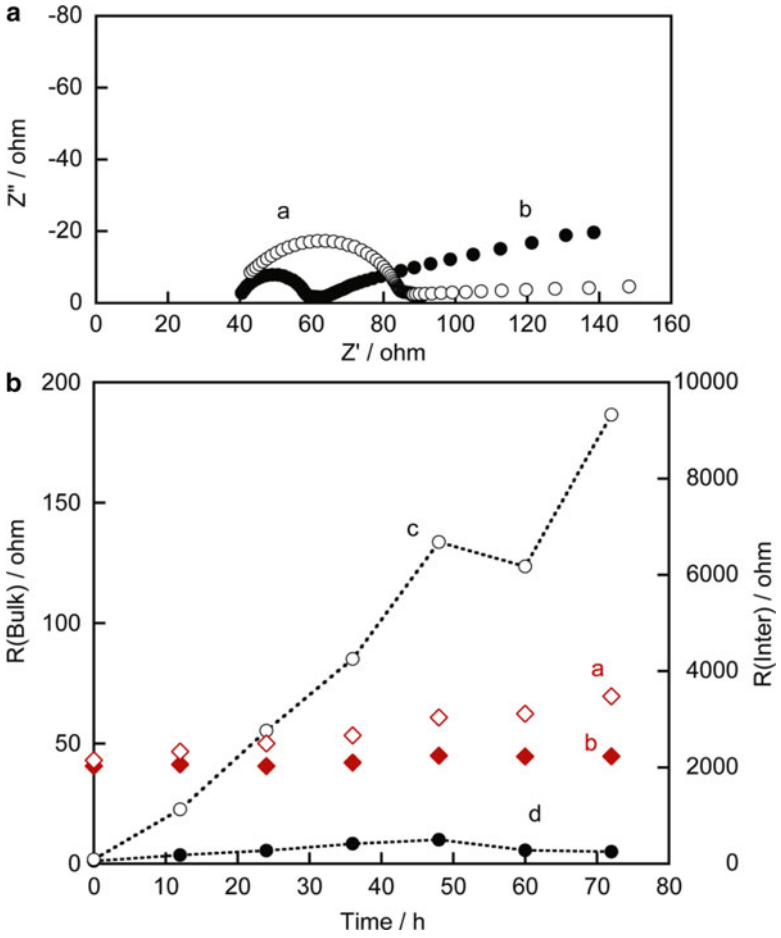

Fig. 2.34 AC impedance responses of Li/gel electrolyte/Li cells: (a) Nyquist plot (*a*: NPGE, *b*: NPGE-LAP), (b) time dependence of bulk resistance (R_{bulk}: *a* and *b*) and interfacial resistance (R_{int}: *c* and *d*), (*a* and *c*: for NPGE, *b* and *d*: for NPGE-LAP)

The improvement of the conductivity by adding LAP is considered to be mainly due to a decrease in the association between the Li^+ cation and the BF_4^- anion. The spectroscopic data of NPGEs with and without LAP prove that the Lewis-acid boron center interacts with the Lewis-base BF_4^-, and there is no ion-pair formation in the LAP-containing NPGE [141]. With respect to the ionic mobility itself, a high value of Li^+ with a transport number (~0.6) is demonstrated as the result of direct-current polarization measurements combined with an ac impedance technique. As smaller values than 0.5 have been usually obtained for conventional organic electrolyte solutions and poly(ethlene oxide)–based solid electrolytes, the above value for NPGE-LAP is regarded to be quite high for Li^+ ion conduction in this kind of gel electrolyte system.

In Fig. 2.34 [141], ac impedance responses of Li metal/NPGE (with and without LAP)/Li metal symmetric cells are shown as an example of the examination of

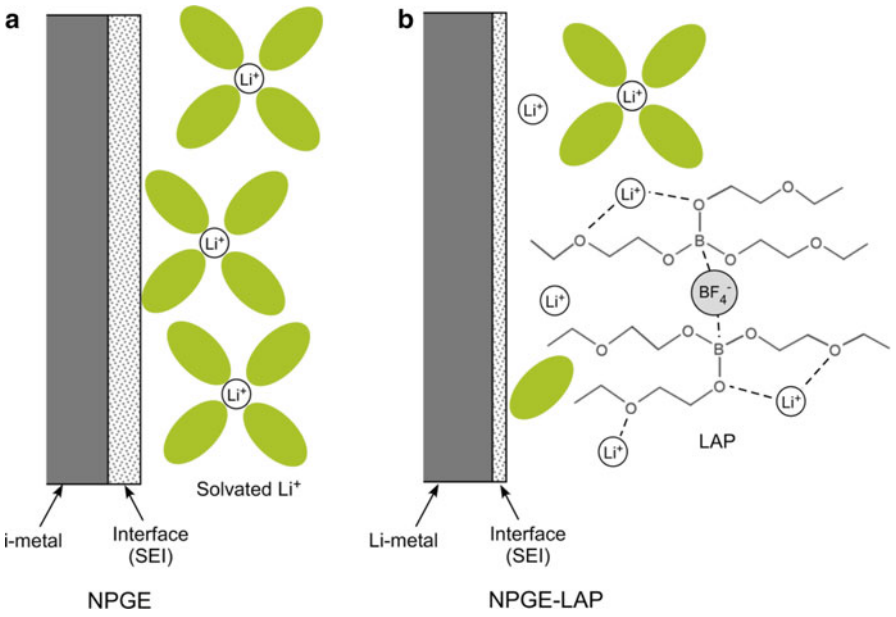

Fig. 2.35 A schematic model for an Li/gel electrolyte interface having interactions between ions and LAP in NPGE. (a) NPGE, (b) NPGE-LAP

influences of LAP on the interface behavior of NPGE. The interfacial resistance, R_{int}, between Li/NPGE (without LAP) increases with the time, while its bulk resistance, R_{bulk}, remains almost constant during the storage. The addition of LAP decreases R_{int} itself by one- to twofold, and reduces the increment during the storage. A model for the additional effects of LAP on the interfacial behavior is presented as shown in Fig. 2.35 [141]. Because Li metal is highly reactive toward organic compounds, it reacts with alkyl carbonate molecules that form Li^+ solvation at the vicinity of the interface between the Li electrode and the gel electrolyte. The decomposition of the organic solvent molecules produces a surface thin layer (SEI). The resistance of the resulting thin layer influences the Li^+ mobility at the interface. A thicker layer with high resistivity hinders the fast movement of Li^+ at the interface. The introduction of LAP in the NPGE leads to the anion trapping by the Lewis-acid interaction, providing free Li^+ at the interface. Thus, the number of Li^+ solvation decreases at the interface, and a thinner layer will be formed as compared to NPGE without LAP.

The results of thermal analyses demonstrated that the introduction of LAP into NPGE also reduces the exothermic heat for thermal decomposition of the liquid component dissolving the Li salt. The charge/discharge characteristics of $LiMn_2O_4$ positive electrode have also been reported. The addition of LAP to NPGE does not have a negative influence on the electrode behavior of $LiMn_2O_4$. There is a high rate capability of the oxide electrode in the present NPGE-LAP system: ca. 80 % or higher of utilization is achieved for the cycling under a 2C-rate at ambient

temperature [141]. We conclude that NPGE-LAP can be used for an LIB system for high-power-density applications with sufficient safety and reliability.

2.4.4 Summary

A variety of organophosphorous compounds, especially in the alkylphosphates family, have been examined as flame-retardant co-solvents or additives in LIB electrolyte systems. Polymeric gel electrolytes containing flame-retardant components would be another choice to produce a battery with a safer and more reliable cell performance. In both cases, nonflammability or the self-extinguishing property of the electrolyte system depends very much on the P/C atomic ratio in the resulting electrolyte. Thus, the higher P/C ratio tends to be effective in establishing nonflammability. However, battery performances, especially for graphite-based negative electrodes, have a tendency to decrease with an increasing P/C ratio. No clear solution has been found for this trade-off behavior. Utilization of an efficient SEI-forming reagent would be a condition to deliver sufficient cell performance for the system using completely nonflammable electrolyte systems.

2.5 Sulfur-Containing Organic Solvents

2.5.1 Introduction

Sulfur has been an important element used for the electrolyte solvents for lithium and lithium-ion batteries. Sulfur-containing organic solvents such as dimethyl sulfoxide and sulfolane are popular solvents for nonaqueous electrolytes [142]. Sulfur-containing inorganic solvents such as SO_2 and $SOCl_2$ have been used as catholytes for lithium cells as listed in Tables 2.6 and 2.7, where typical chemistries for primary and secondary cells are given, respectively [143, 144]. Although no sulfur-containing organic solvent is commercially used in lithium-ion cells, nonaqueous electrolytes containing sulfolane have already been commercially produced for aluminum electrolytic capacitors and double-layer capacitors [145, 146], and have been examined for lithium cells for high-temperature applications. The authors review the papers on lithium and lithium-ion cells using sulfur-containing organic solvents that were published after 1990.

2.5.2 Properties of Organo-Sulfur Compounds

Organo-sulfur compounds are classified into sulfide, sulfoxide, sulfone, sulfite, sulfonate, and sulfate depending on the number and kind of oxygen atoms. The physical properties of acyclic (dimethyl derivatives) and cyclic (five-membered derivatives)

Table 2.6 Primary lithium cells commercialized in the 1970s

Code	Positive electrode	Electrolyte	Voltage	Manufacturer	Year
B	$(CF)_n$	$LiBF_4$/GBL	2.6	Panasonic	1971
–	I_2-PVP	LiI	2.7	Wilson Greatbatch	1972
–	Ag_2CrO_4	$LiClO_4$/PC	3.0	SAFT	1973
–	SO_2	LiBr/AN-SO_2	2.6	(American Cyanamid)	1974
E	$SOCl_2$	$LiAlCl_4/SOCl_2$	3.5	GTE	1974
–	V_2O_5	$LiAsF_6$-$LiBF_4$/MF	2.8	Honeywell	1975
–	CuS	$LiClO_4$/DOL-DME	1.8	DuPont	1975
G	CuO	$LiClO_4$/DOL	1.5	SAFT	1975
F	FeS_2	$LiCF_3SO_3$/MOX-DOL-DME	1.6	Union Carbide	1976
C	MnO_2	$LiClO_4$/PC-DME	2.8	Sanyo Electric	1976

Table 2.7 Secondary lithium cells developed in the 1980s

Type	Negative electrode	Positive electrode	Electrolyte	Manufacturer	Year
Coin	Li-Al	TiS_2	$LiClO_4$/DOL	Exxon	1978
	Li-BiPbSnCd	C	$LiClO_4$/PC-DME	Panasonic	1985
	Li-Al	PAn	$LiBF_4$/PC-DME	Bridestone	1987
	Li-Al	TiS_2	$LiPF_6$/4MeDOL-HMPA	Hitachi Maxwell	1988
	Li-LGH	V_2O_5	$LiClO_4$/PC	Toshiba	1988
	Li-PAS	PAS	$LiBF_4$/PC	Kanebo	1989
	Li-AlMn	Li_xMnO_2	$LiCF_3SO_3$/EC-BC-DME	Sanyo Electric	1989
Cylidrical	Li	TiS_2	$LiAsF_6$/2MeTHF	EIC Lab.	1979
	Li	SO_2	$Li_2B_{10}Cl_{10}/SO_2$	Duracell	1981
	Li	MoS_2	$LiAsF_6$/EC-PC	Moli Energy	1987
	Li	TiS_2	$LiAsF_6$/2MeTHF	W. R. Grace	1987
	Li	$NbSe_3$	$LiAsF_6$/PC-2MeTHF	AT&T Bell Laboratories.	1988
	Li	$CuCl_2$, SO_2	$LiAlCl_4/SO_2$	Altus	1989
	Li	$LiMn_3O_6$	$LiAsF_6$/DOL-TBA	Tadiran	1989

compounds are listed in Table 2.8, where FW, d, mp, bp, fp, ε_r, η, E_{IP}, and E_{EA} are formula weight, density, melting point, boiling point, flash point, relative permittivity, viscosity, ionization potential, and electron affinity, respectively. The ionization potential (IP) and electron affinity (EA) in one-electron oxidation and reduction of a single molecule was calculated by B3LYP/6−311+G(2d,p) without changing the atomic coordinates during the electron transition [147]. The values for DMC and EC are also given for reference. Generally, the ionization potential increases and the electron affinity decreases as the number of oxygen atoms increases.

(a) Sulfides
Sulfides contain a bivalent sulfur atom. Their strong, unpleasant odor is a problem for use. Since lone-pair electrons on the sulfur atoms are easy to oxidize (low IP), there are no recent uses for use in batteries.

Table 2.8 Physical properties of organosulfur compounds at 25 °C

Name	FW	d (g cm^{-3})	mp (°C)	bp (°C)	fp (°C)	ε_r	η (m Pa s)	E_{IP} (eV)	E_{EA} (eV)
Acyclic									
Dimethyl sulfide	62.13	0.85	−98	38	−37			8.65	1.24
Dimethyl sulfoxide (DMSO)	78.13	1.10	18	189	85	46.5	1.99	8.93	1.17
Dimethyl sulfone	94.13	1.16	108	238	143	47.4	1.37	10.60	0.75
Dimethyl sulfite	110.13	1.29	−141	127	41	(110°C)		9.97	0.95
						22.5	0.87		
Methyl methanesulfonate	110.13	1.30	20	203	104			10.64	0.92
Dimethyl sulfate	126.13	1.33	−32	188	83			10.72	0.92
Dimethyl carbonate (DMC)	90.08	1.07	5	90	18	3.2	0.59	10.91	1.09
Cyclic									
Tetramethylene sulfide	88.17	1.00	−96	119	13			8.36	1.09
Tetramethylene sulfoxide (TMSO)	104.17	1.17	−41	236	110	42.9	5.25	8.63	0.90
Tetramethylene sulfone (TMS)	120.17	1.26	28	287	166	43.3	10.28	10.06	0.75
Ethylene sulfite (ES)	108.12	1.43	−17	159	79	(30°C)		10.56	0.88
						39.6	2.06		
Propane sultone (PS)	122.14	1.39	31	295	110			10.69	0.78
Ethylene sulfate	124.12	1.60	96	231	94			11.09	0.74
Ethylene carbonate (EC)	88.06	1.32	37	238	160	90.4	1.93	11.15	0.88
						(40°C)			

(b) Sulfoxides
Dimethyl sulfoxide (DMSO) is a very popular solvent, because it has strong solvating power with a high relative permittivity and an optimum liquid temperature range. Tetramethylene sulfoxide (TMSO) seems to have similar properties with a wider liquid temperature range. Since sulfoxides contain a tetra-valent sulfur atom, they are not as stable toward oxidation as carbonates are due to the existence of lone-pair electrons on the sulfur atoms (low IP). Conductivity and viscosity of $LiClO_4$ in DMSO-ether (THF, DME, DOL) mixtures were extensively studied [148]. Both $LiCF_3SO_3$ and $LiPhSO_3$-DMSO electrolytes were tested for Li/$LiMn_2O_4$ and Li/V_2O_5 cells [149].

(c) Sulfones
Sulfolane (TMS) is the most studied sulfur-containing organic solvent for lithium [150] and lithium-ion [151] cells. Since sulfolane is a solid at room temperature, like EC, it is often mixed with low-viscosity solvents to make electrolyte solutions. Dimethyl sulfone has a high melting point of 108 °C, and it is not easy to handle as a solvent, although it was used for lithium cells in high-temperature operation above 150 °C [152, 153]. Unsymmetrical ethyl methyl sulfone has a relatively low melting point of 37 °C, and it was studied extensively as an electrolyte solvent [154].

(d) Sulfites
Because of the similarity in the structures of sulfites with those of carbonates, the properties of cyclic and acyclic sulfites such as ethylene sulfite [155], propylene sulfite [156], dimethyl sulfite [157], and diethyl sulfite [157] were studied in comparison with EC, PC, DMC, and DEC as an electrolyte additive or co-solvent. Among these, ethylene sulfite (ES) is one of the practical anode SEI-forming additives [158], and dimethyl sulfite is a promising candidate as a co-solvent that improves low-temperature performance of graphite/$LiCoO_2$ cells [159].

(e) Sulfonates
Due to the high chemical reactivity of sulfonates, they are not easy to use as electrolyte solvents. Among sulfonates, 1,3-propane sultone (PS) is one of the practical additives that work as both an anode SEI-forming agent [160–162] and as a cathode protection agent [158, 161].

(f) Sulfates
Due to the high chemical reactivity and toxicity of sulfates, they cannot be used as electrolyte solvents and have been tested only as additives. Among these, ethylene sulfate was tested as an anode SEI-forming agent [163–165].

2.5.3 Electrolyte Formulation and Cell Performance

The oxidation process of electrolyte solutions is complicated. Although electrolyte solutes (lithium salts) are involved, solvents are believed to be the major component responsible for the catalytic decomposition on the cathodes [147, 166]. Angell's

Table 2.9 Electrolytic conductivity of lithium salts in $EMSO_2$

Salt	κ (mS cm^{-1})
$LiN(CF_3SO_2)_2$	5.3
$LiPF_6$	3.2
$LiClO_4$	1.2
$LiCF_3SO_3$	1.0

1 mol dm^{-3}, 25 °C

group in Arizona State University has conducted systematic studies on sulfone solvents in order to increase the anodic stability of the electrolyte solution, which is a recent R&D trend to obtain high-voltage cells. As described in the previous section, sulfones are promising electrolyte solvents for lithium and lithium-ion batteries among sulfur-containing organic solvents. Angell's group introduced an unsymmetrical sulfone, ethyl methyl sulfone ($EMSO_2$), which lowers the melting point (108 °C) of dimethyl sulfone ($DMSO_2$) down to 37 °C by breaking the molecular symmetry [154].

$EMSO_2$ liquefies spontaneously in the presence of lithium salts and the resultant solutions are stable over wide ranges of temperatures from ca.10 °C (when salts or solvate precipitate or $EMSO_2$ crystallizes, depending on lithium salt and concentration) to ca. 220 °C (when $EMSO_2$ begins to evaporate). $EMSO_2$ dissolves various lithium salts readily and it seems to have a special affinity for $LiN(CF_3SO_2)_2$. The electrolytic conductivity of 1 mol dm^{-3} solutions of various lithium salts are given in Table 2.9. A 3:1 mixture of $EMSO_2$ and $DMSO_2$ has an eutectic temperature of 23 °C, and its solution containing $LiN(CF_3SO_2)_2$ is stable to below 0 °C. The anodic stability of $EMSO_2$-based electrolytes was announced to be higher than EC-based electrolytes. It has been confirmed by the successful intercalation of PF_6^- into graphite in $EMSO_2$ up to 5.5 V vs. Li/Li$^+$, whereas EC-based electrolytes are strongly oxidized above 5.2 V, preventing complete loading of graphite with PF_6^- [167], and by the attempt to completely remove lithium ion from $Li_{2/3}Ni_{1/3}Mn_{2/3}O_2$ around 5.4 V [168]. However, its relatively high melting point essentially eliminates the possibility of $EMSO_2$ as a single solvent. Therefore, it must be mixed with a cosolvent to lower the melting point and viscosity for practical use [151].

The studies of Angell's group were extended to other sulfone derivatives as listed in Table 2.10 [151]. The high boiling points of the sulfones correlate reliably with their viscosities at room temperature, and these are high enough to seriously limit the ionic mobilities. The concentration and temperature dependence of electrolytic conductivity of $LiN(CF_3SO_2)_2$ in $EMSO_2$, TMS, and ethyl sec-butyl sulfone (E^sBSO_2) are given in Figs. 2.36 and 2.37, respectively. All sulfones demonstrated a rather uniform high anodic stability toward a $LiMn_2O_4$ cathode despite their different chemical structures. In contrast with the stability on the cathode surface, which is invariant for all sulfones, the ability to form an effective SEI film on the graphite anode is found to be critically sensitive to the sulfone structure. The reductive decomposition of $EMSO_2$ occurred at ca. 0.7 V vs. Li/Li$^+$ without forming an effective SEI on the graphite. Similarly, the coulombic efficiencies for the oxidation-reduction of

Table 2.10 Physical properties of sulfones and their electrolytes

Name	mp (°C)	bp (°C)	ε_r	η (mPa s)	Solubility, m ($LiN(CF_3SO_2)_2$/ $LiPF_6$)	κ^b (mS cm^{-1})
Acyclic						
Dimethyl sulfone	108	238				
Ethyl methyl sulfone	37	239	95 (20˚C)		3.8/2.7	5.3
Diethyl sulfone	74	246				
Ethyl iso-propyl sulfone	<−20	265[a]			2.3/1.0	2.3
Ethyl iso-butyl sulfone	<−20	280[a]				2.5
Ethyl sec-butyl sulfone	−60	290[a]	48 (20˚C)		1.5/0.8	1.5
Dipropyl sulfone	31	266	33 (30˚C)	5.4 (30˚C)		
Dibutyl sulfone	45	295	26 (50˚C)	4.7 (50˚C)		
Cyclic						
Trimethylene sulfone	75	290[a]				
2-Methyltrimethylene sulfone	<−20	270[a]			3.3/–	2.3
Tetramethylene sulfone	28	287	43.3 (30˚C)	10.3 (30˚C)	3.5/2.0	3.1
3-Methyltetramethylene sulfone	6	276	29.4 (25˚C)	11.8 (25˚C)		
2,4-Dimethyltetramethylene sulfone	−3	281	29.7 (25˚C)	9.1 (25˚C)		

[a]Value extrapolated by nomograph
[b]1 mol dm^{-3} $LiN(CF_3SO_2)_2$, 25 °C

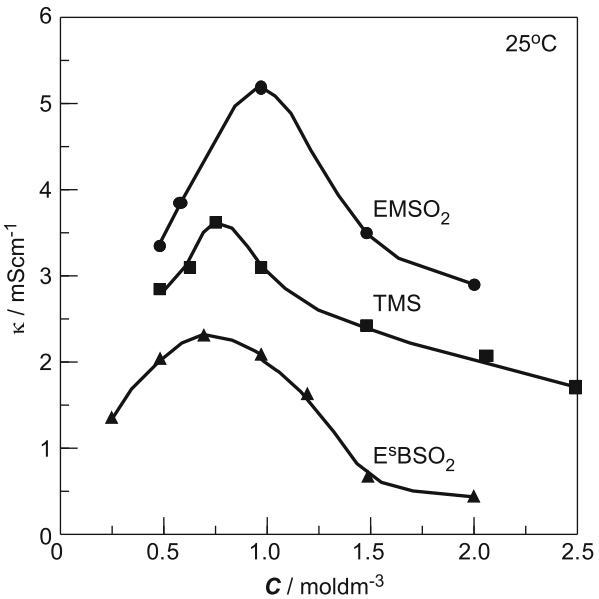

Fig. 2.36 Concentration dependence of electrolytic conductivity of $LiN(CF_3SO_2)_2$ in sulfone solvents

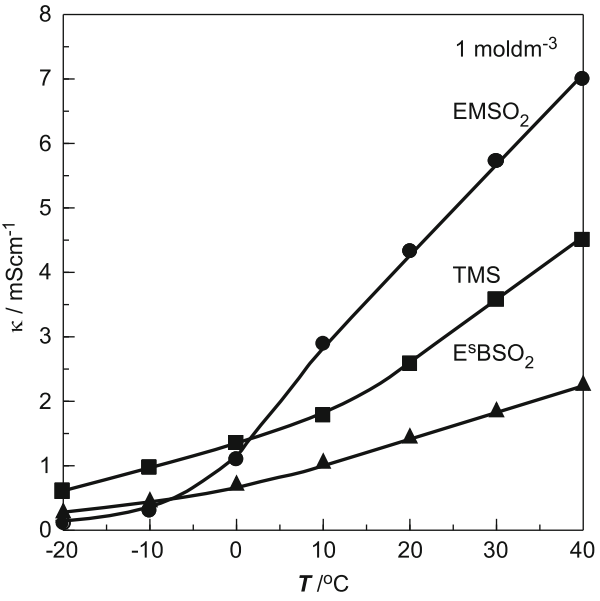

Fig. 2.37 Temperature dependence of electrolytic conductivity of $LiN(CF_3SO_2)_2$ in sulfone solvents

lithium on Pt and Al were low in $EMSO_2$ solvent [169]. Therefore, 1 mol dm^{-3} $LiN(CF_3SO_2)_2$ in $EMSO_2$ or TMS were tested using a $Li_4Ti_5O_{12}$ anode, which does not need a SEI layer to operate [170]. 2.5 V $Li_4Ti_5O_{12}/LiMn_2O_4$ cells containing 1 mol dm^{-3} $LiN(CF_3SO_2)_2$ in $EMSO_2$ or TMS were operated at C/3 rate for 100 cycles with 99 % capacity retention and 100 % coulombic efficiency. Furthermore, a 3 V $Li_4Ti_5O_{12}/LiNi_{1/2}Mn_{3/2}O_4$ cell containing 1 mol dm^{-3} $LiPF_6$ in TMS cycled fairly well at C/12 rate, although a separator wettability problem occurred at the initial cycles.

To lower the melting points of $EMSO_2$, oligoether-containing sulfones [171] and cycloalkyl group-containing sulfones [172] were synthesized and characterized as in Table 2.11. Although these new sulfones showed lower melting points, the electrolytic conductivity of lithium salts in these solvents were always lower than in $EMSO_2$, due to the increased viscosity. The anodic stability decreased by the incorporation of oligoether segments, which was proved by quantum-mechanical calculations [173].

1 mol dm^{-3} $LiPF_6$ in EMES was tested in graphite (MCMB25-28)/Li and $LiCr_{0.015}Mn_{1.985}O_4$/Li half-cells, respectively [171]. The capacity of the first half-cell decreased rapidly with cycling at 0.013 mA cm^{-2} (C/78), presumably due to the ineffective SEI formation, whereas that of the second half-cell decreased gradually with cycling at 0.092 mA cm^{-2} (C/11). A discharge capacity of more than 50 mA h g^{-1} was maintained after 200 cycles with a stable coulombic efficiency around 0.86. Similarly, 1 mol dm^{-3} $LiN(CF_3SO_2)_2$ in ESCP was also tested in graphite (MCMB25-28)/Li and $LiCr_{0.015}Mn_{1.985}O_4$/Li half-cells, respectively [172]. The capacity of the first half-cell decreased rapidly with cycling at 0.068 mA cm^{-2}

Table 2.11 Physical properties of sulfone derivatives and their electrolytes

Name	mp (°C)	bp[a] (°C)	T_g (°C)	T_g[b] (°C)	κ[b](mS cm^{-1})
$CH_3SO_2C_2H_5$ ($EMSO_2$)	37	240	–	–96	5.3
$CH_3OCH_2CH_2SO_2CH_3$ (MEMS)	15	275	–90	–81	1.5
$CH_3OCH_2CH_2SO_2C_2H_5$ (EMES)	2	286	–91	–83	1.4
$CH_3(OCH_2CH_2)_2SO_2C_2H_5$ (EMEES)	<0	>290	–88	–73	0.8
$CH_3(OCH_2CH_2)_3SO_2C_2H_5$ (EMEEES)	<0	>290	–83	–72	0.6
$(CH_3OCH_2CH_2)_2SO_2$ (DMES)	47	>290	–91	–84	1.0
$CH_3SO_2C_5H_9$ (MSCP)	–20	320	–92	–86	0.6
$C_2H_5SO_2C_5H_9$ (ESCP)	38	328	–93	–85	0.6
$CH_3SO_2CH_2C_5H_9$ (MSMCP)	19	325	–87	–80	0.5
$C_2H_5SO_2C_6H_{11}$ (ESCH)	21	337	–76	–72	0.1
$C_2H_5SO_2CH_2C_6H_{11}$ (ESMCH)	9	345	–89	–65	0.1

[a]Value extrapolated by nomograph
[b]1 mol dm^{-3} $LiN(CF_3SO_2)_2$, 25 °C

(C/4.4) due to the incompatibility of the conductivity with the charge/discharge rate, whereas that of the second half-cell decreased gradually with cycling at 0.15 mA cm^{-2} (C/2). A discharged capacity of more than 60 mA h g^{-1} was maintained after 120 cycles with a stable coulombic efficiency around 0.86.

Because these sulfone derivatives have no ability to form an effective SEI, 2 wt% of vinylene carbonate (VC) was added in 1 mol dm^{-3} $LiPF_6$ in EMES or MEMS for graphite/$LiCoO_2$ full cells [174]. 1 mol dm^{-3} $LiPF_6$ in EMES + 2 wt% VC showed a capacity drop, when the rate was raised to 0.50 mA cm^{-2} (C/4.6), whereas 1 mol dm^{-3} $LiPF_6$ in MEMS + 2 wt% VC exhibited almost the same performance as the reference electrolyte, 1 mol dm^{-3} $LiPF_6$ in EC-DMC (50–50 vol.%), at 0.46 mA cm^{-2} (C/5). These results indicated that more fluid versions of the sulfone-based electrolytes are necessary.

To circumvent the low separator wettability and low electrolytic conductivity of single-solvent systems based on sulfone solvents as mentioned before, blending with a low-viscosity solvent such as EMC is a practical approach [170]. Based on this guideline, 1 mol dm^{-3} $LiBF_4$ in TMS-ethyl acetate (50–50 vol.%) + 2 vol.% VC was tested for Li/$LiNi_{1/2}Mn_{3/2}O_4$ cells.

Although sulfone solvents such as $EMSO_2$ and TMS give better performance than EC for high-voltage cells using $LiNi_{0.5}Mn_{1.5}O_4$ cathodes, there is a controversy about the electrochemical stability of sulfone solvents. Xu pointed out that open-chain alkyl sulfones such as $EMSO_2$ are more stable against chemical oxidation and reduction than cyclic sulfones such as TMS [154]. However, their difference seems to be small according to experimental results [170] and IP calculated by density functional theory (cf. Table 2.8). There exists ambiguity in determining the limiting redox potentials because there is always a possibility to include the effect of passivation on the electrode surface by reacted products.

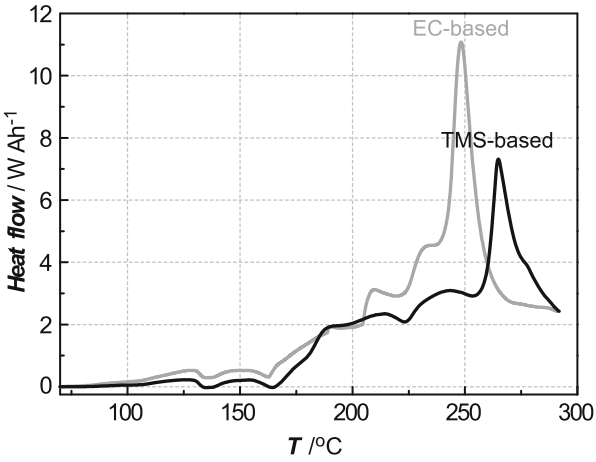

Fig. 2.38 Thermal behavior of 4.4 V graphite/$LiNi_{1/3}Mn_{1/3}Co_{1/3}O_2$ pouch cells

The research on high-voltage cells is going on over the world to meet the requirements for automotive applications, because the utilization of high-voltage cathodes enables is to increase the energy density by enhancing operational voltage such as $LiNi_{0.5}Mn_{1.5}O_4$ and $LiCoPO_4$, or increasing capacity such as $LiNi_xMn_yCo_zO_2$ and Li_2MnO_3-$LiNi_xMn_yCo_zO_2$ ($x+y+z=1$). However, lithium-ion cells intrinsically have serious safety problems, and the cell safety becomes still more severe for the high-voltage cells. Ue's group at Mitsubishi Chemical Corporation have developed high safety electrolytes including a TMS solvent for hybrid electric vehicle applications. One of the ways to avoid the thermal runaway is to apply materials that generate less heat even at elevated temperatures. They have found that the major source of heat generation in conventional electrolytes was EC, and a partial replacement of EC with TMS decreased the heat generation, when graphite/$LiNi_{1/3}Mn_{1/3}Co_{1/3}O_2$ pouch cells (4.1 V, 20 mA h) and 18,650 cylindrical cells (4.1 V, 1.2 A h) were heated up [175]. Encouraged by this result, the charging voltage was raised from 4.1 to 4.4 V and the thermal behavior and cell performance of these cells were examined [176, 177]. A TMS-based electrolyte [1 mol dm^{-3} $LiPF_6$/EC–FEC–SLF–DMC–EMC (5–5–20–40–30 vol.%)] showed lower heat generation rate than the conventional EC-based counterpart [1 mol dm^{-3} $LiPF_6$/EC–EMC (30–70 vol.%)] as shown in Fig. 2.38. A nail penetration test (0.0025 mφ, 0.35 ms^{-1}) of the 18,650 cylindrical cells at room temperature proved that the TMS-based electrolyte is safer than the conventional EC-based counterpart, because the former showed no event, whereas the latter exploded. Although cycle performances of the cells using TMS-based electrolytes are almost equivalent to that of the conventional EC-based counterparts, their output performances were inferior, as shown in Fig. 2.39.

Ue's group have also found that TMS-based electrolytes suppress the crystal change of $LiNi_{1/3}Mn_{1/3}Co_{1/3}O_2$ (layered) to spinel M_3O_4 at elevated temperatures over 280 °C due to passivation on the cathode by sulfur compounds such as Li_2SO_4. Contrary to experimental observations, TMS has lower IP and EA than EC. If it is

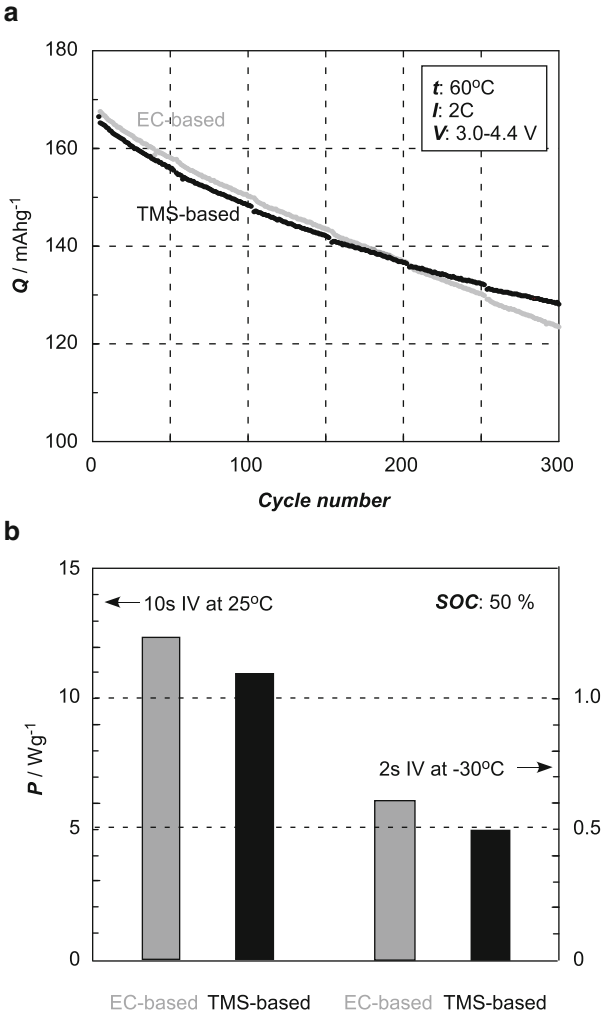

Fig. 2.39 Cell performances of graphite/$LiNi_{1/3}Mn_{1/3}Co_{1/3}O_2$ pouch cells. (**a**) Cycle test and (**b**) output test

true, the observed higher anodic and cathodic stability of sulfones can be explained by the formation of SEI on the electrodes, which must be examined in detail.

2.5.4 Summary

Sulfur-containing organic solvents, particularly sulfones such as $EMSO_2$ and TMS, were examined as electrolyte solvents for high-voltage cells. As single solvents, they have a few disadvantages such as low-anode SEI film–forming ability, and low

electrolytic conductivity, particularly at low temperatures. However, these disadvantages are mitigated by the aids of SEI-forming additives and low-viscosity carbonate co-solvents. Further progress is expected by introducing new sulfone derivatives. For example, a computational study to examine the effect of multiple functionalization with fluorine, cyano, ester, and carbonate groups has recently been reported as a key to achieving high oxidation potentials [178].

References

1. Ue, M., Electrolytes: nonaqueous, In *Encyclopedia of electrochemical power sources*; Garche, J.; Dyer, C.; Moseley, P.; Ogumi, Z.; Rand, D.; Scrosati, B., Eds.; Elsevier: Amsterdam, Netherlands, 2009; Vol. 5; 71–84.
2. Ding, M. S., Liquid-solid phase diagrams of ternary and quaternary organic carbonates, *J. Electrochem. Soc.* **2004**, *151*, A731–A738.
3. Ding, M. S.; Xu, K.; Zhang, S. S.; Amine, K.; Henriksen, G. L.; Jow, T. R., Change of conductivity with salt content, solvent composition, and temperature for electrolytes of $LiPF_6$ in ethylene carbonate-ethyl methyl carbonate, *J. Electrochem. Soc.* **2001**, *148*, A1196–A1204.
4. Sasaki, Y., The status and view for fluorine-containing organic solvents, In *Advanced battery technologies-2011*; *the Electrochemical Society of Japan*: Tokyo, Japan, 2011; 17–30.
5. Sasaki, Y., Organic electrolytes of secondary lithium batteries, *Electrochemistry* **2008**, *76*, 2–15.
6. Prager, J. H., *Cyclic fluorocarbonates*, US Patent 3,455,954: 1969.
7. Adcock, J. L.; Lagow, R. J., The synthesis of the perfluoroethers, "perfluoroglyme" and "perfluorodiglyme" by direct fluorination, *J. Org. Chem.* **1973**, *38*, 3617–3618.
8. Sasaki, Y.; Ebara, R.; Nanbu, N.; Takehara, M.; Ue, M., Direct fluorination of γ-butyrolactone, *J. Fluorine Chem.* **2001**,*108*, 117–120.
9. Hasegawa, M; Ishi, H.; Fuchigami, T., Electroorganic synthesis under solvent-free conditions. Highly regioselective anodic monofluorination of cyclic ethers, lactones and a cyclic carbonate, *Tetrahedron Lett*. **2002**, *43*, 1503–1505.
10. Takehara, M.; Ebara, R.; Nanbu, N.; Ue, M.; Sasaki, Y., Electrochemical properties of fluoro-γ-butyrolactone and its application to lithium rechargeable cells, *Electrochemistry* **2003**, *71*, 1172–1176.
11. Nakajima, T.; Dan, K.; Koh, M., Effect of fluoroesters on the low temperature electrochemical characteristics of graphite electrode, *J. Fluorine Chem.* **1998**, *87*, 221–227.
12. Nakajima, T.; Dan, K.; Koh, M; Ino, T.; Shimizu, T., Effect of addition of fluoroethers to organic solvents for lithium ion secondary batteries, *J. Fluorine Chem.* **2001**, *111*, 167–174.
13. Chandrasekaran, R.; Koh, M; Ozhawa, Y.; Aoyama, H; Nakajima, T., Electrochemical cell studies on fluorinated natural graphite in propylene carbonate electrolyte with difluoromethyl acetate (MFA) additive for low temperature lithium battery application *J. Chem. Sci.* **2009**, *121*, 339–346.
14. Yamaki, J.; Yamazaki, I.; Egashira, M.; Okada, S., Thermal studies of fluorinated ester as a novel candidate for electrolyte solvent of lithium metal anode rechargeable cells, *J. Power Sources* **2001**, *102*, 288–293.
15. Sato, K.; Yamazaki, I.; Okada, S.; Yamaki, J., Mixed solvent electrolytes containing fluorinated carboxylic acid esters to improve the thermal stability of lithium metal anode cells, *Solid State Ionics* **2002**, *148*, 463–466.
16. Yamaki, J.; Tanaka, T.; Ihara, M.; Sato, K.; Egashira, M.; Watanabe, I.; Okada, S., Thermal stability of methyl difluoroacetate as a novel electrolyte solvent for lithium batteries electrolytes, *Electrochemistry* **2003**, *71*, 1154.

17. Ihara, M.; Hang, B. T.; Sato, K.; Egashira, M.; Okada, S.; Yamaki, J., Properties of carbon anodes and thermal stability in $LiPF_6$/methyl difluoroacetate electrolyte, *J. Electrochem. Soc.* **2003**, *150*, A1476–A1483.
18. Nanbu, N.; Suzuki, Y.; Ohtsuki, K.; Meguro, T.; Takehara, M.; Ue, M.; Sasaki, Y., Physical and electrochemical properties of monofluorinated ethyl acetates for lithium rechargeable batteries, *Electrochemistry* **2010**, *78*, 446–449.
19. Sato, K.; Zhao, L.; Okada, S.; Yamaki, J., $LiPF_6$/methyl difluoroacetate electrolyte with vinylene carbonate additive for Li-ion batteries, *J. Power Sources* **2011**, *196*, 5617–5622.
20. Kobayashi, M.; Inoguchi, T.; Iida, T.; Tanioka, T.; Kumase, H.; Fukai, Y., Development of direct fluorination technology for application to materials for lithium battery, *J. Fluorine Chem.* **2003**, *120*, 105–110.
21. McMillan, R.; Slegr, H.; Shu, Z. X.; Wang, W., Fluoroethylene carbonate electrolyte and its use in lithium ion batteries with graphite anodes, *J. Power Sources* **1999**, *81–82*, 20–26.
22. Mogi, R.; Inaba, M.; Jeong, S.-K.; Iriyama, Y.; Abe, T.; Ogumi, Z., Effects of some organic additives on lithium deposition in propylene carbonate, *J. Electrochem. Soc.* **2002**, *149*, A1578–A1583.
23. Choi, N.-S.; Yew, K. H.; Lee, K. Y.; Sung, M.; Kim, H.; Kim, S.-S., Effect of fluoroethylene carbonate additive on interfacial properties of silicon thin-film electrode, *J. Power Sources* **2006**, *161*, 1254–1259.
24. Profatilova, I. A.; Kim, S.-S.; Choi, N.-S., Enhanced thermal properties of the solid electrolyte interphase formed on graphite in an electrolyte with fluoroethylene carbonate, *Electrochim. Acta* **2009**, *54*, 4445–4450.
25. Hagiyama, K.; Suzuki, K.; Ohtake, M.; Shimada, M.; Nanbu, N.; Takehara, M.; Ue, M.; Sasaki, Y., Physical properties of substituted 1,3-dioxolan-2-ones, *Chem. Lett.* **2008**, *37*, 210–211.
26. Sasaki, Y.; Takimoto, K.; Nanbu, N.; Takehara, M.; Ue, M., Direct fluorination of propylene carbonate, In *Meeting abstracts of the 6th Japan-France joint seminar on lithium ion batteries*; Kohu, Yamanashi, Japan, 2006; 24.
27. Nanbu, N.; Takimoto, K.; Suzuki, K.; Ohtake, M.; Hagiyama, K.; Takehara, M.; Ue, M.; Sasaki, Y., Temperature dependence of physical constants of monofluororinated propylene carbonate as highly polar liquid, *Chem. Lett.* **2008**, *37*, 476–477.
28. Nanbu, N.; Takimoto, K.; Takehara, M.; Ue, M.; Sasaki, Y., Electrochemical properties of fluoropropylene carbonate and its application to lithium-ion batteries, *Electrochem. Commun.* **2008**, *10*, 783–786.
29. Inaba, M.; Kawatate, Y.; Funabiki, A.; Jeong, S.-K.; Abe, T.; Ogumi, Z., STM study on graphite/electrolyte interface in lithium-ion batteries: solid electrolyte interface formation in trifluoropropylene carbonate solution, *Electrochim. Acta* **1999**, *45*, 99–105.
30. Arai, J.; Katayama, H.; Akahoshi, H., Binary mixed solvent electrolytes containing trifluoropropylene carbonate for lithium secondary batteries, *J. Electrochem. Soc.* **2002**, *149*, A217–A226.
31. Achiha, T.; Nakajima, T.; Ohzawa, Y.; Koh, M.; Yamauchi, A.; Kagawa, M.; Aoyama, H., Electrochemical behavior of nonflammable organo-fluorine compounds for lithium ion batteries, *J. Electrochem. Soc.* **2009**, *156*, A483–A488.
32. Achiha, T.; Nakajima, T.; Ohzawa, Y.; Koh, M.; Yamauchi, A.; Kagawa, M.; Aoyama, H., Thermal stability and electrochemical properties of fluorine compounds as nonflammable solvents for lithium-ion batteries, *J. Electrochem. Soc.* **2010**, *157*, A707–A712.
33. Takehara, M.; Watanabe, S.; Nanbu, N.; Ue, M.; Sasaki, Y., Synthesis of fluorinated dimethyl carbonates by direct fluorination, *Synth. Commun.* **2004**, *34*, 1367–1375.
34. Takehara, M.; Watanabe, S.; Nanbu, N.; Ue, M.; Sasaki, Y., Physical properties of monofluorodimethyl carbonate, *Chem. Lett.* **2004**, *33*, 338–339.
35. Sasaki, Y.; Takehara, M.; Watanabe, S.; Oshima, M.; Nanbu, N.; Ue, M., Electrolytic behavior and application to lithium batteries of monofluorinated dimethyl carbonate, *Solid State Ionics* **2006**, *177*, 299–303.

36. Nanbu, N.; Watanabe, S.; Takehara, M.; Ue, M.; Sasaki, Y., Electrolytic characteristics of fluoromethyl methyl carbonate for lithium rechargeable batteries, *J. Electroanal. Chem.* **2009**, *625*, 7–15.
37. Nanbu, N.; Takehara, M.; Watanabe, S.; Ue, M.; Sasaki, Y., Polar effect of successive fluorination of dimethyl carbonate on physical properties, *Bull. Chem. Soc. Jpn.* **2007**, *80*, 1302–1306.
38. Sasaki, Y.; Takehara, M.; Watanabe, S.; Nanbu, N.; Ue, M., Physical and electrolytic properties of difluorinated dimethyl carbonate, *J. Fluorine Chem.* **2004**, *125*, 1205–1209.
39. Takehara, M., Tsukimori, N.; Nanbu, N.; Ue, M.; Sasaki, Y., Physical and electrolytic properties of fluoroethyl methyl carbonate, *Electrochemistry* **2003**, *71*, 1201–1204.
40. Handa, M.; Kataoka, M.; Watanabe, M.; Sasaki, Y., Physical and donor–acceptor properties of 3-propyl-4-ethylsydnone, *Bull. Chem. Soc. Jpn.* **1997**, *70*, 315–320.
41. Tsukimori, N.; Nanbu, N.; Takehara, M.; Ue, M.; Sasaki, Y., Electrolytic properties of ethyl fluoroethyl carbonate and its application to lithium battery, *Chem. Lett.* **2008**, *37*, 368–369.
42. Sasaki, Y.; Satake, H.; Tsukimori, N.; Nanbu, N.; Takehara, M.; Ue, M., Physical and electrolytic properties of partially fluorinated methyl propyl carbonate and its application to lithium batteries, *Electrochemistry* **2010**, *78*, 467–470.
43. Smart, M. C.; Ratnakumar, B. V.; Ryan-Mowrey, V. S.; Surampudi, S.; Prakash, G. K. S.; Hu, J.; Cheung, I., Improved performance of lithium-ion cells with the use of fluorinated carbonate-based electrolytes, *J. Power Sources* **2003**, *119–121*, 359–367.
44. Kitagawa, T; Azuma, K.; Koh, M.; Yamaguchi, A.; Kagawa, M.; Sakata, H.; Miyawaki, H.; Nakazono, A.; Arima, H.; Yamagata, M.; Ishikawa, M., Application of fluorine-containing solvents to $LiCoO_2$ cathode in high voltage operation, *Electrochemistry* **2010**, *78*, 345–348.
45. Arai, J., A novel non-flammable electrolyte containing methyl nonafluorobutyl ether for lithium secondary batteries, *J. Appl. Electrochem.* **2002**, *32*, 1071–1079.
46. Arai, J., Nonflammable methyl nonafluorobutyl ether for electrolyte used in lithium secondary batteries, *J. Electrochem. Soc.* **2003**, *150*, A219–A228.
47. Arai, J., No-flash-point electrolytes applied to amorphous carbon/$Li_{1+x}Mn_2O_4$ cells for EV use, *J. Power Sources* **2003**, *119–121*, 388–392.
48. Morita, M.; Kawasaki, T.; Yoshimoto, N.; Ishikawa, M., Nonflammable organic electrolyte solution based on perfluoro-ether solvent for lithium ion batteries, *Electrochemistry* **2003**, *71*, 1067–1069.
49. Naoi, K.; Iwama, E.; Ogihara, N.; Nakamura, Y.; Segawa, H.; Ino, Y., Nonflammable hydrofluoroether for lithium-ion batteries: enhanced rate capability, cyclability, and low-temperature performance, *J. Electrochem. Soc.* **2009**, *156*, A272–A276.
50. Naoi, K.; Iwama, E.; Honda, Y.; Shimodate, F., Discharge behavior and rate performances of lithium-ion batteries in nonflammable hydrofluoroethers(II), *J. Electrochem. Soc.* **2010**, *157*, A190–A195.
51. Iwama, E.; Shimodate, F.; Oki, Y.; Naoi, K., Super-enhanced lithium-ion transport by an effective shift of solvation shell structure in branched hydrofluoroether electrolyte, *Electrochemistry* **2010**, *78*, 266–272.
52. Ikeda, K.; Kawasato, T.; Hiratsuka, K.; Morimoto, T., *Nonaqueous electrolytic secondary battery*; JP 3,557,724 (B2): 2004.
53. Sasaki, Y.; Shimazaki, G.; Nanbu, N.; Takehara, M.; Ue, M., Physical and electrolytic properties of partially fluorinated organic solvents and its application to secondary lithium batteries: partially fluorinated dialkoxyethanes, *ECS Trans.* **2009**, *16(35)*, 23–31.
54. Blomgren, G. E., Properties, structures and conductivity of organic and inorganic electrolytes for lithium battery systems, In *Lithium batteries*; Gabano, J.-P., Ed.; Academic Press: London, United Kingdom, 1983; Ch. 2; 13–41.
55. Ue, M.; Ida, K.; Mori, S., Electrochemical properties of organic liquid electrolytes based on quaternary onium salts for electrical double-layer capacitors, *J. Electrochem. Soc.* **1994**, *141*, 2989–2996.
56. Nanbu, N.; Hagiyama, K.; Takehara, M.; Ue, M.; Sasaki, Y., Physical and electrolytic properties of difluorinated 3-methyl-2-oxazolidinones and their application to lithium rechargeable batteries, *Electrochemistry* **2010**, *78*, 450–453.

57. Suzuki, K.; Shin-Ya, M.; Ono, Y.; Matsumoto, T., Nanbu, N.; Takehara, M.; Ue, M.; Sasaki, Y., Physical and electrochemical properties of fluoroacetonitrile and its application to electric double-layer capacitors, *Electrochemistry* **2007**, *75*, 611–614.
58. Hagiyama, K.; Nanbu, N.; Takehara, M.; Ue, M.; Sasaki, Y., Electrolytic properties of α-fluorinated 1-methyl-2-pyrrolidinone, In *Meeting abstracts of the 2002 fall meeting of the Electrochemical Society of Japan*; Atsugi, Kanagawa, Japan, 2002; 99.
59. (a) Lu, Z.; MacNeil, D. D.; Dahn, J. R., Layered cathode materials $Li[Ni_xLi_{(1/3-2x/3)}Mn_{(2/3-x/3)}]O_2$ for lithium-ion batteries, *Electrochem. Solid-State Lett.* **2001**, *4*, A191–A194; (b) Ohzuku, T.; Makimura, Y., Layered lithium insertion material of $LiCo_{1/3}Ni_{1/3}Mn_{1/3}O_2$ for lithium-ion batteries, *Chem. Lett*. **2001**, *(7)*, 642–643; (c) Ohzuku, T.; Makimura, Y., Layered lithium insertion material of $LiNi_{1/2}Mn_{1/2}O_2$: a possible alternative to $LiCoO_2$ for advanced lithium-ion batteries, *Chem. Lett*. **2001**, *(8)*, 744–745; (d) Ohzuku, T.; Ariyoshi, K.; Yamamoto, S.; Makimura, Y., A 3-volt lithium-ion cell with $Li[Ni_{1/2}Mn_{3/2}]O_4$ and $Li[Li_{1/3}Ti_{5/3}]O_4$: a method to prepare stable positive-electrode material of highly crystallized $Li[Ni_{1/2}Mn_{3/2}]O_4$, *Chem. Lett.* **2001**, *(12)*, 1270–1271; (e) Lu, Z. H.; Beaulieu, L. Y.; Donaberger, R. A.; Thomas, C. L.; Dahn, J. R., Synthesis, structure, and electrochemical behavior of $Li[NixLi_{1/3-2x/3}Mn_{2/3-x/3}]O_2$, *J. Electrochem. Soc*. **2002**, *149*, A778–A791; (f) Lu, Z. H.; Chen, Z. H.; Dahn, J. R., Lack of cation clustering in $Li[Ni_xLi_{1/3-2x/3}Mn_{2/3-x/3}]O_2$ ($0 < x \leq 1/2$) and $Li[Cr_xLi_{(1-x)/3}Mn_{(2-2x)/3}]O_2$ ($0 < x < 1$), *Chem. Mater.* **2003**, *15*, 3214–3220; (g) Makimura, Y.; Ohzuku, T., Lithium insertion material of $LiNi_{1/2}Mn_{1/2}O_2$ for advanced lithium-ion batteries, *J. Power Sources* **2003**, *119–121*, 156–160.
60. (a) Xu, K.; Angell, C. A., High anodic stability of a new electrolyte solvent: unsymmetric noncyclic aliphatic sulfone, *J. Electrochem. Soc.* **1998**, *145*, L70–L72; (b) Xu, K.; Angell, C. A., Sulfone-based electrolytes for lithium-ion batteries, *J. Electrochem. Soc.* **2002**, *149*, A920–A926; (c) Abouimrane, A.; Belharouak, I.; Amine, K., Sulfone-based electrolytes for high-voltage Li-ion batteries, *Electrochem. Commun.* **2009**, *11*, 1073–1076; (d) Sun, X,; Angell, C. A., Doped sulfone electrolytes for high voltage Li-ion cell applications, *Electrochem.Commun.* **2009**, *11*, 1418–1421.
61. Abu-Lebdeh, Y.; Davidson, I., New electrolytes based on glutaronitrile for high energy/power Li-ion batteries, *J. Power Sources* **2009**, *189*, 576–579.
62. (a) Sasaki, Y.; Takehara, M.; Watanabe, S.; Oshima, M.; Nanbu, N.; Ue, M., Electrolytic behavior and application to lithium batteries of monofluorinated dimethyl carbonate, *Solid State Ionics* **2006**, *177*, 299–303; (b) Nanbu, N.; Takimoto, K.; Takehara, M.; Ue, M.; Sasaki, Y., Electrochemical properties of fluoropropylene carbonate and its application to lithium-ion batteries, *Electrochem. Commun.* **2008**, *10*, 783–786.
63. Gaussian 09 is the current integrated program including several molecular orbital methods, see Gaussian Inc. http://www.gaussian.com/
64. For example, *Minerals yearbook*, *Volume I. Metals and minerals*, USGS: 2009.
65. *Merck Index*, 13th Edition, 2001.
66. (a) Kidd, R. G., In *NMR of newly accessible nuclei, Vol. 2*; Laszlo, P., Ed.; Academic Press: New York, NY, 1983; (b) Noeth, H.; Wrackmeyer, B., In *Nuclear magnetic resonance spectroscopy of boron compounds*; Springer: Berlin, 1987; (c) Kennedy, J. D., In *Multinuclear NMR*; Mason, J., Ed.; Plenum Press: New York, NY, 1987.
67. Tanaka, Y.; Kaneko, J.; Minoshima, M.; Iriyama, Y.; Fujinami, T., Electrochemical properties of a mixed boric ester as a novel electrolyte solvent, *Electrochemistry* **2010**, *78*, 397–399.
68. Hirono, T.; Tamada, H.; Kishimoto, A.; Kaneko, J.; Iriyama, Y.; Tanaka, Y.; Fujinami, T., High voltage stability of interfacial reaction at the $LiMn_2O_4$ thin-film electrodes/liquid electrolytes with boroxine compounds, *J. Electrochem. Soc.* **2010**, *157*, A667–A681.
69. Shanmukaraj, D.; Grugeon, S.; Gachot, G.; Laruelle, S.; Mathiron, D.; Tarascon, J.-M.; Armand, M., Boron esters as tunable anion carriers for non-aqueous batteries electrochemistry, *J. Am. Chem. Soc.* **2010**, *132*, 3055–3062.
70. (a) Lee, H. S.; Yang, X. Q.; Sun, X.; McBreen, J., Synthesis of a new family of fluorinated boronate compounds as anion receptors and studies of their use as additives in lithium battery electrolytes, *J. Power Sources* **2001**, *97–98*, 566–569; (b) Sun, X.; Lee, H. S.; Yang, X. Q.;

McBreen, J., A new additive for lithium battery electrolytes based on an alkyl borate compound, *J. Electrochem. Soc.* **2002**, *149*, A355–A359; (c) Li, L. F.; Lee, H. S.; Lee, H.; Yang, X. Q.; Nam, K. W.; Yoon, W. S.; McBreen, J.; Huang, X. J., New electrolytes for lithium ion batteries using LiF salt and boron based anion receptors, *J. Power Sources* **2008**, *184*, 517–521.

71. (a) Lee, H. S.; Sun, X.; Yang, X. Q.; McBreen, J., Synthesis and study of new cyclic boronate additives for lithium battery electrolytes, *J. Electrochem. Soc.* **2002**, *149*, A1460–A1465; (b) Lee, H. S.; Ma, X. Z. F.; Yang, X. Q.; Sun, X.; McBreen, J., Synthesis of a series of fluorinated boronate compounds and their use as additives in lithium battery electrolytes, *J. Electrochem. Soc.* **2004**, *151*, A1429–A1435; (c) Chen, Z.; Amine, K., Bifunctional electrolyte additive for lithium-ion batteries, *Electrochem. Commun.* **2007**, *9*, 703–707; (d) Chen, Z.; Amine, K., Computational estimates of fluoride affinity of boron-based anion receptors, *J. Electrochem. Soc.* **2009**, *156*, A672–A676; (e) Weng, W.; Zang, Z.; Schlueter, J. A.; Redfern, P. C.; Curtiss, L. A.; Amine, K., Improved synthesis of a highly fluorinated boronicester as dual functional electrolyte additive for lithium-ion batteries, *J. Power Sources,* **2011**, *196*, 2171–2178.
72. (a) Xu, W.; Angell, C. A., LiBOB and its derivatives. Weakly coordinating anions, and the exceptional conductivity of their nonaqueous solutions, *Electrochem. Solid-State Lett.* **2001**, *4*, E1–E4; (b) Xu, W.; Shusterman, A. J.; Videa, M.; Velikov, V.; Marzke, R.; Angell, C. A., Structures of orthoborate anions and physical properties of their lithium salts in nonaqueous solutions, *J. Electrochem. Soc.* **2003**, *150*, E74–E80.
73. (a) Xu, K.; Lee, U.; Zhang, S. S.; Alen, J. L.; Jow, T. R., Graphite/electrolyte interface formed in LiBOB-based electrolytes, *Electrochem.Solid-State Lett.* **2004**, *7*, A273–A277; (b) Xu, K.; Lee, U.; Zhang, S. S.; Jow, T. R., Graphite/electrolyte interface formed in LiBOB-based electrolytes, *J. Electrochem. Soc.* **2004**, *151*, A2106–A2112.
74. (a) Zhang, S. S., An unique lithium salt for the improved electrolyte of Li-ion battery, *Electrochem. Commun.* **2006**, *8*, 1423–1428; (b) Zhang, S. S., Electrochemical study of the formation of a solid electrolyte interface on graphite in a $LiBC_2O_4F_2$-based electrolyte, *J. Power Sources* **2007**, *163*, 713–718.
75. (a) Barthel, J.; Buestrich, R.; Gores, H. J.; Schmidt, M.; Wuhr, M., A new class of electrochemically and thermally stable lithium salts for lithium battery electrolytes, *J. Electrochem. Soc*. **1997**, *144*, 3866–3870; (b) Sasaki, Y.; Handa, M.; Kurashima, K.; Tonuma, T.; Usami, K., Application of lithium organoborate with salicylic ligand to lithium battery electrolyte, *J. Electrochem. Soc*. **2001**, *148*, A999–A1003; (c) Sasaki, Y.; Handa, M.; Sekiya, S.; Kurashima, K.; Usami, K., Application to lithium battery electrolyte of lithium chelate compound with boron, *J. Power Sources* **2001**, *97–98*, 561–565; (d) Xue, Z.-M.; Ding, Y.-Z.; Chen, C.-H., A DFT study of electronic structures, energies, and molecular properties of lithium bis[croconate]borate and its derivatives, *Electrochim. Acta* **2007**, *53*, 990–997.
76. (a) Nanbu, N.; Shibazaki, T.; Sasaki, Y., Thermal and electrolytic behavior of lithium chelatoborates and application to lithium batteries, *Electrochemistry* **2003**, *71*, 1205–1213; (b) Xue, Z.-M.; Wu, K.-N.; Liu, B.; Chen, C.-H., New lithium salts with croconato-complexes of boron for lithium battery electrolytes, *J. Power Sources* **2007**, *171*, 944–947.
77. (a) Barthel, J.; Buestrich, R.; Carl, E.; Gores, H. J., A new class of electrochemically and thermally stable lithium salts for lithium battery electrolytes. III. Synthesis and properties of some lithium organo borates *J. Electrochem. Soc*. **1996**, *143*, 3572–3575; (b) Barthel, J.; Buestrich, R.; Gores, H. J.; Schmidt, M.; Wuhr, M., A new class of electrochemically and thermally stable lithium salts for lithium battery electrolytes, *J. Electrochem. Soc*. **1997**, *144*, 3866–3870; (c) Xue, Z.-M.; Chen, C.-H., Density functional theory study on lithium bis[1,2-benzenediolato (2-)-O,O′] borate and its derivatives: electronic structures, energies, and molecular properties, *Electrochim. Acta* **2004**, *49*, 5167–5175; (d) Aurbach, D.; Gnanaraj, J. S.; Geissler, W.; Schmidt, M., Vinylene Carbonate and Li salicylatoborate as additives in $LiPF_3(CF_2CF_3)_3$ solutions for rechargeable Li-ion batteries, *J. Electrochem. Soc*. **2004**, *151*, A23–A30.

78. Lisbona, D.; Snee, T., A review of hazards associated with primary lithium and lithium-ion batteries, *Process Safety and Environmental Protection* **2011**, *89*, 434–442.
79. Scrosati, B.; Garch, J., Lithium batteries: status, prospects and future, *J. Power Sources* **2010**, *195*, 2419–2430.
80. Murata, K.; Izuchi, S; Yoshihisa, Y., An overview of the research and development of solid polymer electrolyte batteries, *Electrochim. Acta* **2000,** *45*, 1501–1508.
81. Aihara, Y.; Kuratomi, J.; Bando, T.; Iguchi, T.; Yoshida, H.; Ono, T.; Kuwana, K., Investigation on solvent-free solid polymer electrolytes for advanced lithium batteries and their performance, *J. Power Sources* **2003**, *114*, 96–104.
82. Rodrigues, L. C.; Barbosa, P. C.; Silva, M. M.; Smith, M. J., Electrochemical and thermal properties of polymer electrolytes based on poly(epichlorohydrin-co-ethylene oxide-co-allyl glycidyl ether), *Electrochim. Acta* **2007**, *53*, 1427–1431.
83. Koura, N.; Iizuka, K.; Idemoto, Y., Ui, K., Li and Li-Al negative electrode characteristics for the lithium secondary battery with a nonflammable $SOCl_2$, Li added, LiCl saturated $AlCl_3$-EMIC molten salt electrolyte, *Electrochemistry* **1999**, *67*, 706–712.
84. Nakagawa, H.; Izuchi, S.; Kuwana, K.; Nukuda, T.; Aihara, Y., Liquid and polymer gel electrolytes for lithium batteries composed of room-temperature molten salt doped by lithium salt, *J. Electrochem. Soc.* **2003**, *150*, A695–A700.
85. Seki, S.; Kobayashi, Y.; Miyashiro, H.; Ohno, Y.; Usami, A.; Mita, Y.; Kihira, N.; Watanabe, M.; Terada, N., Lithium secondary batteries using modified-imidazolium room temperature ionic liquids, *J. Phys. Chem. B* **2006**, *110*, 10228–10230.
86. Ui, K.; Yamamoto, K.; Ishikawa, K.; Minami, T.; Takeuchi, K.; Itagaki, M.; Watanabe, K.; Koura, N., Development of non-flammable lithium secondary battery with room-temperature ionic liquid electrolyte: performance of electroplated Al film negative electrode, *J. Power Sources* **2008**, *183*, 347–350.
87. Wang, X. M.; Yasukawa, E.; Kasuya, S., Nonflammable trimethyl phosphate solvent-containing electrolytes for lithium-ion batteries, I. Fundamental properties, *J. Electrochem. Soc.* **2001**, *148*, A1058–A1065.
88. Arai, J., A novel non-flammable electrolytes containing methyl nonafluorobutyl ether for lithium secondary batteries, *J. Appl. Electrochem.* **2002**, *32*, 1071–1079.
89. Morita, M.; Kawasaki, T.; Yoshimoto, N.; Ishikawa, M., Nonflammable organic electrolyte solution based on perfluoro-ether solvent for lithium ion batteries, *Electrochemistry* **2003**, *71*, 1067–1069.
90. Zhang, S. S.; Xu, K.; Jow, T. R., Tris(2,2,2-trifluoroethyl)phosphate as a co-solvent for non-flammable electrolytes in Li-ion batteries, *J. Power Sources* **2003**, *113*, 166–172.
91. Xiang, H. F.; Xu, H. Y.; Wang, Z. Z.; Chen, C. H., Dimethylmethylphosphonate (DMMP) as an efficient flame retardant additives for the lithium-ion battery electrolytes, *J. Power Sources* **2007**, *173*, 562–564.
92. Murayama, M.; Sonoyama, N.; Yamada, A.; Kanno, R., Material design of new lithium ionic conductor, thio-LISICON, in the Li_2S-P_2S_5 system, *Solid State Ionics* **2004**, *170*, 173–180.
93. Nagao, M.; Hayashi, A.; Tatsumisago, M., All-solid-state lithium secondary batteries with high capacity using black phosphorus negative electrode, *J. Power Sources* **2011**, *196*, 6902–6905.
94. Morita, M.; Niida, Y.; Yoshimoto, N.; Adachi, K., Polymeric gel electrolyte containing alkylphosphate for lithium ion batteries, *J. Power Sources* **2005**, *146*, 427–430.
95. Hayashi, A.; Harayama, T.; Mizuno, F.; Tatsumisago, M., Mechanochemical synthesis of hybrid electrolytes from the Li_2S-P_2S_5 glasses and polyethers, *J. Power Sources* **2006**, *163*, 289–293.
96. Noda A.; Watanabe, M., Highly conductive polymer electrolytes prepared by in situ polymerization of vinyl monomers in room temperature molten salts, *Electrochim. Acta* **2000**, *45*, 1265–1270.
97. Shin, J.-H.; Henderson, W. A.; Passerini, S., Ionic liquids to rescue? Overcoming the ionic conductivity limitations of polymer electrolytes, *Electrochem. Commun.* **2003**, *5*, 1016–1020.

98. Egashira, M.; Todo, H.; Yoshimoto, N.; Morita, M., Lithium ion conduction in ionic liquid-based gel polymer electrolyte, *J. Power Sources* **2008**, *178*, 729–735.
99. Lalia, B. S.; Yoshimoto, N.; Egashira, M.; Morita, M., A mixture of triethylphosphate and ethylene carbonate as a safe additives for ionic liquid-based electrolytes of lithium ion batteries, *J. Power Sources* **2010**, *195*, 7426–7431.
100. Annakutty, K. S.; Kishore, K., A novel approach to structure-flammability correlation in polyphosphate esters, *Polymer* **1988**, *29*, 1273–1276.
101. Wang, X.; Yasukawa, E.; Kasuya, S., Nonflammable trimethyl phosphate solvent-containing electrolytes for lithium-ion batteries, II. The use of amorphous carbon anode, *J. Electrochem. Soc.* **2001**, *148*, A1066–A1071.
102. Wang, C. S.; Shieh, J. Y.; Sun, Y. M., Synthesis and properties of phosphorus containing PET and PEN (I), *J. Applied Polymer Science* **1998**, *70*, 1959–1964.
103. Xu, K.; Ding, M. S.; Zhang, S.; Allen, J. L.; Jow, T. R., An attempt to formulate nonflammable lithium ion electrolytes with alkyl phosphates and phosphazenes, *J. Electrochem. Soc.* **2002**, *149*, A622–A626.
104. Ota, H.; Kominato, A.; Chun, W. J.; Yasukawa, E.; Kasuya, S., Effect of cyclic phosphate additive in non-flammable electrolyte, *J. Power Sources* **2003**, *119–121*, 393–398.
105. Xu, K.; Zhang, S.; Allen, J. L.; Jow, T. R., Nonflammable electrolytes for Li-ion batteries based on a fluorinated phosphate, *J. Electrochem. Soc.* **2002**, *149*, A1079–A1082.
106. Morimoto, E.; Yoshimoto, N.; Egashira, M.; Morita, M., Cathode performance of $LiMn_2O_4$ in nonflammable organic electrolyte solutions containing alkylphosphate, In *Extended abstract of 56th annual meeting of international society of electrochemistry (56th ISE), Busan, Korea*, 2005; 1132.
107. Shigematsu, Y.; Ue, M.; Yamaki, J.-I., Thermal behavior of charged graphite and Li_xCoO_2 in electrolytes containing alkylphosphates for lithium-ion cell, *J. Electrochem. Soc.* **2009**, *156*, A176–A180.
108. Aurbach, D.; Ein-Eli, Y., The study of Li-graphite intercalation process in several electrolyte systems using *in situ* X-ray diffraction, *J. Electrochem. Soc.* **1995**, *142*, 1746–1752.
109. Ein-Eli, Y.; McDevitt, S. F.; Aurbach, D.; Markovsky, B.; Schecheter, A., Methyl propyl carbonate: A promising single solvent for Li-ion battery, *J. Electrochem. Soc.* **1997**, *144*, L180–L184.
110. Zhang, S. S., A review on electrolyte additives for lithium-ion batteries, *J. Power Sources* **2006**, *162*, 1379–1394.
111. Wang, X.; Yamada, C.; Naito, H.; Segami, G.; Kibe, K., High-concentration trimethyl phosphate-based nonflammable electrolytes with improved charge-discharge performance of a graphite anode for lithium-ion cells, *J. Electrochem. Soc.* **2006**, *153,* A135–A139.
112. Feng, J. K.; Sun, X. J.; Ai, X. P.; Cao, Y. L.; Yang, H. X., Dimethyl methyl phosphate: a new nonflammable electrolyte solvent for lithium-ion batteries, *J. Power Sources* **2008**, *184*, 570–573.
113. Yamaki, J.; Yamazaki, I.; Egashira, M.; Okada, S., Thermal studies of fluorinated ester as a novel candidate for electrolyte solvent of lithium metal anode rechargeable cells, *J. Power Sources* **2001**, *102*, 288–293.
114. Ding, M. S.; Xu, K.; Jow, T. R., Effects of tris(2,2,2-trifluoroethyl) phosphate as a flame-retarding cosolvent on physicochemical properties of electrolytes of $LiPF_6$ in EC-PC-EMC of 3:3:4 weight ratios, *J. Electrochem. Soc.* **2001**, *149*, A1489–1498.
115. Xu, K.; Ding, M. S.; Zhang, S.; Allen, J. L.; Jow, T. R., Evaluation of fluorinated alkylphosphates as flame retardants in electrolytes for Li-ion batteries I. Physical and electrochemical properties, *J. Electrochem. Soc.* **2003**, *150*, A161–A169.
116. Xu, K.; Zhang, S.; Allen, J. L.; Jow, T. R., Evaluation of fluorinated alkylphosphates as flame retardants in electrolytes for Li-ion batteries II. Performance in cell. *J. Electrochem. Soc.* **2003**, *150*, A170–A175.
117. Xiang, H. F.; Jin, Q. Y.; Chen, C. H.; Ge, X. W.; Guo, S.; Sun, J. H., Dimethyl methylphosphonate-based nonflammable electrolyte and high safety lithium-ion batteries, *J. Power Sources* **2007**, *174*, 335–341.

118. Xiang, H. F.; Jin, Q. Y.; Wang, R.; Chen, C. H.; Ge, X. W., Nonflammable electrolyte for 3-V lithium-ion battery with spinel materials $LiNi_{0.5}Mn_{1.5}O_4$ and $Li_4Ti_5O_{12}$, *J. Power Sources* **2008**, *179*, 351–356.
119. Dalavi, S.; Xu, M.; Ravdel, B.; Zhou, L.; Lucht, B. L., Nonflammable electrolytes for lithium-ion batteries containing dimethyl methylphosphonate, *J. Electrochem. Soc.* **2010**, *157*, A1113–A1120.
120. Wu, L.; Song, Z.; Liu, L.; Guo, X.; Kong, L.; Zhan, H.; Zhou, Y.; Li, Z., A new phosphate-based nonflammable electrolyte solvent for Li-ion batteries, *J. Power Sources* **2009**, *188*, 570–573.
121. Yao, X. L.; Xie, S.; Chen, C. H.; Wang, Q. S.; Sun, J. H.; Li, Y. L.; Lu, S. X., Comparative study of trimethyl phosphite as electrolyte additives in lithium ion batteries, *J. Power Sources* **2005**, *144*, 170–175.
122. Xu, H. Y.; Xie, S.; Wang, Q. Y.; Yao, X. L.; Wang, Q. S.; Chen, C. H., Electrolyte additive trimethyl phosphite for improving electrochemical performance and thermal stability of $LiCoO_2$ cathode, *Electrochim. Acta* **2006**, *52*, 636–642.
123. Zhang, S. S.; Xu, K.; Jow, T. R., A thermal stabilizer for $LiPF_6$-based electrolytes of Li-ion cells, *Electrochem. Solid-State Lett,* **2002**, *5*, A206–A208.
124. Wang, Q.; Sun, J.; Yao, X.; Chen, C., 4-isopropyl phenyl diphenyl phosphate as flame-retardant additive for lithium-ion battery electrolyte, *Electrochem. Solid-State Lett.* **2005**, *8*, A467–A470.
125. Wang, Q.; Sun, J.; Chen, C., Enhancing the thermal stability of $LiCoO_2$ electrode by 4-isopropyl phenyl diphenyl phosphate in lithium ion batteries, *J. Power Sources* **2006**, *162*, 1363–1366.
126. Wang, Q.; Ping, P.; Sun, J.; Chen, C., Improved thermal stability of lithium ion battery by using cresyl diphenyl phosphate as an electrolyte additive, *J. Power Sources* **2010**, 195, 7457–7461.
127. Zhou, D.; Li, W.; Tan, C.; Zuo, X.; Huang, Y., Cresyl diphenyl phosphate as flame retardant additive for lithium-ion batteries, *J. Power Sources* **2008**, *184*, 589–592.
128. Feng, J. K.; Yao, Y. L.; Ai, X. P.; Yang, H. X., Tri-(4-methokythphenyl) phosphate: a new electrolyte additive with both fire-retardancy and overcharge protection for Li-ion batteries, *Electrochim. Acta* **2008**, *53*, 8265–8268.
129. Tsujikawa, T.; Yabuta, K.; Matsushita, T.; Matsushima, T.; Hayashi, K.; Arakawa, M., Characteristics of lithium-ion battery with non-flammable electrolyte, *J. Power Sources* **2009**, *189*, 429–434.
130. Lee, C. W.; Venkatachalapathy, R.; Prakash, J., A novel flame-retardant additive for lithium batteries, *Electrochem. Solid-State Lett,* **2000**, *3*, 63–65.
131. Sazhin, S. V.; Harrup, M. K.; Gering, K. L., Characterization of low flammability electrolytes for lithium-ion batteries, *J. Power Sources* **2011**, *196*, 3433–3438.
132. Hu, J.; Jin, Z.; Zhong, H.; Zhan, H.; Zhou, Y.; Li, Z., A new phosphonamidate as flame retardant additive in electrolytes for lithium ion batteries, *J. Power Sources* **2012**, *197*, 297–300.
133. Morford, R. V.; Kellam III, E. C.; Hofmann, M. A.; Allcock, H. R., A fire-retardant organophosphorus gel polymer electrolyte additive for use in rechargeable lithium batteries, *Solid State Ionics* **2000**, *133*, 171–177.
134. Yoshimoto, N.; Niida, Y.; Egashira, M.; Morita, M., Nonflammable gel electrolyte containing alkyl phosphate for rechargeable lithium batteries, *J. Power Sources* **2006**, *163*, 238–242.
135. Yoshimoto, N.; Goto, D.; Egashira, M.; Morita, M., Alkylphosphate-based nonflammable gel electrolyte for $LiMn_2O_4$ positive electrode in lithium-ion battery, *J. Power Sources* **2008**, *185*, 1425–1428.
136. Lalia, B. S.; Fujita, T; Yoshimoto, N.; Egashira, M.; Morita, M., Electrochemical performance of nonflammable gel electrolyte containing triethylphosphate, *J. Power Sources* **2009**, *186*, 211–215.
137. Lalia, B. S.; Yoshimoto, N.; Egashira, M.; Morita, M., Electrochemical performances of nonflammable gel electrolyte for lithium ion battery using $LiFePO_4$ positive electrode, *Electrochemistry* **2010**, *78*, 332–335.

138. McBreen, J.; Lee, H. S.; Yang, X. Q.; Sun, X., New approaches to the design of polymer and liquid electrolytes for lithium batteries, *J. Power Sources* **2000**, *89*, 163–167.
139. Tabata, S.; Hirakimoto, T.; Nishimura, M.; Watanabe, M., Synthesis of Lewis-acid boric acid ester monomer and effect of its addition to electrolyte solutions and polymer gel electrolytes on their ion transport properties, *Electrochim. Acta* **2003**, *48*, 2105–2112.
140. Xu, W.; Sun, X. G.; Angell, C. A., Anion-trapping and polyanion electrolytes based on acid-in-chain borate polymers, *Electrochim. Acta* **2003**, *48*, 2255–2266.
141. Lalia, B. S.; Yoshimoto, N.; Egashira, M.; Morita, M., Effects of Lewis-acid polymer on the electrochemical properties of alkylphosphate-based non-flammable gel electrolyte, *J. Power Sources* **2009**, *194*, 531–535.
142. Blomgren, G. E., Properties, structures and conductivity of organic and inorganic electrolytes for lithium battery systems, In *Lithium batteries*; Gabano, J.-P., Ed.; Academic Press: London, United Kingdom, 1983; Ch. 2; 13–41.
143. Ue, M., Thinking way in electrolyte materials, In *50th Electrochemistry seminar*; Kansai branch of the Electrochemical Society of Japan: Osaka, Japan, 2010.
144. Ue, M., Electrolyte technologies supporting the progress of lithium batteries, In *2012 Taipei forum on large format lithium batteries*; Taipei, Taiwan, 2012.
145. Tamamitsu, K., Aluminum electrolytic capacitors using sulfolane as an electrolyte solvent, *J. Technology and Education* **2003**, *10*, 115–120.
146. Ue, M.; Takehara, M.; Takeda, M., Triethylmethylammonium tetrafluoroborate as a highly soluble supporting electrolyte salt for electrochemical capacitors, *Denki Kagaku* **1997**, *65*, 969–971.
147. Ue, M.; Murakami, A.; Nakamura, S., Anodic stability of several anions examined by ab initio molecular orbital and density functional theories, *J. Electrochem. Soc.* **2002**, *149*, A1572–A1577.
148. Kumar, T. P.; Prabhu, P. V. S. S.; Srivastava, A. K.; Kumar, U. B.; Ranganathan, R.; Gangadharan, R., Conductivity and viscosity studies of dimethyl sulfoxide (DMSO)-based electrolyte solutions at 25°C, *J. Power Sources* **1994**, *50*, 283–294.
149. Prisyazhnii, V. D.; Sirenko, V. I.; Potapenko, O. V.; Zmievs'ka, T. A., Solutions of lithium benzenesulfonate in dimethyl sulfoxide as electrolytes for lithium-based batteries, *Dopov. Nats. Akad. Nauk Ukr.* **2007**, 136–141.
150. Fouache-Ayoub, S.; Garreau, M.; Prabhu, P. V. S. S.; Thevenin, J., Mass-transport properties of lithium surface layers formed in sulfolane-based electrolytes, *J. Electrochem. Soc.* **1990**, *137*, 1659–1665.
151. Xu, K.; Angell, C. A., Sulfone-based electrolytes for lithium-ion batteries, *J. Electrochem. Soc.* **2002**, *149*, A920–A926.
152. Giwa, C. O., Feasibility study of sulfone-based electrolytes for a medium-temperature reserve cell concept, *J. Power Sources* **1993**, *42*, 389–397.
153. Bach, S.; Baffier, N.; Pereira-Ramos, J. P.; Messina, R., Rechargeable γ-MnO_2 for lithium batteries using a sulfone-based electrolyte at 150°C, *J. Power Sources* **1993**, *43–44*, 569–575.
154. Xu, K.; Angell, C. A., High anodic stability of a new electrolyte solvent: unsymmetric non-cyclic aliphatic sulfone, *J. Electrochem. Soc.* **1998**, *145*, L70–L72.
155. Wrodnigg, G. H.; Besenhard, J. O.; Winter, M., Ethylene sulfite as electrolyte additive for lithium-ion cells with graphitic anodes, *J. Electrochem. Soc.* **1999**, *146*, 470–472.
156. Wrodnigg, G. H.; Wrodnigg, T. M.; Besenhard, J. O.; Winter, M., Propylene sulfite as film-forming electrolyte additive in lithium ion batteries, *Electrochem. Commun.* **1999**, *1(3), 148–150*,
157. Wrodnigg, G. H.; Besenhard, J. O.; Winter, M., Cyclic and acyclic sulfites: new solvents and electrolyte additives for lithium ion batteries with graphitic anodes?, *J. Power Sources* **2001**, *97–98*, 592–594.
158. Ue, M., Role-assigned electrolytes: additives, In *Lithium-ion batteries*; Yoshio, M.; Brodd, R. J.; Kozawa, A., Eds.; Springer: New York, NY, 2009; Ch. 4; 75–115.
159. Yu, B. T.; Qiu, W. H.; Li, F. S.; Cheng, L., A study on sulfites for lithium-ion battery electrolytes, *J. Power Sources* **2006**, *158*, 1373–1378.

160. Park, G.; Nakamura, H.; Lee, Y.; Yoshio, M., The importance role of additives for improved lithium ion battery safety, *J. Power Sources* **2009**, *189*, 602–606.
161. Xu, M.; Li, W.; Lucht, B. L., Effect of propane sultone on elevated temperature performance of anode and cathode materials in lithium-ion batteries, *J. Power Sources* **2009**, *193*, 804–809.
162. Jeong, S. K.; Lee, H. N.; Kim, Y. S., Thermal stability of surface film formed on a graphite negative electrode in lithium secondary batteries, *J. Korean Electrochem. Soc.* **2011**, *14*, 157–162.
163. Han, Y. K.; Lee, S. U.; Ok, J. H.; Cho, J. J.; Kim, H. J., Theoretical studies of the solvent decomposition by lithium atoms in lithium-ion battery electrolyte, *Chem. Phys. Lett.* **2002**, *360*, 359–366.
164. Sano, A.; Maruyama, S., Decreasing the initial irreversible capacity loss by addition of cyclic sulfate as electrolyte additives, *J. Power Sources* **2009**, *192*, 714–718.
165. Yao, Y. W.; Xu, J.; Yao, W. H.; Wang, Z. C.; Yang, Y., Effect of ethylene sulfate as electrolyte additive on performance of Li-ion batteries, *Yingyong Huaxue* **2010**, *27*, 823–828.
166. Guyomard, D.; Tarascon, J. M., Rechargeable $Li_{1+x}Mn_2O_4$/carbon cells with a new electrolyte composition: potentiostatic studies and application to practical cells, *J. Electrochem. Soc.* **1993**, *140*, 3071–3081.
167. Seel, J. A.; Dahn, J. R., Electrochemical intercalation of PF_6 into graphite, *J. Electrochem. Soc.* **2000**, *147*, 892–898.
168. Lu, Z. H.; Dahn, J. R., Can all the lithium be removed from T/2 $Li_{2/3}[Ni_{1/3}Mn_{2/3}]O_2$?, *J. Electrochem. Soc.* **2001**, *148*, A710–A715.
169. Park, S. H.; Winnick, J.; Kohl, P. A., Investigation of the lithium couple on Pt, Al, and Hg electrodes in lithium imide-ethyl methyl sulfone, *J. Electrochem. Soc.* **2002**, *149*, A1196–A1200.
170. Abouimrane, A.; Belharouak, I.; Amine, K., Sulfone-based electrolytes for high-voltage Li-ion batteries, *Electrochem. Commun.* **2009**, *11*, 1073–1076.
171. Sun, X. G.; Angell, C. A., New sulfone electrolytes for rechargeable lithium batteries. part I. oligoether-containing sulfones, *Electrochem. Commun.* **2005**, *7*, 261–266.
172. Sun, X. G.; Angell, C. A., New sulfone electrolytes, *Solid State Ionics* **2004**, *175*, 257–260.
173. Shao, N.; Sun, X. G.; Dai, S.; Jiang, D. E., Electrochemical windows of sulfone-based electrolytes for high-voltage Li-ion batteries, *J. Phys. Chem. B* **2011**, *115*, 12120–12125.
174. Sun, X. G.; Angell, C. A., Doped sulfone electrolytes for high voltage Li-ion cell applications, *Electrochem. Commun.* **2009**, *11*, 1418–1421.
175. Watarai, A.; Tokuda, H.; Kawai, T.; Ue, M., Development of electrolytes for highly safe lithium-ion batteries, In *216th Electrochemical society meeting*; Vienna, Austria, 2009.
176. Ue, M.; Kagimoto, J.; Tokuda, H.; Kawai, T., Sulfolane-based LIB electrolytes for HEV applications, In *5th International conference on polymer batteries and fuel cells*; Argonne, IL, 2011.
177. Ue, M.; Kagimoto, J.; Tokuda, H.; Kawai, T., High-safety LIB electrolytes for HEV applications, In *6th Asian conference on electrochemical power sources*; Chennai, India, 2012.
178. Shao, N.; Sun, X. G.; Dai, S.; Jiang, D. E., Oxidation potentials of functionalized sulfone solvents for high-voltage Li-ion batteries: a computational study, *J. Phys. Chem. B* **2012**, *116*, 3235–3238.

http://www.springer.com/978-1-4939-0301-6

Electrolytes for Lithium and Lithium-Ion Batteries

Jow, R.T.; Xu, K.; Borodin, O.; Ue, M. (Eds.)
2014, XVIII, 476 p. 300 illus., 130 illus. in color.,
Hardcover
ISBN: 978-1-4939-0301-6